

**Membrane glycoprotein M6a: expression and regulation
by stress in the brain**

Ph.D. Thesis

**In partial fulfilment of the requirements for the degree "Doctor of Philosophy"
In the Graduate Program Neuroscience
At the Georg-August University, Göttingen
Faculty of Biology**

Submitted by

Benjamin Cooper

Born in

Blenheim, New Zealand

2007

"It is not stress that kills us, it is our reaction to it."

Hans Selye

Declaration

I hereby declare that this submission is my own work and that, to the best of my knowledge and belief, it contains no materials previously published or written by another person nor material which to a substantial extent has been accepted for the award of any other degree of the university or other institute of higher education, except where due acknowledgement has been made in the text.

Signature

Name

Date and place

.....

.....

.....

Table of Contents

Abbreviations	6
Abstract	7
Introduction	9
Glycoprotein M6a	9
<i>Structure and membrane topology of M6a</i>	9
<i>Expression and localisation of M6a</i>	11
<i>Function of M6a</i>	12
Chronic stress and neuronal remodelling	14
<i>Hippocampus</i>	15
<i>Prefrontal cortex</i>	18
Stress regulation of gene expression	19
Stress regulates M6a expression in the hippocampal formation	21
Chronic restraint stress paradigm	21
Aims of the thesis	22
Methods and materials	24
Experimental animals	24
<i>In situ</i> hybridisation	24
<i>Cloning of rat M6a cDNA</i>	24
<i>Tissue preparation and hybridisation procedure</i>	25
<i>Quantitative in situ hybridisation</i>	26
Immunocytochemistry	28
<i>Immunofluorescence experiments</i>	29
Confocal laser scanning microscopy	30
Chronic restraint stress	31
Quantitative real-time RT-PCR	32
<i>Data analysis</i>	34
Quantitative immunocytochemistry	35
Statistical analyses	36

Results	37
<i>In situ</i> hybridisation	37
Immunocytochemistry	39
<i>Specificity of the M6a antibody</i>	39
<i>Immunocytochemical detection of M6a in the hippocampal formation.</i>	40
<i>Immunocytochemical detection of calbindin in the hippocampal formation</i>	40
<i>Immunocytochemical detection of MAP-2 in the hippocampal formation</i>	44
<i>Immunocytochemical detection of NF200 in the hippocampal formation</i>	45
<i>Immunocytochemical detection of synaptophysin in the hippocampal formation</i>	45
<i>Immunocytochemical detection of VGLUT1 in the hippocampal formation</i>	46
<i>Immunocytochemical detection of VGAT in the hippocampal formation</i>	46
<i>Immunocytochemical detection of SV2B in the hippocampal formation</i>	47
<i>Immunocytochemical detection of MOR1 in the hippocampal formation</i>	47
Confocal laser scanning microscopy	48
<i>Calbindin immunoreactivity detected by confocal LSM</i>	48
<i>MAP-2 immunoreactivity detected by confocal LSM</i>	48
<i>NF200 immunoreactivity detected by confocal LSM</i>	56
<i>Synaptophysin immunoreactivity detected by confocal LSM</i>	56
<i>VGLUT1 immunoreactivity detected by confocal LSM</i>	57
<i>VGAT immunoreactivity as detected by confocal LSM</i>	58
<i>SV2B immunoreactivity detected by confocal LSM</i>	58
<i>MOR1 immunoreactivity detected by confocal LSM</i>	59
Real-time RT-PCR	61
<i>Constitutive expression of M6a isoforms in the brain and kidneys</i>	61
<i>Effects of chronic stress on M6a expression in the brain</i>	61
Quantitative <i>in situ</i> hybridisation	64
Quantitative immunocytochemistry	64
Discussion	67
Antibody specificity	67
M6a is targeted to the axonal membrane of glutamatergic neurons	67
<i>Dentate gyrus: mossy fibre pathway</i>	68
<i>Pyramidal neurons: hippocampus</i>	69
<i>Pyramidal neurons: prefrontal cortex</i>	70
<i>Cerebellar granule cells: parallel fibres</i>	71

M6a and GABAergic neurons	71
Colocalisation of M6a with synaptic vesicle markers	72
Chronic stress regulation of M6a expression	74
<i>M6a is downregulated by chronic stress in the hippocampus</i>	74
<i>M6a is upregulated by chronic stress in the ventromedial prefrontal cortex</i>	75
<i>Chronic stress selectively regulates expression of neuronal M6a isoform Ib</i>	76
<i>Time-course of stress-effects on M6a expression</i>	77
Functional implications of M6a in glutamatergic axon terminals	78
<i>Cell adhesion</i>	78
<i>Ion channel function</i>	79
<i>Opioid receptor interactions</i>	80
<i>Potential interaction with cholesterol and lipid-enriched microdomains</i>	81
Conclusion	84
List of References	85
List of Figures	96
List of Tables	97
Publications	98
Acknowledgements	99
Curriculum Vitae	100

Abbreviations

AC	anterior cingulate cortex
CAM	cellular adhesion molecule
C _t	threshold cycle
EMA	edge membrane antigen
EST	expressed sequence tag
gcl	granule cell layer; dentate gyrus
gl	granule layer; cerebellum
GR	glucocorticoid receptor
GRE	glucocorticoid response element
HPA	hypothalamo-pituitary-adrenal
IL	infralimbic cortex
LSM	laser scanning microscopy
MAP-2	microtubule-associated protein 2
MDD	major depressive disorder
MF	mossy fibre
ml	molecular layer
MOR	μ-opioid receptor
mPFC	medial prefrontal cortex
MR	mineralocorticoid receptor
NA	numerical aperture
NCAM	neuronal cellular adhesion molecule
NF200	neurofilament subunit 200 kDa
NGF	nerve growth factor
NR	nuclear receptor
PFC	prefrontal cortex
PL	prelimbic cortex
PLP	proteolipid protein
TMD	transmembrane domain
ROD	relative optical density
RT-PCR	reverse-transcription polymerase chain reaction
SiRNA	small inhibitory RNA
SSRI	selective serotonin reuptake inhibitor
SV2B	synaptic vesicle protein type 2B
VGAT	vesicular gamma-amino butyric acid (GABA) transporter
VGLUT1	vesicular glutamate transporter type 1

Abstract

Glycoprotein M6a is a neuronally expressed transmembrane protein belonging to the myelin proteolipid protein (PLP) family. *In vitro* studies have identified M6a as a key modulator of neurite outgrowth and spine formation, however, the precise location of M6a within neurons in the adult brain remains obscure. M6a was previously identified as a stress-responsive gene in the hippocampus of psychosocially stressed animals, but it is not known whether stress also regulates M6a expression in other brain regions. It is generally accepted that stress induces aberrant neuronal plasticity and it has been hypothesised that stress-induced morphological changes in the hippocampal formation and prefrontal cortex may contribute to the development of stress-related neuropathologies such as depression. Therefore, the aim of the present thesis was to characterise the regional neuronal expression of membrane glycoprotein M6a in the brain and to investigate the effects of stress on M6a expression within the prefrontal cortex of chronically restrained rats.

A combination of *in situ* hybridisation and immunocytochemistry was performed to characterise the expression of M6a within the hippocampal formation, prefrontal cortex and cerebellum. *In situ* hybridisation confirmed that M6a is abundantly expressed in pyramidal and granule neurons in the hippocampal formation, in cortical pyramidal and in cerebellar granule neurons. Neurons bearing the morphological characteristics of inhibitory interneurons do not express M6a. Confocal laser microscopy demonstrated that M6a immunoreactivity colocalises with synaptophysin and the vesicular glutamate transporter (VGLUT1) indicating that the glycoprotein is targeted to the terminals of glutamatergic axons. M6a immunoreactivity was not detected within neuronal somata and did not colocalise with MAP-2 in any brain region investigated, demonstrating that M6a is not expressed in dendrites. In the hippocampus M6a immunoreactivity was visualised as focal puncta localised to distinct sites within the terminal regions of granule cell mossy fibre axons that were visualised by immunoreactivity for the cytoplasmic calcium-binding protein calbindin. Analysis of giant mossy fibre terminals, which contact dendrites of CA3 pyramidal neurons in the hippocampal *stratum lucidum*, revealed that M6a immunoreactivity was associated primarily with the membrane of axon fibres and their terminals, but not with synaptic vesicles. M6a and the vesicular GABA transporter (VGAT) exhibited largely contrasting patterns of immunoreactivity and colocalisation was observed only

rarely, indicating that M6a is not expressed in inhibitory neurons but that colocalisation might be observed when GABAergic terminals are situated in close proximity to glutamatergic axons.

The second part of the thesis investigated the effects of stress on M6a expression in the brains of rats exposed to 21 days chronic restraint stress. Stress experiments were performed to investigate the effects of chronic restraint on M6a expression using: i) quantitative real-time RT-PCR and ii) quantitative *in situ* hybridisation. RT-PCR analysis revealed that M6a is regulated in a region-specific manner in the brains of chronically restrained rats. M6a was significantly downregulated in the hippocampus, whereas the prefrontal cortex demonstrated a non-significant increase in expression. No effect of stress was observed in the cerebellum. Since the prefrontal cortex comprises several anatomically and functionally distinct areas, of which only some may be responsive to stress, regional changes in M6a expression may be masked in RT-PCR analyses performed on prefrontal samples containing multiple subregions. Therefore, quantitative *in situ* hybridisation was performed to provide a means of localising potential stress-induced changes in M6a expression to specific neuronal populations. M6a was found to be significantly upregulated in layer II/III pyramidal neurons in the infralimbic and prelimbic, but not in the anterior cingulate cortex.

In conclusion, the present data show that M6a is expressed in pyramidal and granule cells and that the glycoprotein is targeted to distinct sites within the axonal plasma membrane of these excitatory neurons. Stress was found to regulate M6a expression in a region-specific manner. Moreover, changes in M6a expression correlate with brain regions exhibiting maladaptive alterations in neuronal morphology in response to chronic stress. Stress-induced changes in M6a expression may influence the structural integrity of presynaptic terminals and impair the induction of neuroplastic mechanisms designed to protect against the deleterious effects of chronic stress.

Introduction

Glycoprotein M6a

The M6a gene encodes a highly hydrophobic transmembrane glycoprotein belonging to the phylogenetically archaic proteolipid family of tetraspan proteins (Schweitzer *et al.*, 2006; Gow, 1997). Proteolipids possess both protein and lipid moieties and consequently exhibit distinct biochemical properties that distinguish them from other known lipoproteins: proteolipids are insoluble in water, but soluble in chloroform-methanol mixtures (Folch & Lees, 1951). Members of the mammalian proteolipid family include M6a, M6b, PLP and its splice isoform DM20 (Yan *et al.*, 1993; Nave, 1987). M6a (also known as edge membrane antigen; EMA; Baumrind *et al.*, 1992) represents the only member of the proteolipid family to be expressed exclusively by neurons in the central nervous system. M6b is expressed in both neuronal and glial populations (Yan *et al.*, 1996; Werner *et al.*, 2001), whereas PLP and DM20 are expressed exclusively by oligodendrocytes and collectively represent the major protein component of myelin in the brain (Lees & Brostoff, 1984).

Structure and membrane topology of M6a

Structural analyses indicate that proteolipids assume common topologies with respect to the phospholipid bilayer (Popot *et al.*, 1991; Gow *et al.*, 1997). M6a is composed of four putative transmembrane domains (TMDs) connected via three hydrophilic domains, two of which are exposed to the extracellular environment. The larger, second extracellular domain (spanning TMD 3-4) possesses two potential N-linked glycosylation sites and four conserved cysteine residues presumed to participate in the formation of two intramolecular disulfide (S-S) bridges. Two putative phosphorylation sites for protein kinase C (PKC) and one for casein kinase 2 (CK2)

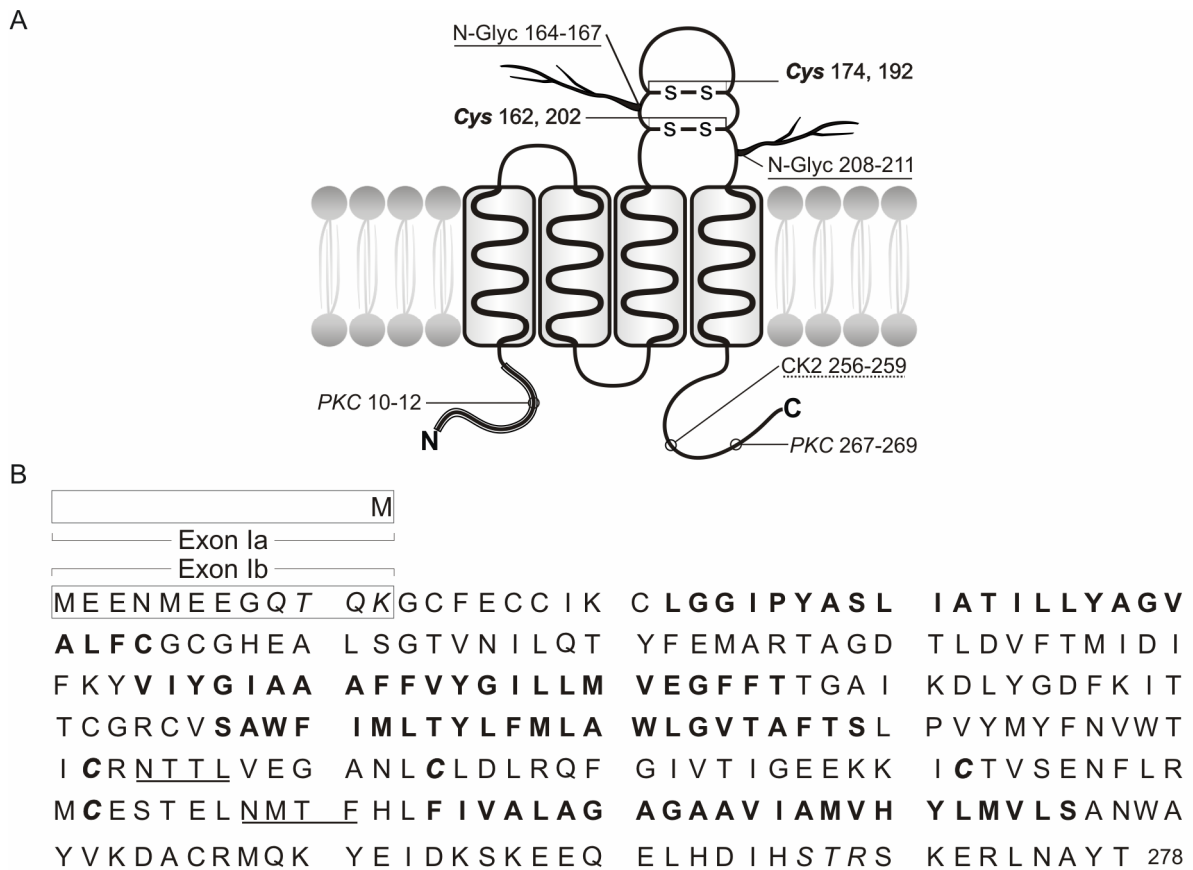


FIGURE 1. Schematic illustrating the basic structure of membrane glycoprotein M6a (**A**). The amino acid sequence of M6a (**B**) including the N-terminus peptide fragment encoded by exon 1b (enclosed in black box). Features listed include transmembrane domains (sequence appears in bold), PKC phosphorylation sites (*PKC*, sequence appears in italic), N-linked glycosylation sites (N-Glyc, sequence underlined) indicating position of oligosaccharide moieties, casein kinase 2 phosphorylation site (CK2, sequence underlined; dotted), and the alternative N-terminus peptide fragment for exon 1a (enclosed in black box).

are located in the hydrophilic domains of the N- and C-termini, both of which face the cytoplasm (see **Fig.1**). Immunoaffinity-purified M6a separated by SDS-PAGE migrates with a size of 35 kDa (Yan *et al.*, 1993). Cleavage of carbohydrate moieties with neuraminidase treatment causes M6a to migrate with a size of 31 kDa (Lagenaur *et al.*, 1992). All proteolipids are believed to have evolved from a common ancestral gene (Schweitzer *et al.*, 2006), and the considerable homology observed between different members of the mammalian proteolipid family appears to reflect this evolutionary relationship: M6a is 56% and 43% homologous with M6b and PLP/DM20 at the amino acid level, respectively; Yan *et al.*, 1993). TMDs are highly

conserved within the family, however, studies indicate that the amino acid composition of hydrophilic domains profoundly influences the conformational properties of proteolipids within membranes (Gow, 1997).

Expression and localisation of M6a

M6a was first identified in studies investigating growth cone dynamics in cultured cerebellar monolayers (Lagenaur *et al.*, 1992). Antibodies generated against the M6 antigen revealed that M6a is localised to the membranes of neuronal processes in cultured neurons (Baumrind *et al.*, 1992; Lagenaur *et al.*, 1992; Alfonso *et al.*, 2005a) and time-lapse video microscopy was used to visualise the 'entrapment' of EMA at the leading edge of lamellipodia (Sheetz *et al.*, 1990). It was subsequently shown that disruption of tubulin assembly with vinblastine severely impairs transport of M6a to neurites, implying that M6a is trafficked to the membranes of neuronal processes via microtubule-dependent anterograde transport (Obayashi *et al.*, 2002).

The temporal pattern of M6a expression in mice indicates that M6a is one of the first molecules to be expressed by differentiating neurons in the developing CNS (Yan *et al.*, 1996). M6a mRNA is first detectable at embryonic (E) day 10 in the marginal zone of the neural tube and by E11 is distributed throughout the brain with expression in the cerebellum, hippocampus, and cortex remaining throughout adulthood (Yan *et al.*, 1996). In the adult cerebellum *in situ* hybridisation provided preliminary evidence that M6a is differentially expressed in certain neuronal populations: M6a mRNA was strongly expressed within the cerebellar granule layer but absent from the Purkinje cell and molecular layers (Yan *et al.*, 1996). M6a immunoreactivity was, however, detected in both granule and molecular layers and ultrastructural analyses indicate that M6a synthesized in cerebellar granule cells is targeted to the membranes of presynaptic terminals and synaptic vesicles of parallel

fibres (Roussel *et al.*, 1998). M6a mRNA was found to be strongly expressed in all major cell layers of the murine hippocampus and *in vitro* studies report that M6a is distributed throughout the entire plasma membrane of primary hippocampal neurons, but enriched in neuronal processes and spine-like filopodia (Alfonso *et al.*, 2005a). However, the precise location of M6a in the hippocampal formation is yet to be described in the adult brain. The highly related proteolipid M6b has been detected in numerous peripheral tissues (Werner *et al.*, 2001). In contrast, the non-neuronal expression of M6a appears restricted to the apical membranes of polarised epithelial cells within the choroid plexus, olfactory bulb, and proximal renal tubules (Lagenaur *et al.*, 1984).

Function of M6a

The precise function of neuronally expressed proteolipids remains unclear. Potential roles for M6a may include regulation of neurite outgrowth, cellular adhesion, ion transport, and receptor internalisation.

During brain development M6a exhibits a temporal pattern of expression coinciding with specific periods of neuronal differentiation and neurite outgrowth (Yan *et al.*, 1996). Moreover, neurite formation was severely impaired in cerebellar neurons treated with monoclonal M6 antibody: neurites appeared shorter, fewer in number and irregularly shaped (Lagenaur *et al.*, 1992). In primary hippocampal neurons forced overexpression of M6a promotes neurite outgrowth and the formation of filopodial protrusions in primary hippocampal neurons (Alfonso *et al.*, 2005a). In contrast, targeted depletion of endogenous M6a expression with small inhibitory RNA (siRNA) technology severely attenuated neurite outgrowth and impaired synaptogenesis as visualised by a reduction in the number of synaptophysin-positive clusters (Alfonso *et al.*, 2005a).

Cellular adhesion molecules (CAMs) are similarly localised to the neurites of developing neurons where their functions include axonal growth (Doherty *et al.*, 1990; Zhang *et al.*, 1992), fasciculation (Acheson *et al.*, 1991; Yin *et al.*, 1995), guidance (Tang *et al.*, 1992) and synaptic arrangement (Seki & Rutishauser, 1998; Venero, 2004; Kiss *et al.*, 2001). The observed tendency for isolated M6a to co-aggregate (Lund *et al.*, 1986) and its preferential localisation to regions of dynamic membrane outgrowth (Lagenaur *et al.*, 1992) has led some authors to ascribe a potential adhesive function to this neuronally expressed proteolipid (Lund *et al.*, 1986). M6a immunoreactivity was localised to axon bundles of the corpus callosum early in development, but is lost prior to the onset of myelination (Lund *et al.*, 1986). Interactions between surface-bound M6a may therefore promote the stability of bundled axon fasciculi prior to the onset of myelination, at which point adhesive bonds should be dissolved to promote accessibility to the ensheathing processes of oligodendrocytes.

A potential role for M6a in ion transport was first based intuitively on the immunolocalisation of M6a to neuronal plasma membranes and the apical surface of polarised epithelia, both of which rely heavily on the coordinated transport of ions across membranes. Indeed, members of the proteolipid family were initially hypothesised to act as membrane-bound pore-forming units and reconstituted lipid bilayers comprised of M6a were found to exhibit a cation channel-like function (White & Lagenaur, 1993). More recently, Mukobata and coworkers reported that exogenous expression of M6a in PC12 cells imparts a heightened sensitivity to NGF-induced neuronal differentiation accompanied by increased intracellular calcium (Mukobata *et al.*, 2002). The increased calcium conductance induced by NGF was abolished via inhibition of PKC activity, but unaffected by pharmacological blockade of voltage-

gated calcium currents, suggesting that M6a may represent a novel, NGF-sensitive calcium channel.

A new perspective on potential M6a function has arisen from studies identifying protein interactions between M6a and the μ -opioid receptor (MOR). Yeast two-hybrid analysis revealed a potential interaction between MOR isoform 1 (MOR1) and a peptide fragment from the C-terminus of M6a (Liang, 2004). Moreover, M6a was found to co-precipitate with MOR1 and bioluminescent resonant energy transfer (BRET) performed in living HEK 293 cells providing further evidence that these two proteins interact *in vitro*. While the nature of this proposed interaction remains to be investigated in detail, the observation that M6a expression is correlated with the internalisation of MOR-1 suggests that M6a may be involved in opioid receptor desensitisation and the development of opioid tolerance (Liang, 2004; Wu, 2006).

Chronic stress and neuronal remodelling

Prior to the publication of Hans Selye's seminal paper: "A syndrome produced by diverse noxious agents" (1936) the term 'stress' was applied exclusively in the field of engineering to describe a pressure or tension that exerts physical force on a structure. In a biological sense, any condition challenging the physical/psychological homeostasis of an organism may be defined as a stressor: the cascade of physiological and behavioural reactions to stress directed at restoring homeostatic balance are referred to collectively as the 'stress response'. Acute exposure to stress triggers a rapid succession of physiological responses designed to enhance an organism's ability to react effectively to environmental threats, the most prominent of which include an activation of the hypothalamo-pituitary-adrenal (HPA) axis and

sympathetic nervous system. However, systems mediating the response to severe or chronic stress are vulnerable to dysregulation, the consequences of which are known to contribute to the etiology of stress-related mood disorders such as major depressive disorder (MDD) (Holsboer *et al.*, 1984). Neuroimaging studies have revealed volumetric and metabolic abnormalities in depressed patients, most prominently within limbic brain regions, including the hippocampus, and in the prefrontal cortex (Sheline *et al.*, 1996; Drevets *et al.*, 1997; Botteron *et al.*, 2002). Significantly, animal models of depression utilising chronic stress paradigms exhibit comparable changes in brain structure and provide an experimental platform on which the mechanisms underlying these changes can be investigated. Increasing evidence indicates that structural alterations resulting from stress or depressive illness represent a dramatic reorganisation occurring at the level of neuronal processes rather than a reduction in the total number of neurons: stereological analyses have found no evidence of substantial neuronal death in brain regions exhibiting stress-induced reductions in brain volume (Vollmann-Honsdorf *et al.*, 1997) and structural changes induced by stress exposure are ultimately reversible (Sandi *et al.*, 2003).

Hippocampus

The deleterious effects of chronic stress on hippocampal-dependent cognitive function have been described in numerous species (Luine *et al.*, 1994; Conrad *et al.*, 1996; Krugers *et al.*, 1997; Joels *et al.*, 2004) and have been temporally and functionally correlated with localised changes in neuronal morphology (Sandi *et al.*, 2003). Neuronal remodelling has been observed in all major hippocampal cell types in response to severe or prolonged stress, however, CA3 pyramidal neurons appear especially sensitive and exhibit dramatic reductions in the length and branching

complexity of apical dendritic arborizations in animals subjected to chronic restraint (Watanabe *et al.*, 1992a; Magarinos *et al.*, 1996), psychosocial stress (Sousa *et al.*, 2000; McKittrick *et al.*, 2000; Fuchs *et al.*, 2001), and corticosteroid treatment (Woolley *et al.*, 1990; Watanabe *et al.*, 1992b). The extent of remodelling is proportional to the duration of stress exposure: structural changes in CA3 dendrites are first detectable 10-14 days after the onset of stress, maximally expressed by 21 days, and (Magarinos & McEwen, 1995b). Stress-induced dendritic atrophy in the CA3 region is fully reversed after 10-20 days of stress-free recovery (Sandi *et al.*, 2003).

Furthermore, specialised spine-like structures, termed 'thorny excrescences', receiving afferent mossy fibre (MF) input on the proximal portions of CA3 apical dendrites (Gonzales *et al.*, 2001; see **Fig.2**), exhibited reduced length and volume in chronically restrained rats as revealed by quantitative electron microscopic analysis (Stewart *et al.*, 2005). However, the effects of stress are not limited to postsynaptic structures. Ultrastructural analyses have detected reductions in the plasmalemmal surface area and synaptic density of giant MF terminal inputs to CA3 pyramidal neurons in rats exposed to chronic unpredictable stress (Sousa *et al.*, 2000). Moreover, MF terminals of chronically restrained rats exhibit a marked reorganisation of synaptic vesicles consistent with modified neurotransmitter release: the total population of synaptic vesicles is significantly depleted and remaining vesicles exhibited an increased packing density in proximity to active zones (Magarinos *et al.*, 1997). The data indicates that the efficacy transmission at the MF-CA3 synapse is susceptible to modification by exposure to severe or prolonged stress.

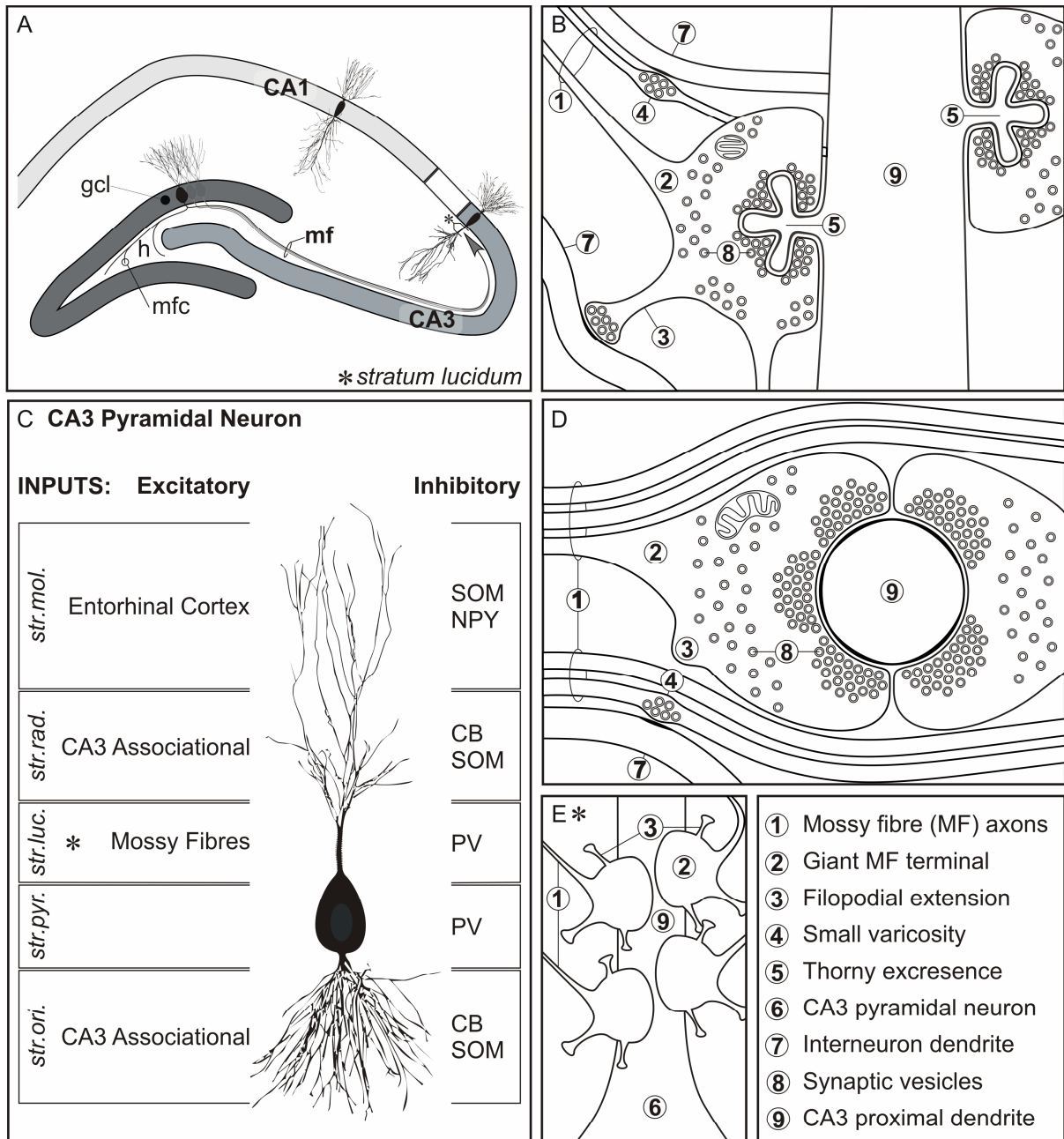


FIGURE 2. Synaptic organization of the hippocampal mossy fibre pathway. The major hippocampal cell types including dentate granule cells (**gcl**) and pyramidal neurons belonging to the CA3 and CA1 subfields are shown in their respective locations in the dorsal hippocampus (**A**). The mossy fibre pathway, comprised of mossy fibre collaterals (**mfc**) innervating neuronal targets in the hilus (**h**) and mossy fibre projections (**mf**) innervating CA3 pyramidal neurons in the *stratum lucidum* (*), represents the primary route of information transfer between granule cells of the dentate gyrus and CA3 pyramidal neurons of the hippocampus (**A**). An illustrative summary of synaptic inputs and their laminar organization in CA3 pyramidal neurons: mossy fibre terminals are shown to target *stratum lucidum* (**C**; according to Matsuda *et al.*, 2004). Detailed schematics illustrating the divergence and target specificity of mossy fibre terminals, presented in two perpendicular planes of focus (**B**, **D**; modified according to Acsady *et al.*, 1998). Schematic illustrating multiple giant mossy fibre terminals making synaptic contact with proximal dendrites of CA3 pyramidal neurons in the *stratum lucidum* (**E**).

Prefrontal cortex

The perception of stress and its 'controllability' relies on prefrontal cognitive processes that ultimately determine the susceptibility of an organism to the adverse effects of chronic stress exposure and the extent to which they are manifest (Kim & Diamond, 2002; Shors *et al.*, 1989). The medial prefrontal cortex (mPFC) is selectively activated in response to psychological and social stressors (Van Eden, 2000; Thierry, 1976; Ostrander *et al.*, 2003; Kuipers *et al.*, 2003). The mPFC of rats comprises three anatomically and functionally distinct cortical subareas: the anterior cingulate cortex (AC) represents the dorsomedial aspect of the PFC, whereas the prelimbic (PL) and infralimbic (IL) cortices collectively represent the ventromedial PFC (Van Eden *et al.*, 1990; Uylings *et al.*, 2003). Tract tracing studies have exposed a vast and highly interconnected network connecting the mPFC with both cortical and subcortical nuclei (Uylings *et al.*, 2003; Vertes *et al.*, 2004) and deficits induced by anatomically restricted prefrontal lesions suggest that nuclei within the mPFC function cooperatively to direct adaptive behavioural responses to emotive stimuli via the integration of cognitive and visceral information (Fryszak & Neafsey, 1991; Sullivan & Gratton, 1999; Dalley *et al.*, 2004). Vastly simplified, the functions assigned to subareas of the mPFC include temporal ordering and sequencing of motor behaviour, limbic / cognitive processes supporting working memory, and autonomic modulation (visceromotor) for the AC, PL, and IL, respectively (reviewed by Vertes, 2004). Moreover, the results of recent studies indicate that subareas of the mPFC may be functionally lateralised with respect to modulation of the autonomic and endocrine response to chronic stress since focal lesions within the right, but not left, mPFC significantly attenuated stress-induced HPA activation and the development of gastric pathologies (Sullivan & Gratton, 1999).

Pyramidal neurons in layer II-III of the rat mPFC undergo significant remodelling of apical dendritic arborizations in response to chronic restraint (Cook & Wellman, 2004; Radley *et al.*, 2004) or chronic corticosterone administration (Wellman *et al.*, 2001). Stress-induced alterations in neuronal morphology were observed in mildly restrained rats as early as 7 days following the initiation of stress (Brown *et al.*, 2005). Moreover, dendritic retraction (Wellman, 2001) and alterations in spine morphology (Seib & Wellman, 2003) are induced in response to daily vehicle injections alone. Pyramidal neurons within the mPFC therefore exhibit an exceptional sensitivity to stress indicating that neuronal networks governing our perception of stress are particularly vulnerable to adverse environmental stimuli and their deleterious effects on neuronal morphology (Perez-Cruz *et al.*, in press).

Stress regulation of gene expression

The induction and maintenance of adaptive neuronal plasticity relies upon a neuron's ability to respond to environmental challenges via the induction and regulated maintenance of an altered pattern of gene expression. Under stressful conditions gene expression is susceptible to regulation via multiple, potentially interactive, mediators of the stress response.

In both stress and depressive disorders structural modifications are primarily observed in brain regions in which glucocorticoid receptors are abundantly expressed, such as the hippocampus (Sapolsky *et al.*, 1983) and medial prefrontal cortex (Diorio *et al.*, 1993; Helm *et al.*, 2002). Glucocorticoid receptors belong to the nuclear receptor (NR) family (Lozovaya & Miller 2003; Evans. 1988) of ligand-induced transcription factors and are expressed in two forms: i) mineralocorticoid receptors (Type I; MR) exhibit a high affinity for glucocorticoids; and ii) glucocorticoid receptors (Type II; GR) bind glucocorticoids with low affinity and are principally

activated during stress-induced hypercortisolaemia (Reul & de Kloet, 1985). Activated GRs translocate to the nucleus where they either dimerise, recruit transcriptional co-activators (Meijer, 2002), and promote transcription at glucocorticoid response elements (GREs), or alternatively remain as monomers and potentially interfere with non-receptor transcription factors to repress expression of their respective gene targets (Auphan *et al.*, 1995). Moreover, stress regulates GR mRNA expression in the hippocampus (Sapolsky *et al.*, 1984; Meyer *et al.*, 2001).

Stress has also been shown to regulate gene expression by influencing the transcriptional activity of cyclic AMP response element binding protein (CREB) (Trentani *et al.*, 2002). Phosphorylated CREB recruits the transcriptional coactivator CREB binding protein (CBP) (Chrivia *et al.*, 1993) and modulates transcription at promoters containing cAMP response elements (CRE) (Sheng *et al.*, 1990). Intracellular signalling cascades facilitating CREB phosphorylation are sensitive to various cellular conditions including cAMP elevations and growth factor reception (West *et al.*, 2001). Stress-induced perturbations in monoamine transmission (reviewed by Flügge *et al.*, 2004) influence intracellular cAMP concentrations modulated via the G protein receptor-coupled stimulation/inhibition of adenylate cyclase. Receptor tyrosine kinases (trk) mediate growth hormone signalling (eg. BDNF, NGF) via downstream activation of the mitogen activated protein kinase/extracellular signal-regulated kinase) MAPK/ERK signalling pathway (Trentani *et al.*, 2002; Grewal *et al.*, 1999). CREB is one of several nuclear targets phosphorylated by activated MAPK. The transcriptional activity of BDNF and NGF is also susceptible to regulation by chronic stress (Alfonso *et al.*, 2005b)

Stress regulates M6a expression in the hippocampal formation

In a previous study investigating differential gene expression regulated by chronic corticosterone treatment in the hippocampus of male tree shrews (*Tupaia belangeri*), membrane glycoprotein M6a was identified via subtractive hybridisation as a potentially stress-responsive gene (Alfonso *et al.*, 2004a). Real-time RT-PCR analysis subsequently confirmed that hippocampal M6a expression is reduced in psychosocially stressed tree shrews (Alfonso *et al.*, 2004b) and chronically restrained mice (Alfonso *et al.*, 2006). Moreover stress-induced reductions in M6a expression were sensitive to chronic antidepressant treatment: the tricyclic antidepressant clomipramine and selective serotonin reuptake enhancer tianeptine were found to inhibit the effects of stress on M6a expression (Alfonso *et al.*, 2004b, 2006).

Chronic restraint stress paradigm

Repetitive restraint has proved a reliable stress paradigm that has been extensively used in studies investigating stress-induced changes in neuronal morphology and their consequences on brain function (Watanabe *et al.*, 1992; Wellman, 2001; Radley *et al.* 2004; Prez-Cruz *et al.*, in press). Restrained animals exhibit a reduced rate of body weight gain compared to controls resulting from a glucocorticoid-mediated shift in energy metabolism favouring fat loss from both central and peripheral adipose stores (Gomez *et al.*, 2002). The HPA axis response to chronic restraint is characterised by progressive habituation: the initial peak in plasma glucocorticoid levels initiated at the onset of daily restraint gradually declines over subsequent days of stress (McEwen 2001; Watanabe *et al.*, 1992a; Magarinos & McEwen, 1995b). The cumulative effects of chronic restraint stress include impaired cognitive performance in spatial recognition tasks (Luine *et al.*, 1994), increased anxiety and enhanced fear conditioning (Conrad *et al.*, 1999), and increased aggression (Wood *et al.*, 2003).

Aims of the thesis

The main objective of the present thesis was to investigate the potential involvement of membrane glycoprotein M6a in the development of stress-induced changes in neuronal morphology. Accordingly, experiments were designed to characterise; i) the *in vivo* localisation of M6a, and ii) the effects of chronic stress on M6a expression within specific brain regions.

In the first part of the thesis, *in situ* hybridisation was used to map the pattern of M6a mRNA expression in the brain. Since strong hybridisation signals were detected in the hippocampus and prefrontal cortex, immunocytochemistry was performed to characterise the precise localisation of M6a protein within these regions. M6a exhibited a pattern of immunoreactivity consistent with expression in axonal membranes, but not dendrites. To further define the subcellular distribution of M6a, immunofluorescent experiments were conducted with a selected range of axonal (calbindin, NF200) and synaptic markers (synaptophysin, VGlut1, VGAT, SV2B) to identify potential sites of colocalisation.

In the second part of the thesis, the effects of stress on M6a expression were investigated in rats subjected to 21 days chronic restraint stress. Previous studies have identified M6a as a stress-responsive gene in the hippocampus. Therefore, expression levels were quantified by real-time RT-PCR analysis within the hippocampus, prefrontal cortex, and cerebellum to investigate whether the regulatory effects of stress on M6a expression are confined to the hippocampus or conserved within other brain regions. Primers distinguishing N-terminus variants of M6a (isoforms Ia & Ib) were designed to identify potential isoform-specific effects of chronic stress on M6a expression. Quantitative *in situ* hybridisation was subsequently performed to correlate stress-induced changes in M6a expression to specific neuronal populations within the hippocampus (dentate granule cells, CA3

pyramidal neurons) and prefrontal cortex (infralimbic, prelimbic, and anterior cingulate cortices). Finally, to investigate the effects of chronic stress and antidepressant treatment on M6a protein expression, quantitative immunocytochemistry was performed in the hippocampus of rats subjected to chronic psychosocial stress and fluoxetine treatment.

Methods and materials

Experimental animals

Experimental animals (adult male Sprague-Dawley rats and C57/Bl mice; Harlan-Winkelmann, Borchon, Germany) were used for *in situ* hybridisation and immunocytochemical studies, respectively. M6a knockout mice (generously donated by Prof. Klaus-Armin Nave, Göttingen) were used to validate antibody specificity in immunocytochemical experiments. In transgenic mice, the transcriptional capacity of M6a is negated via the insertion of a neomycin selection cassette bearing a translational stop codon into exon 2 of the M6a gene. Animals were housed under standard 12 hr: 12 hr light/dark conditions (lights on 07:00; unless otherwise specified in stress experiments). The ambient temperature was maintained at 21°C. Food and water was available *ad libitum*. All animal experiments were in accordance with the European Communities Council Directive of November 24, 1986, (86/EEC) and with the National Institutes of Health Guide for the Care and Use of Laboratory Animals, and were approved by the Government of Lower Saxony, Germany.

In situ hybridisation

Cloning of rat M6a cDNA

Adult male Sprague-Dawley rats were decapitated and brains were rapidly removed. Hippocampus and cerebellum were dissected, immediately frozen in liquid nitrogen, and stored at -80°C until RNA isolation. Dissected brain regions were weighed and homogenised in Trizol[®] reagent (Life Technologies, Rockville, MD, USA) using a teflon-coated glass dounce. Total RNA was isolated from Trizol[®] homogenates according to the manufacturers' instructions. Synthesis of cDNA from mRNA transcripts was performed by reverse transcription using Superscript II RT

(Invitrogen™, life technologies, New York, USA) with poly (dT)₁₅ primer. Rat M6a cDNA was amplified by PCR with gene-specific primers as follows; forwards primer: 5'-TGG AAG AAG GAC AGA CAC and reverse primer: 5'-TTG AGC CGC TCT TTA GAG. PCR product was verified by electrophoresis in 1% agarose gel and subsequently isolated according to the Gel Extraction Kit protocol (Qiagen, Hilden, Germany). M6a was ligated into p-Drive plasmid (Qiagen, Hilden, Germany) and transformed into 50 µl competent *E.Coli* by electroporation at 1.6 kV (Genepulser®II; Bio-Rad, Hercules, USA). Transformed bacteria were incubated in 450 µl SOC medium for 60 min at 37°C, plated on LB agar, then incubated overnight at 37°C. Positive colonies (white) were selected according to blue/white galactosidase activity and grown overnight at 37°C in 2 ml ampicillin-treated LB medium: 1ml LB medium was withheld as glycerol stock and 1 ml was used to verify the plasmid construct via restriction digest and PCR with M6a- specific primers.

Tissue preparation and hybridisation procedure

Frozen brains from adult male Sprague-Dawley rats were cut on a cryostat and 10 µm cryosections were thaw-mounted on gelatin-coated slides. Sections were dried at room temperature for 20 min, fixed in 4% buffered paraformaldehyde (PFA, pH 7.2), rinsed in phosphate-buffered saline (PBS), dehydrated through graded alcohols, air dried and frozen at -80°C. Prior to , sections were rehydrated through graded alcohols, fixed in 4% PFA, washed in PBS, acetylated (0.1M triethanolamine, 0.25% acetic anhydride), washed in PBS and dehydrated once again through graded alcohols. Plasmid DNA was linearised and riboprobes were synthesized with T7 and SP6 RNA polymerases (Promega, Madison, USA) for the antisense and sense probe, respectively, in the presence of 9.25 MBq of ³³P-UTP (ICN; specific activity 3000 Ci/mmol) for 1 h at 37°C. Probes were purified with Microspin S-400 HR

columns (Amersham Pharmacia, Freiburg, Germany) and buffer (50% deionised formamide, 10% dextran sulphate, 0.3 M NaCl, 1 mM EDTA, 10 mM Tris-HCl, pH 8.0, 500ug/ml tRNA, 0.1 M dithiothreitol, and 1 x Denhard's solution) was added to give a final probe activity of 5×10^4 CPM. mixture containing probe was denatured at 70°C for 10 min, cooled to 55°C, and pipetted directly onto sections (80 µl/section). Hybridisation was performed at for 18 hrs at 43°C. Sections were subsequently washed in 4 x SSC (0.6 M NaCl, 0.06 M citric acid), 2 x SSC, and 0.5 x SSC for 10 min each at 37°C. Following 1 hr incubation at 70°C in 0.2 x SSC, sections were washed twice in 0.1 x SSC, once at 37°C and again at room temperature, for 10 min each. Sections were dehydrated through graded alcohols, air dried, and exposed to Bio-Max MR film (Amersham Pharmacia, Freiburg, Germany) for 4 days at 4°C. Films were developed and fixed with GBX (Kodak, Rochester, New York, USA).

Quantitative in situ hybridisation

Quantitative *in situ* hybridisation was performed on adult male Sprague-Dawley rats exposed to 21 days chronic restraint stress. Brains were prepared for cryosectioning under mRNAse-free conditions and serial cryosections were made through the entire brain of both stressed (n=9) and control animals (n=9). The collection of sections for began at specific anatomical coordinates (Paxinos & Watson, 1986; Bregma position -1.88 mm and 3.7 mm for hippocampus and prefrontal cortex, respectively) and anatomically matched sections from both control and stress groups were thaw-mounted on gelatine-coated slides. Hippocampal cryosections were mounted in pairs (one control, one stress section per slide) and prefrontal cortical sections in groups of four (two control and two stress sections per slide). Individual slides thus held sections from each experimental group to minimise variations in conditions between experimental groups. Following (as described above), sections were coated with

photoemulsion (Kodak NBT) at 42°C, dried for 90 min at RT, and stored for 7 weeks at 4°C in a light-proof container to permit exposure of the photoemulsion to hybridised riboprobes. Exposed slides were developed at 15°C for 5 min (developer; Kodak D-19), rinsed twice briefly in H₂O, fixed 5 min at RT (fixer; Kodak polymax). Sections were counterstained with methyl-green (M-8884, Sigma), cleared in xylol, and coverslipped with Eukitt mounting medium (Bodo Schmidt GmbH, Goettingen). Hybridised sections were visualised with a 40x objective (NA=1.4) under a light microscope (Axioscope, Zeiss, Jena, Germany) and silver grain quantification was performed on a cell by cell basis using the silver grain count function of MCID Basic software (Imaging Research Inc., St. Catharines, Ontario, Canada). ROD (relative optical density) threshold intensities were optimised to exclusively detect exposed silver grains: background interference from methyl-green was eliminated by the introduction of a green filter during quantification. The number of pixels contained within an individual silver grain was determined and used in subsequent calculations to extrapolate the number of silver grains contained within the area of interest. Circular counting masks of 125 pixel diameter were used to estimate silver grain number in hippocampal region CA3 and in prefrontal pyramidal neurons, whereas a smaller counting mask of 100 pixel diameter corresponding approximately to the size of a granule neuron was used in the dentate gyrus to accommodate the tight packing of neurons within the granule cell layer. Boundaries delineating cortical laminae and the subareas of the prefrontal cortex were determined according to the published anatomical findings of Gabbott *et al* (1997). Silver grain estimates were calculated from 2 sections per animal and 100 neurons per section within the dentate gyrus, CA3 pyramidal cell layer, anterior cingulate cortex, prelimbic cortex, and infralimbic cortex.

Immunocytochemistry

Immunocytochemistry was performed on adult male; i) Sprague-Dawley rats, ii) C57/Bl mice, and iii) M6a knockout mice (generously donated by Prof. Nave, Göttingen). Animals received a lethal dose of GMII ("Goettinger Mischung II" containing ketamine, 50mg/ml; xylazine, 10mg/ml; atropine, 0.1 mg/ml) and were transcardially perfused with 4% paraformaldehyde in 0.1 M PBS (pH 7.2). Brains were removed, washed overnight in 0.1 M PBS (pH 7.2) and immersed in cryoprotectant (2% DMSO, 20% glycerol in 0.125 M PBS, pH 7.2) until saturation. Coronal cryosections (40 μ m) were collected through prefrontal and hippocampal regions, washed briefly in PBS (0.9% NaCl in 0.1 M PBS, pH 7.2), and quenched of endogenous peroxidase activity by 30 min incubation at RT in 0.5% H₂O₂ in distilled water. Sections were washed in 0.5% Triton X-100 (TX-100) in PBS, blocked for 1 hr at RT (5% normal rabbit serum and 0.5% TX-100 in PBS), incubated 48 hr at 4 °C with monoclonal anti-M6a rat IgG (Medical & Biological Laboratories Co., Ltd, Japan; 1:1000 dilution in 1% normal rabbit serum and 0.5% TX-100 in PBS), and washed again. Sections were then incubated in blocking solution (5% normal rabbit serum and 0.5% TX-100 in PBS) for 1 hr at RT, incubated with biotin-conjugated rabbit anti-

Table 1. Antibody list

Antibody	Host	Type	Manufacturer	Optimal dilution
Anti-M6a	Rat	Monoclonal	MBL	1:1500
Anti-Calbindin D-28k	Rabbit	Polyclonal	Chemicon	1:1000
Anti-NF200	Rabbit	Polyclonal	Sigma	1:2000
Anti-MAP-2	Mouse	Monoclonal	Sigma	1:2000
Anti-Synaptophysin	Rabbit	Polyclonal	Synaptic Systems	1:1000
Anti-VGLUT1	Rabbit	Polyclonal	Synaptic Systems	1:1000
Anti-VGAT	Rabbit	Polyclonal	Synaptic Systems	1:1000
Anti-SV2B	Rabbit	Polyclonal	Synaptic Systems	1:1000
Anti-rMOR1	Rabbit	Polyclonal	ABCAM	1:500

rat IgG (DAKO, Hamburg, Germany; 1:400 dilution in 1% normal rabbit serum and 0.5% TX-100 in PBS) for 4 hr at RT, then washed overnight at 4 °C. The sections were treated with streptavidin-HRP (DAKO, Hamburg, Germany; 1:200 dilution in 1% normal rabbit serum and 0.5% TX-100 in PBS) for 2 hr at RT, washed in PBS and then again in 0.05 M Tris/HCl (pH 7.2) prior to DAB detection (DAB detection was performed according to the manufacturer's instructions; DAB-Kit, Vector Laboratories, USA). Sections were washed in 0.05 M Tris/HCl (pH 7.6) and again in 0.1 M PBS prior to xylol clearance, dehydration, and coverslipping with Eukitt mounting medium (Bodo Schmidt).

Immunofluorescence experiments

Immunofluorescent experiments were performed on C57/Bl mice. M6a knockout mice served as negative controls to validate antibody specificity. Antibodies used in double-labelling experiments were applied sequentially and blocking steps were performed using normal serum of host species from which respective secondary antibodies were derived. Cryosections (40 µm) from prefrontal cortex and hippocampus were rinsed in normal PBS (33 mM phosphate, pH 7.4), quenched of endogenous peroxidase activity by 30 min incubation at RT in 0.5% H₂O₂ in distilled water, and blocked (3% normal serum, 0.3% TX-100 in PBS) 1 hr at 4°C. Sections

Table 2. Antibodies and fluorophores used in confocal colocalisation experiments

1° antibody	2° antibody + fluorophore	1° antibody	2° antibody + fluorophore
Anti-M6a	Alexa 488-coupled goat anti-rat IgG	Anti-calbindin D-28k Anti-VGAT Anti-SV2B	Alexa 568-coupled goat anti-rabbit IgG
	Alexa 594-coupled donkey anti-rat	Anti-NF200 Anti-synaptophysin Anti-VGLUT1 Anti rMOR1	Alexa 488-coupled goat anti-rabbit IgG
		Anti-MAP-2	Alexa 488-coupled goat anti-mouse IgG

were then incubated in monoclonal anti-M6a (1:1500; in 3% normal serum, and 0.3% TX-100 in PBS) for 24 hr at 4°C, washed, and incubated in secondary antisera (Alexa Fluor IgG; 1:300; in 0.3% TX-100 in PBS) for 2 hr in a light proof container. Efforts were taken to minimise light exposure in all subsequent steps. Sections were washed, incubated in primary antisera directed against the second targeted antigen (see **Table 1** for appropriate dilutions; in 3% normal serum, 0.5% TX-100 in PBS), washed, and then incubated 2 hr at 4°C in secondary antisera (1:300; in 0.5% TX-100 in PBS). Sections were floated/mounted on Histobond slides in PBS, allowed to dry overnight at 4°C, then coverslipped with fluorescent mounting medium (DAKO).

Confocal laser scanning microscopy

Confocal microscopy was performed with a Zeiss LSM Pascal 5 laser scanning microscope (LSM) equipped with three lasers: i) argon 488 nm, ii) helium/neon 543 nm, and iii) helium/neon 633 nm. Colocalisation experiments were analysed in multiple tracking (multi-track) mode to avoid cross-talk/bleed-through between channels: the excitation and subsequent detection of emitted light was performed sequentially for each fluorophore /channel used in multiple tracking mode. The 543-nm laser was always used with a smaller detection pinhole diameter than the 488-nm laser to obtain the same optical slice thickness (slice thickness typically between 0.5–1.0 µm). The maximum image resolution (D) obtainable with a conventional LSM is determined by the following formula:

$$D = 0.61\lambda / NA$$

where resolution is proportional to the numerical aperture (NA) of the objective and inversely proportional to the wavelength of emitted light (λ) (Born & Wolf, 1999). For Confocal analysis at high magnification images were obtained with an Apochromat

63x oil objective (Zeiss; NA=1.4) and Immersol immersion oil (Zeiss; refractive index = 1.518) permitting a maximum axial resolution ranging between 200-250 nm.

Chronic restraint stress

Male SpragueDawley rats (Harlan-Winkelmann, Borchon, Germany) weighing between 250-300g on arrival were housed individually and maintained on a 12/12 hour light/dark cycle (lights on 19:00) under controlled temperature between 18°C and 22°C. Animals were randomly divided into two groups (Control, 9 animals; Stress, 9 animals) and allowed to habituate to housing conditions and daily handling for 10 days prior to the onset of experimentation. Animals of the 'Stress' group were restrained daily (10 AM - 4 PM) during the dark phase for a total of 21 days in well-ventilated polypropylene tubes without access to food and water. Food was withheld from control animals during the restraint period to ensure that any difference in body weight gain observed between groups was not simply a result of limited food availability. Animals were not physically compressed and did not experience pain. Bodyweights were recorded daily for the duration of the experiment. All animals were weighed and subsequently sacrificed 24 hrs following the last restraint period. Adrenal glands were removed immediately after sacrifice and weighed for analysis of relative adrenal weight. Stress experiments were performed to enable the independent analysis of M6a expression in the brain of chronically restrained rats by i) quantitative RT-PCR and ii) quantitative *in situ* hybridisation.

Quantitative real-time RT-PCR

Total RNA was isolated from individual tissue samples using a modified version of the established Trizol method (Life Technologies, Rockville, MD, USA). Modifications improving the yield of isolated RNA included a 30 sec sonification step and the addition of linear acrylamide (5µg/ml) to Trizol homogenates. DNaseI digestion was performed to eliminate potential DNA contaminants and total RNA was purified using phenol/isoamyl/chloroform and subsequent isopropyl/sodium acetate precipitation. The integrity and quantity of purified RNA was assessed by spectrophotometry and subsequently confirmed with RNA 6000 Nano Labchip technology (Agilent Technologies Sales, Waldbronn, Germany). Complementary DNA (cDNA) was synthesized from mRNA transcripts using oligo (dT)₁₂₋₁₈ primers and Superscript II reverse transcriptase (Invitrogen) according to manufacturers' instructions. Primer Express software v2.0 (Applied Biosystems; Darmstadt, Germany) was used to design gene-specific primers with amplicons ranging between 50-150 bp in length. Primers were initially designed to selectively amplify sequences within the 3'-untranslated region (UTR) of the M6a transcript. Subsequently, isoform-specific primers distinguishing isoforms 1a and 1b of the M6a gene were designed to recognise two variants of M6a encoding N-termini of short and full length, respectively. The intron-exon organisation of murine M6a and M6b genes has been previously described (Werner *et al.*, 2001). M6a isoform 1a encodes a short N-terminal domain, whereas M6a isoform 1b encodes a longer N-terminal domain

Table 3. Primer list for quantitative RT-PCR

Primer Pairs	Forwards	Reverse
M6a 3'UTR	5'-TTCAACGTGTGGACCATCTGC	5'-AGAGATTTGCTCCCTCCACGAG
M6a Isoform 1a	5'-GCCTGCCTGGTCTTTACACTTC	5'-CACTCAAACACCCCATATCCA
M6a Isoform 1b	5'-CCTGAAGAAAGGTAGCCATGGA	5'-GCAGCACTCAAACACCCCTTTT
Cyclophilin	5'-CAAATGCTGGACCCAACACA	5'-TGCCATCCAACCACTCAGTCT

containing a putative PKC phosphorylation site (see **Fig. 1**). Rat ESTs corresponding to M6a isoforms Ia & Ib were identified in the NCBI database and intron-exon boundaries were mapped according to genomic rat DNA (Contig Accession No. NW_001084718). Thus, three types of primers were synthesized for real-time RT-PCR analysis; i) primers recognising the 3'-UTR region of M6a (common to all isoforms of M6a); ii) primers specific for M6a isoform Ia; and iii) primers specific for M6a isoform Ib.

A quantitative analysis of gene expression was performed using the 7500 Real-time PCR (Applied Biosystems, Darmstadt, Germany) in combination with Quantitect SYBR green technology (Qiagen, Hilden, Germany). SYBR green is incorporated into DNA during primer elongation and is designed to emit fluorescence exclusively in double-stranded PCR products. Real-time detection of SYBR green emission therefore provides a quantitative measure of amplicon abundance with respect to the number of amplification PCR cycles. The light cycler was programmed to the following conditions: an initial PCR activation step of 10 min at 95°C, followed by cycling steps; denaturation for 15 sec at 95°C, annealing for 30 sec at 60°C, and elongation for 60 sec at 72°C; these steps were repeated for 40 cycles.

Dissociation curves were generated for all PCR products to confirm that SYBR green emission is detected from a single PCR product (Ririe *et al.*, 1997). To achieve this, the light cycler is programmed to monitor fluorescent SYBR green signals throughout an increasing temperature gradient (65-95°C). Double stranded PCR products generated from specific primer interactions dissociate at a precise temperature (melting point) and are detected as a dramatic reduction in SYBR green emission. Primer dimerisation or non-specific primer interactions may produce multiple PCR products, however, such contamination can be detected as multiple deviations in the dissociation curve dictated by their respective melting points.

Data analysis

During the exponential phase of PCR amplification the abundance of the targeted gene within a given cDNA sample can be extrapolated by applying the formula:

$$X_n = X_0 \times (1 + E)^n$$

where X_n is the concentration of template cDNA at cycle n , X_0 is the initial concentration of template prior to amplification, and E refers to the efficiency of amplification (an E value of 1 corresponds to 100% efficiency; Peirson *et al.*, 2003). Assuming an E value of 1, the SYBR green fluorescent emission (R) measured at a specified threshold cycle (C_t) can be used to determine initial concentration of cDNA templates within a sample:

$$R_0 = R_{C_t} \times 2^{-C_t}$$

R_{C_t} refers to the fluorescent signal detected at the specified cycle threshold (C_t) and R_0 refers to the starting concentration of cDNA templates within the sample. All cDNA samples were analysed in triplicate and normalised to i) a passive reference dye (ROX) included within the SYBR green reagent, controlling for volume differences between individual samples (pipetting errors), and ii) a housekeeping gene (endogenous control), controlling for variations in the initial abundance of cDNA between individual samples. Cyclophilin has been previously identified as an appropriate endogenous control for the study of stress-induced changes in gene expression and was selected as the housekeeping gene in the present study in order to compare results with previous studies investigating the effects of stress on M6a expression in other species (Alfonso *et al.*, 2004b, 2005a). Data was normalised as follows:

$$\% \text{ cyclophilin} = R_{0(M6a)} \times 100 / R_{0(\text{cyclophilin})}$$

Thus, R_0 for M6a was calculated and expressed as a percentage of R_0 cyclophilin for each sample. Samples from stressed and control animals were compared.

Quantitative immunocytochemistry

Quantitative immunocytochemistry was performed to investigate the effects of chronic stress and antidepressant treatment on M6a protein expression in the hippocampal region *stratum lucidum*. Chronic social stress was performed as previously described (Rygula *et al.*, 2006) in the resident-intruder paradigm. Male Wistar rats and Lister Hooded rats served as intruder and resident populations, respectively. Four groups *Control*, *Stress*, *Stress Fluoxetine*, and *Control Fluoxetine* were used to quantify levels of M6a immunoreactivity in mossy fibre terminals within the hippocampal region *stratum lucidum*. The *Control* group was handled on a daily basis with no exposure to stress or drug treatment for the duration of the experimental period. The *Stress* group was exposed to chronic psychosocial stress on a daily basis for 5 weeks and received no drug. The *Stress Fluoxetine* group was stressed for 5 weeks and received chronic fluoxetine treatment via oral administration for 4 weeks beginning after the first week of stress. The *Control Fluoxetine* group was handled for the duration of the experiment and chronically treated with fluoxetine for the final 4 weeks. Fluoxetine was administered orally in doses designed to produce systemic concentrations comparable with the therapeutic range in humans. All animals (n=6/group) were transcardially perfused 24 hr following the last stress exposure and brains were processed for immunocytochemistry (see Methods; Immunocytochemistry). Immunocytochemical detection of M6a was performed on cryosections (40 μm) from all groups under identical conditions. Relative optical density (ROD) of M6a immunoreactive fibres within the *stratum lucidum* was quantified using the MCID Basic software (Imaging Research Inc., St. Catharines, Ontario, Canada). ROD data was collected as follows: 100 estimates/section; 2 sections/animal. Baseline ROD values were measured in the corpus callosum for each section and subtracted from raw ROD estimates.

Statistical analyses

Statistical analysis was performed with GraphPad Prism 4.0 (GraphPad Software., San Diego, USA). All data were tested for normality (95% confidence interval). Statistical analyses and comparisons were performed using two-tailed unpaired Student's *t*-test or two-factorial ANOVA followed by Bonferroni *post hoc* test.

Results

In situ hybridisation

In situ hybridisation performed with ³³P-dUTP labelled riboprobes specific for rat M6a mRNA yielded a distinct pattern of expression with no evidence of non-specific probe interactions (**Fig.3**). Hybridisation performed with 'sense' probes failed to produce specific signals in any brain region examined (not shown). As can be seen in the parasagittal section (**Fig.3; A**), strong hybridisation signals were obtained in the hippocampus (**HIP**), and cerebral cortex (**CTX**), and cerebellum (**CER**).

M6a expression in the hippocampus was detected in both major cell types: granule cells of the dentate gyrus and pyramidal neurons of the CA1-CA3 subfields (**Fig.3; B, C**). Hybridisation signals were specifically confined to regions containing cell bodies (granule cell layer, **gcl**; *stratum pyramidale*, **str.pyr**) and were not detected elsewhere in the hippocampus.

Hybridisation signals within the cerebral cortex exhibited a laminar pattern of expression indicating stronger expression of M6a by neurons in deeper cortical laminae (**Fig.3; A**). Such a laminar distribution of cortical expression was also clearly visible in coronal sections through the prefrontal cortex (**Fig.3; C**). In the prefrontal cortex hybridisation were distributed through multiple nuclei, however, expression appeared strongest in neurons of the piriform cortex (**PIR**) and subareas of the medial prefrontal cortex including the anterior cingulate cortex (**AC**), prelimbic cortex (**PL**), and infralimbic cortex (**IL**). Interestingly, the laminar gradient of cortical M6a expression was less apparent within medial prefrontal cortical subareas due to comparable levels of expression in deep and superficial cortical laminae.

Cerebellar expression of M6a is restricted to neurons within the granule cell layer, whereas hybridisation signals detected in the molecular layer and cerebellar white

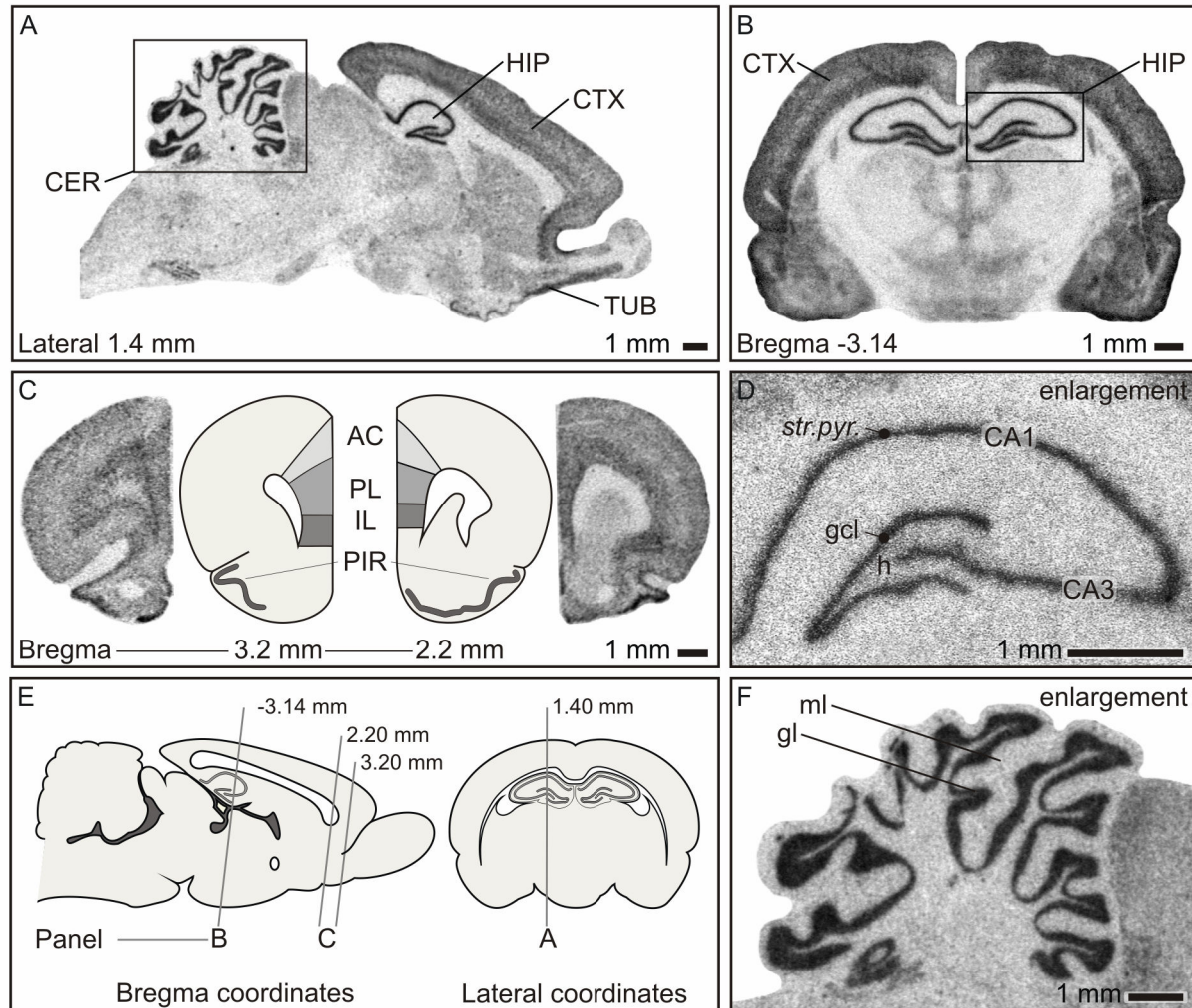


FIGURE 3. M6a mRNA expression in the rat brain as determined by radioactive *in situ* hybridisation with ^{33}P -dUTP-labeled riboprobes. Strong hybridisation signals were detected in the hippocampus (HIP; **A**, **B**, **D**), subregions of the prefrontal cortex (**C**), olfactory tubercle (TUB; **A**) and the cerebellum (CER; **A**, **F**). In the hippocampus (HIP) M6a expression was localized to cell bodies of two specific neuronal populations; i) the granule cell layer (gcl) of the dentate gyrus and ii) pyramidal neurons (pyr) of the CA fields (CA1, CA3). Hybridisation signals in the cortex exhibited a tendency towards stronger M6a expression in deep cortical laminae. M6a mRNA expression in the prefrontal cortex (**C**) was localised to cell bodies in the infralimbic (IL), prelimbic (PL), piriform (PIR) and anterior cingulate (AC) cortices. The neuroanatomical levels according to Paxinos and Watson (1986) are indicated in the lower left corner of each picture: neuroanatomical levels are summarised (**E**). Abbreviations: CER, cerebellum; gl, cerebellar granule cell layer; ml, cerebellar molecular layer; HIP, hippocampus; gcl, dentate granule cell layer; *str.pyr.*, *stratum pyramidale*; CTX, cerebral cortex; AC, anterior cingulate cortex; PL, prelimbic cortex; IL, infralimbic cortex; PIR, cortex piriformis; TUB, olfactory tubercle.

were negligible and attributable to background (**Fig.3; E**). M6a was also found to be strongly expressed in the olfactory tubercle (**Fig.3; A; TUB**). M6a mRNA was not detected in the corpus callosum or other white matter regions.

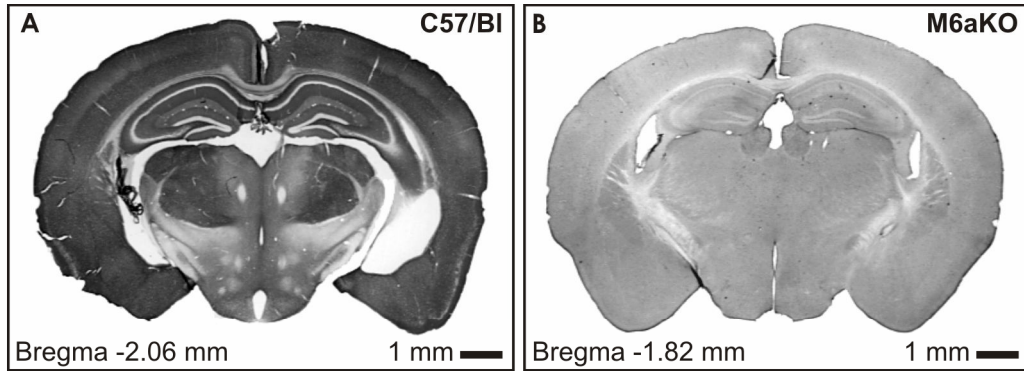


FIGURE 4. M6a immunoreactivity in the mouse brain The specificity of monoclonal anti-M6a antibody was tested by performing immunocytochemistry on control (C57/BI) (**A**) and M6a-knockout (M6aKO) (**B**) mice. A distinct pattern of immunoreactivity is detected in C57/BI mice, whereas no specific staining is observed in M6a-knockout mice. The neuroanatomical levels according to Paxinos and Franklin (2001) are indicated in the lower left corner of each picture.

Immunocytochemistry

Specificity of the M6a antibody

Information on the commercially available monoclonal anti-M6a antibody (MBL) used in this study specified it as being suitable for flow cytometry, however, no information was available regarding the suitability of this antibody for immunocytochemical purposes. To test the specificity of anti-M6a antibody, sections from control (C57/BI strain) (**Fig.4; A**) and M6a-knockout mice (**Fig.4; B**) were processed in parallel for immunocytochemical detection of M6a antigen. In C57/BI mice a distinct pattern of immunoreactivity was obtained. In contrast, M6a knockout mice exhibited only indiscriminate background staining comparable to that obtained in C57/BI sections processed without primary antibody (negative control). These results indicate that anti-M6a antibody is; i) suitable for immunocytochemistry performed on cryosections from transcardially perfused mouse brain, and ii) anti-M6a antibody is specific for the M6a antigen with no indication of non-specific interactions.

Immunocytochemical detection of M6a in the hippocampal formation

In the hippocampus (**Fig.5; A**), M6a immunoreactivity is absent from all major cell body layers: granule cell layer of the dentate gyrus and *stratum pyramidale* of the CA subfields. Interestingly, a laminated pattern of immunoreactivity was detected in the molecular layer of the dentate gyrus, a region comprised of granule cell dendrites and synaptic inputs of both hippocampal and extrahippocampal origin (Amaral & Witter, 1989). M6a immunoreactivity in the middle third of the molecular layer appeared noticeably weaker than that observed in the innermost and outermost laminae. Strong M6a immunoreactivity was detected in the hilus (**h**) and *stratum lucidum* (**Fig.5; B; str.luc.**), regions in which axons of the hippocampal mossy fibre pathway terminate upon hilar targets and proximal dendrites of CA3 pyramidal neurons, respectively (**see Fig.1**). M6a was moderately expressed in *stratum radiatum* (**Fig.5; B; str.rad.**) and *stratum oriens* (**Fig.5; B; str.ori.**) throughout CA subfields, but was not detected within *stratum pyramidale* (**Fig.5; B; str.pyr.**).

Immunocytochemical detection of calbindin in the hippocampal formation

The observed pattern of calbindin immunoreactivity accurately reflects its selective expression within certain neuronal populations in the hippocampus (**Fig.5; C**): dentate granule cell bodies, dendrites, mossy fibre axon projections (**mf**) to the *stratum lucidum* (**Fig.5; D; str.luc.**) and axon collaterals extending into to the hilus are calbindin-immunopositive; CA3 pyramidal cell bodies within *stratum pyramidale* (**Fig.5; D; str.pyr.**), dendrites and axonal projections (Schaffer's collaterals) to CA1 are calbindin-immunonegative; CA1 pyramidal neuron cell bodies, dendrites, and axonal projections to extrahippocampal regions are calbindin-immunopositive (**Fig.5; C; CA1**).

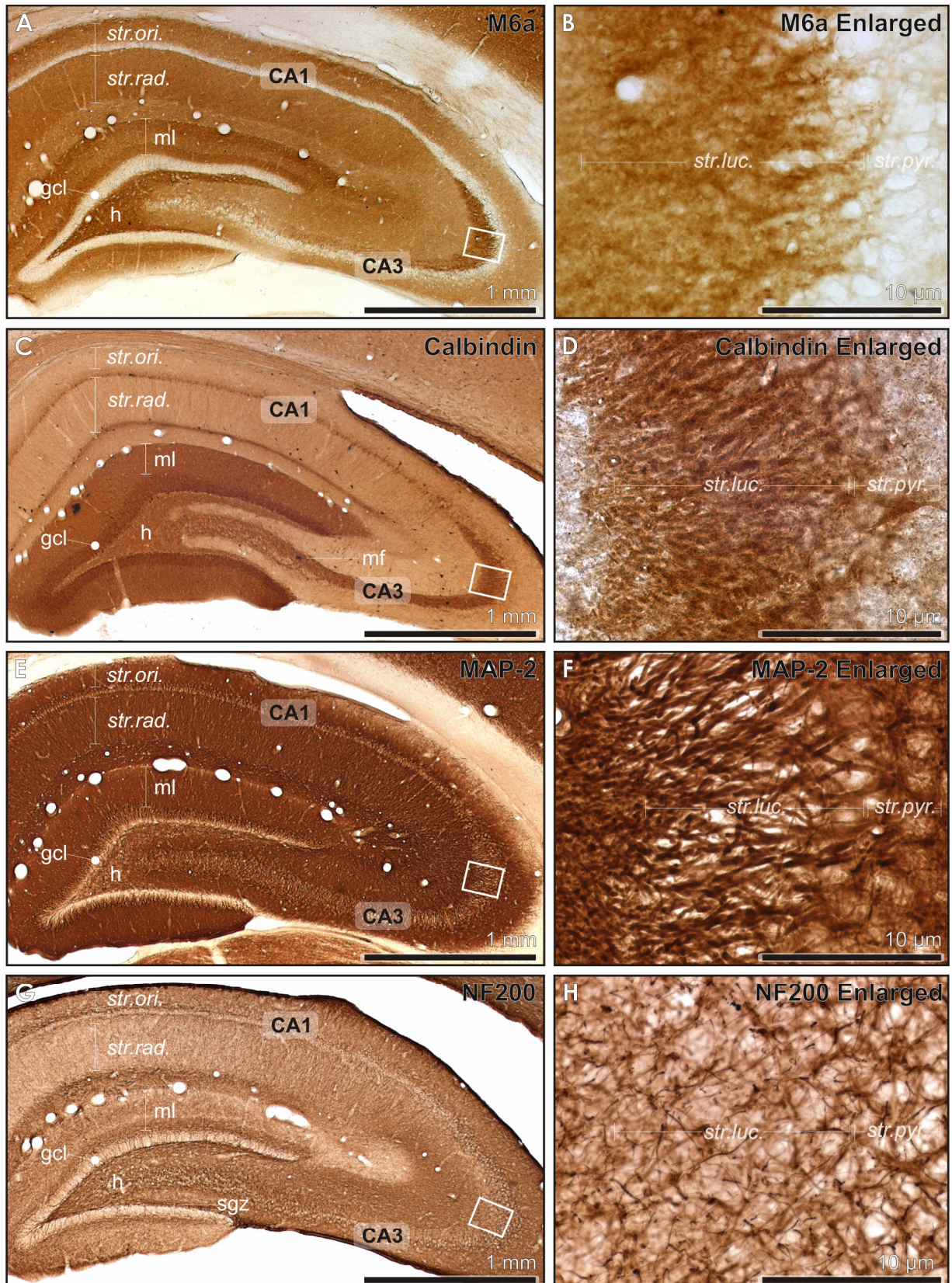


FIGURE 5: A-H. Immunocytochemical detection of different antigens in the hippocampus of the rat. Boxes in the left panel denote the enlargements shown in the right panel.

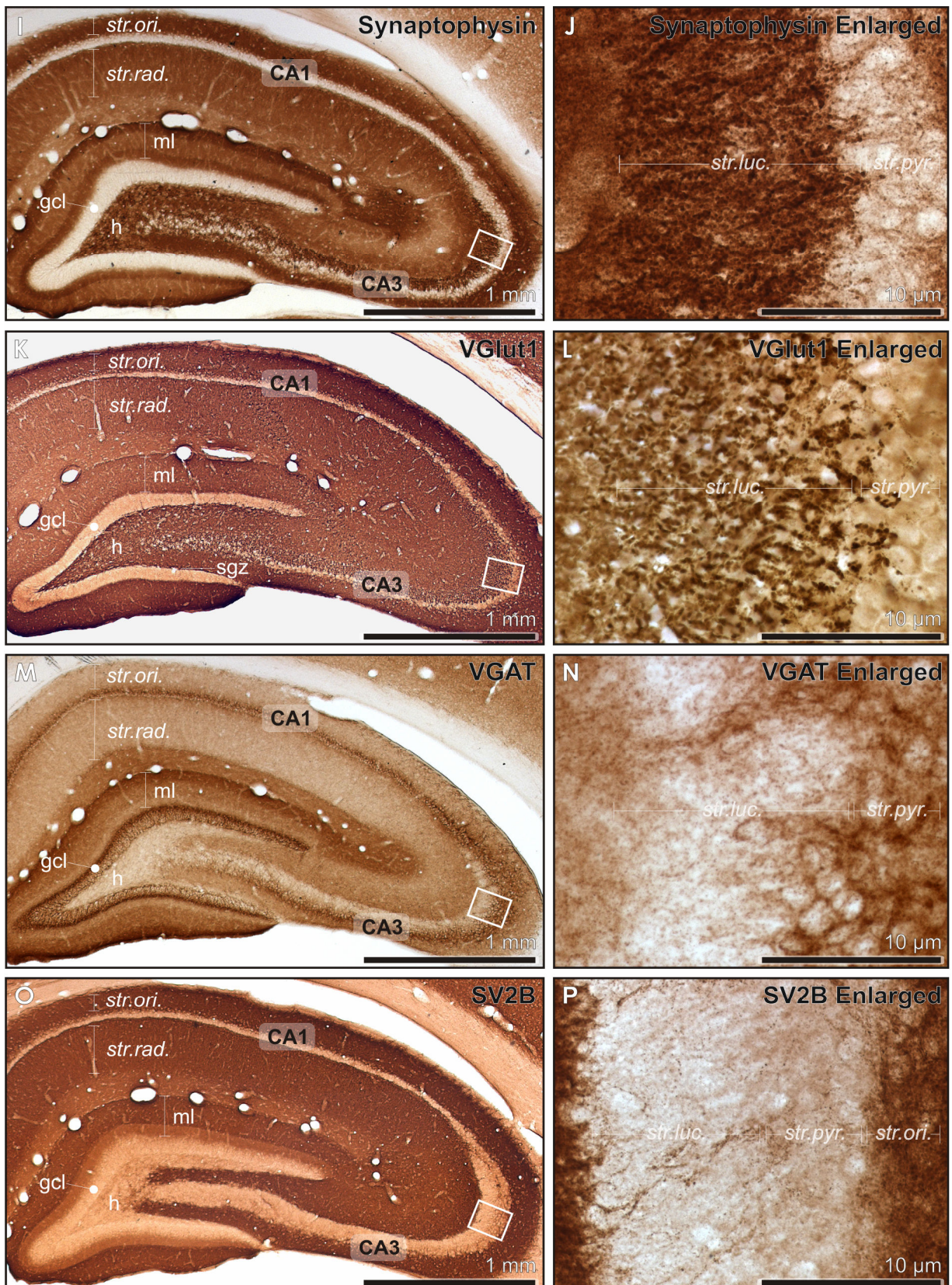


FIGURE 5: I-P. Immunocytochemical detection of different antigens in the hippocampus of the rat. Boxes in the left panel denote the enlargements shown in the right panel.

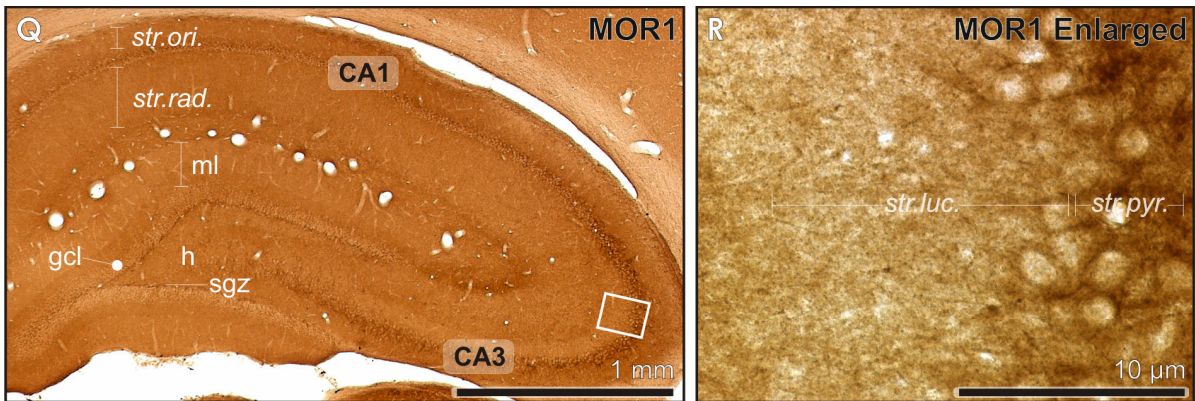


FIGURE 5: Q,R. Immunocytochemical detection of different antigens in the hippocampus of the rat. Boxes in the left panel denote the enlargements shown in the right panel.

A, B: Immunocytochemical detection of glycoprotein M6a in the hippocampus reveals an absence of immunoreactivity in the granule cell layer (**gcl**) and *stratum pyramidale* (**str.pyr.**). Strong immunoreactivity was detected in CA3 *stratum lucidum* (**str.luc.**, **B**) and a laminated pattern of immunoreactivity was detected in the molecular layer (**ml**) of the dentate gyrus: the inner and outer thirds of the molecular layer exhibit a comparable level of stain intensity, whereas immunoreactivity in the middle third appears noticeably weaker.

C, D: Calbindin is a cytoplasmic protein expressed by the granule cells of the dentate gyrus and CA1 pyramidal neurons in the hippocampus (**E**). CA3 pyramidal neurons, however, do not express calbindin. Calbindin immunoreactivity in the dentate molecular layer represents granule cell dendrites (**E**), whereas immunoreactivity in the hilus (**E**) and in *stratum lucidum* (**str.luc.**, **F**) represents mossy fibre (**mf**) axon collaterals and axon projections, respectively.

E, F: Microtubule-associated protein 2 (MAP-2) immunoreactivity is known to be located in dendrites and cell bodies throughout all hippocampal subfields (**C**). MAP-2 immunoreactivity in *stratum lucidum* (**str.luc.**) represents apical dendrites from CA3 pyramidal neurons (**D**).

G, H: Neurofilament protein NF200 immunoreactivity in the hippocampus (**G**) is detected in the molecular layer of the dentate gyrus where it exhibits a laminar gradient with stronger expression detected in the inner portion. Strong immunoreactivity was also observed in the subgranular zone (**sgz**) and hilus. In the CA3 subfield immunoreactivity was found in *stratum radiatum* (**str.rad.**) and surrounding pyramidal cell bodies in *stratum pyramidale* (**str.pyr.**). In contrast, NF200 immunoreactivity was relatively weak in the *stratum lucidum* (**str.luc.**, **H**).

I, J: The distribution of synaptophysin immunoreactivity in the hippocampus (**I**) is prominent in the dentate molecular layer (**ml**), where it exhibits a laminar pattern reminiscent of that observed with M6a; the inner and outer thirds of the molecular layer exhibit a comparable level of stain intensity, whereas immunoreactivity in the middle third appears noticeably weaker. Strong immunoreactivity is also observed surrounding hilar neurons and in *stratum lucidum* (**str.luc.**, **J**), but not at the level of pyramidal cell bodies in *stratum pyramidale* (**str.pyr.**, **J**).

FIGURE 5 continued. Immunocytochemical detection of different antigens in the hippocampus of the rat. Boxes in the left panel denote the enlargements shown in the right panel.

K, L: Immunoreactivity for the vesicular glutamate transporter 1 (VGLut1) in the hippocampus (**K**) is expressed in the inner dentate molecular layer (**ml**), subgranular zone (**sgz**), and surrounding cell bodies of hilar neurons. In *stratum lucidum* (**str.luc.**, **L**) VGLut1 immunoreactivity was detected as large, strongly immuno-positive puncta in close apposition to proximal dendrites of CA3 pyramidal neurons. VGLut1 immunoreactivity was absent from all major cell body layers in the hippocampus.

M, N: Vesicular GABA transporter (VGAT) presents a distinctive pattern of immunoreactivity in the hippocampus consistent with its specificity for synaptic vesicles of GABAergic axon terminals. VGAT immunoreactivity is detected in the dentate granule cell layer (**gcl**) and *stratum pyramidale* (**str.pyr.**) of both CA1 and CA3 subfields (**M**). The dentate molecular layer (**ml**) exhibits a laminar gradient of VGAT immunoreactivity with more intense staining detected in outer laminae. A distinctive absence of immunoreactivity is noticeable within the hilus (**h**) and *stratum lucidum* (**str.luc.**, **N**).

O, P: Synaptic vesicle protein 2B (SV2B) is not expressed by dentate granule cells as is clearly seen by the pattern of SV2B immunoreactivity in the hippocampus (**O**). SV2B immunoreactivity is extremely weak within the hilus (**h**) and inner dentate molecular layer (**ml**) and absent from the dentate granule cell layer (**gcl**), *stratum pyramidale* (**str.pyr.**, **P**), and mossy fibre projections to *stratum lucidum* (**str.luc.**, **P**).

Q, R: Mu-opioid receptor isoform 1 (MOR1) immunoreactivity in the hippocampus (**Q**) is localised to the inner third of the molecular layer (**ml**), granule cell layer (**gcl**), and subgranular zone (**sgz**) of the dentate gyrus. MOR1 is also expressed in *stratum pyramidale* (**str.pyr.**) and appears enriched within the CA3 subfield, however, little evidence of specific MOR1 immunoreactivity was detected in *stratum lucidum* (**str.luc.**, **R**).

Abbreviations: gcl, granule cell layer; ml, molecular layer; sgz, subgranular zone; mf, mossy fibre axons; *str.ori.*, *stratum oriens*; *str.rad.*, *stratum radiatum*; *str.luc.*, *stratum lucidum*; *str.pyr.*, *stratum pyramidale*.

Immunocytochemical detection of MAP-2 in the hippocampal formation

Microtubule-associated protein 2 (MAP-2) immunoreactivity was localised to dendrites of all major hippocampal cell groups including the dentate gyrus, the hilus, and pyramidal neurons of *stratum pyramidale* (**Fig.5; E**). The specificity for dendritic processes is exemplified by the pattern of MAP-2 immunoreactivity observed in the *stratum lucidum* (**Fig.5; F; str.luc.**): proximal dendrites emerging from CA3 pyramidal neurons are clearly stained, whereas regions surrounding the dendrites are immunonegative despite the abundance of mossy fibre axon terminals in this region.

Immunocytochemical detection of NF200 in the hippocampal formation

NF200 has been used in previous studies as a marker of mature myelinated axons (Kriz *et al.*, 2000) and the pattern of NF200 immunoreactivity observed in the present study (**Fig.5; G**) appears to correlate with the previously described distribution of myelinated fibres in the hippocampus of adult rats (Meier *et al.*, 2004). In the molecular layer of the dentate gyrus NF-200 immunoreactivity exhibited a laminar gradient with stronger expression detected within the innermost laminae. Strong immunoreactivity was also observed in the hilus (**Fig.5; G; h**). In the CA3 region immunoreactivity was localised to *stratum radiatum* (**Fig.5; G; str.rad.**) and surrounding pyramidal cell bodies in *stratum pyramidale* (**Fig.5; H; str.pyr.**). In contrast, NF200 immunoreactivity was relatively weak in the *stratum lucidum* (**Fig.5; H; str.luc.**).

Immunocytochemical detection of synaptophysin in the hippocampal formation

Synaptophysin immunoreactivity was clearly distributed in regions of dense synaptic contact (**Fig.5; I**). In the dentate molecular layer, synaptophysin exhibits a laminar pattern of immunoreactivity (**Fig.5; I; ml**) comparable with that observed in M6a-stained sections (**Fig.5; A; ml**): the inner and outer thirds of the molecular layer are intensely stained, whereas immunoreactivity in the middle third appears noticeably weaker. Strong immunoreactivity is also observed surrounding hilar neurons (**h**) and is clearly enriched within the *stratum lucidum* (**Fig.5; J; str.luc.**). Synaptophysin immunoreactivity is detected in *stratum radiatum* (**Fig.5; I; str.rad.**) and *stratum oriens* (**Fig.5; J; str.ori.**) throughout the CA subfields, but was found to be absent from all major cell layers in the hippocampus.

Immunocytochemical detection of VGLUT1 in the hippocampal formation

VGLUT1 (**Fig.5; K**) exhibits a more homogenous pattern of immunoreactivity than that observed with other vesicular proteins tested in this study, a result perhaps attributable to the widespread distribution of glutamatergic terminals in the hippocampus. In the dentate gyrus VGLUT1 immunoreactivity is strongly expressed in the inner molecular layer, subgranular zone, and surrounding cell bodies of hilar neurons (**Fig.5; K; h**). In *stratum lucidum* VGLUT1 immunoreactivity was detected as large, strongly immunopositive puncta in close apposition to proximal dendrites of CA3 pyramidal neurons (**Fig.5; L; str.luc.**). VGLUT1 immunoreactivity was also observed throughout the CA1 subfield in apposition to pyramidal neuron dendrites within the *stratum radiatum* (**Fig.5; K; str.rad.**) and *stratum oriens* (**Fig.5; L; str.luc.**), but was absent from all major cell body layers in the hippocampus.

Immunocytochemical detection of VGAT in the hippocampal formation

VGAT exhibits a distinctive pattern of immunoreactivity in the hippocampus (**Fig.5; M**) consistent with its specificity for synaptic vesicles of GABAergic axon terminals. VGAT immunoreactivity is detected in the dentate granule cell layer (**Fig.5; M; gcl**) and *stratum pyramidale* (**Fig.5; N; str.pyr.**) of both CA1 and CA3 subfields. The dentate molecular layer exhibits a laminar gradient of VGAT immunoreactivity with more intense staining detected in outer laminae. Immunoreactivity is noticeably absent within the hilus (**Fig.5; M; h**) and *stratum lucidum* (**Fig.5; N; str.luc.**), regions targeted by axon collaterals and projections of the glutamatergic mossy fibre pathway, respectively. Examination of *stratum lucidum* at high magnification reveals sparsely distributed VGAT-immunoreactive puncta and, occasionally, beaded axons extending across the border from *stratum radiatum* (**Fig.5; N; str.rad.**).

Immunocytochemical detection of SV2B in the hippocampal formation

The observed pattern of SV2B immunoreactivity accurately reflects the selective absence of SV2B expression within granule cells of the dentate gyrus (**Fig.5; O**). Thus, the terminal portions of mossy fibre collaterals and projections, in the hilus (**Fig.5; O; h**) and *stratum lucidum* (**Fig.5; P; str.luc.**), respectively, appear unlabelled (SV2B-immunonegative). However, at high magnification discrete SV2B-immunoreactive puncta can be seen in *stratum radiatum* (**Fig.5; N**) associated with beaded axons extending across the border to the stratum radiatum. SV2B immunoreactivity is comparable in *stratum radiatum* and *stratum oriens* in all CA subfields with no obvious laminar gradient of intensity.

Immunocytochemical detection of MOR1 in the hippocampal formation

The distribution of hippocampal MOR1-immunoreactivity observed in the present study (**Fig.5; Q**) is consistent with previous descriptions in the rat hippocampus (Arvidsson *et al.*, 1995). MOR1 immunoreactivity is localised to the inner third of the molecular layer (**Fig.5; Q; ml**), the granule cell layer (**Fig.5; Q; gcl**), and subgranular zone of the dentate gyrus (**Fig.5; Q; sgz**). Within the *stratum pyramidale* (**Fig.5; R; str.pyr.**) MOR1 immunoreactivity is abundantly expressed within the CA3 subfield, however, no evidence of specific MOR1 immunoreactivity was detected in *stratum lucidum* (**Fig.5; R; str.luc**).

Confocal laser scanning microscopy

Calbindin immunoreactivity detected by confocal LSM

Calbindin immunoreactivity (**Alexa 568, red**) as detected by confocal microscopy in the *stratum lucidum* (**str.luc.**) is distributed homogeneously throughout the axonal cytoplasm of dentate mossy fibre projections (**Fig.6; B; mf**) and is visualised as calbindin-immunopositive fibres ensheathing unlabelled dendrites of CA3 pyramidal neurons (**d**). M6a (**Alexa 488, green; Fig.6; A**) exhibits a punctate pattern of immunoreactivity and colocalises with calbindin-positive mossy fibres (**yellow; Fig.6; C**). Viewed at high magnification, M6a-immunopositive puncta (diameter ~0.2-0.5 μm) appear superimposed at discrete sites on the plasma membrane of mossy fibre axons (**Fig.6; F**). Strong colocalisation is also observed in the hilus (**yellow; Fig.6; E; h**), indicating that M6a is similarly expressed within the axons of calbindin-positive mossy fibre collaterals innervating hilar targets. No colocalisation was observed with pyramidal neurons in the CA1 subfield (**Fig.6; D; pyr**).

MAP-2 immunoreactivity detected by confocal LSM

In the CA3 subfield of the hippocampus MAP-2-immunoreactivity (**Alexa 488, green; Fig.7; B**) was localised to cell bodies (**pyr**) and dendrites (**d**) of CA3 pyramidal neurons. Apical dendrites emerging from CA3 pyramidal neurons intersect the plane of focus and thus regularly appear in cross section at this anatomical level of the dorsal hippocampus. In the *stratum lucidum* (**str.luc.**) M6a-immunoreactive mossy fibres (**Alexa 594, red**) are detected as parallel, fibre-like structures possessing a lengthwise orientation in the medio-septal direction (**Fig.7; A; mf**). M6a immunoreactivity was not detected in the *stratum pyramidale* (**str.pyr.**). M6a is visible as small immunoreactive puncta situated in apposition to MAP-2-labelled granule

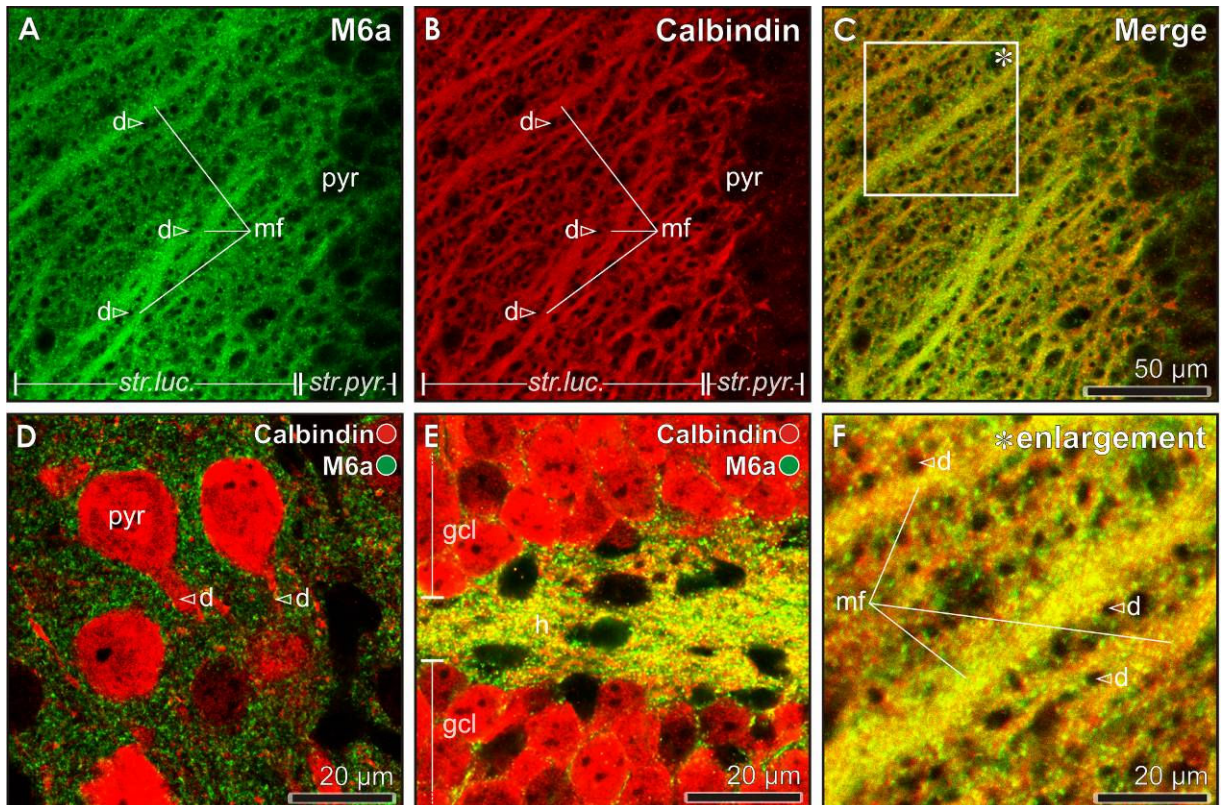


FIGURE 6. Immunolocalisation of M6a (Alexa 488, **green**) and calbindin (Alexa 568, **red**) in the hippocampus and prefrontal cortex.

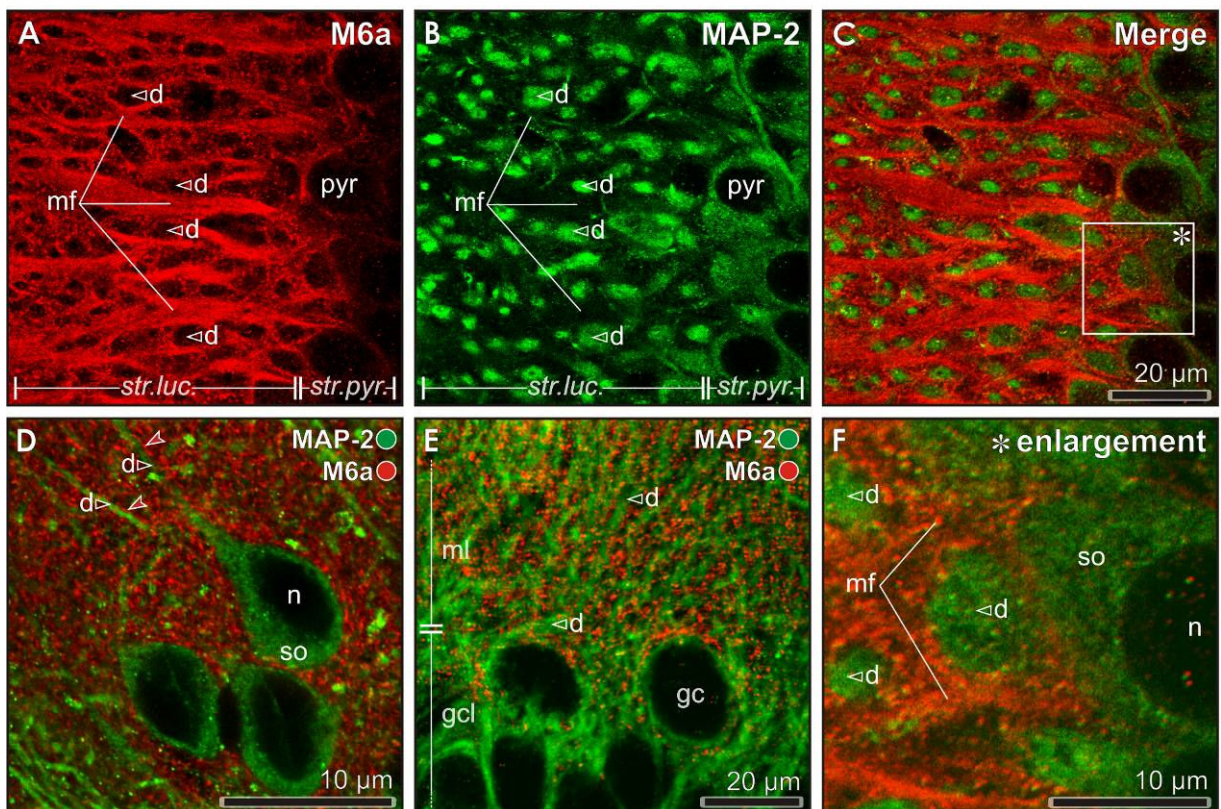


FIGURE 7. Immunolocalisation of M6a (Alexa 594, **red**) and microtubule-associated protein 2 (MAP-2) (Alexa 488, **green**) in the hippocampus and prefrontal cortex.

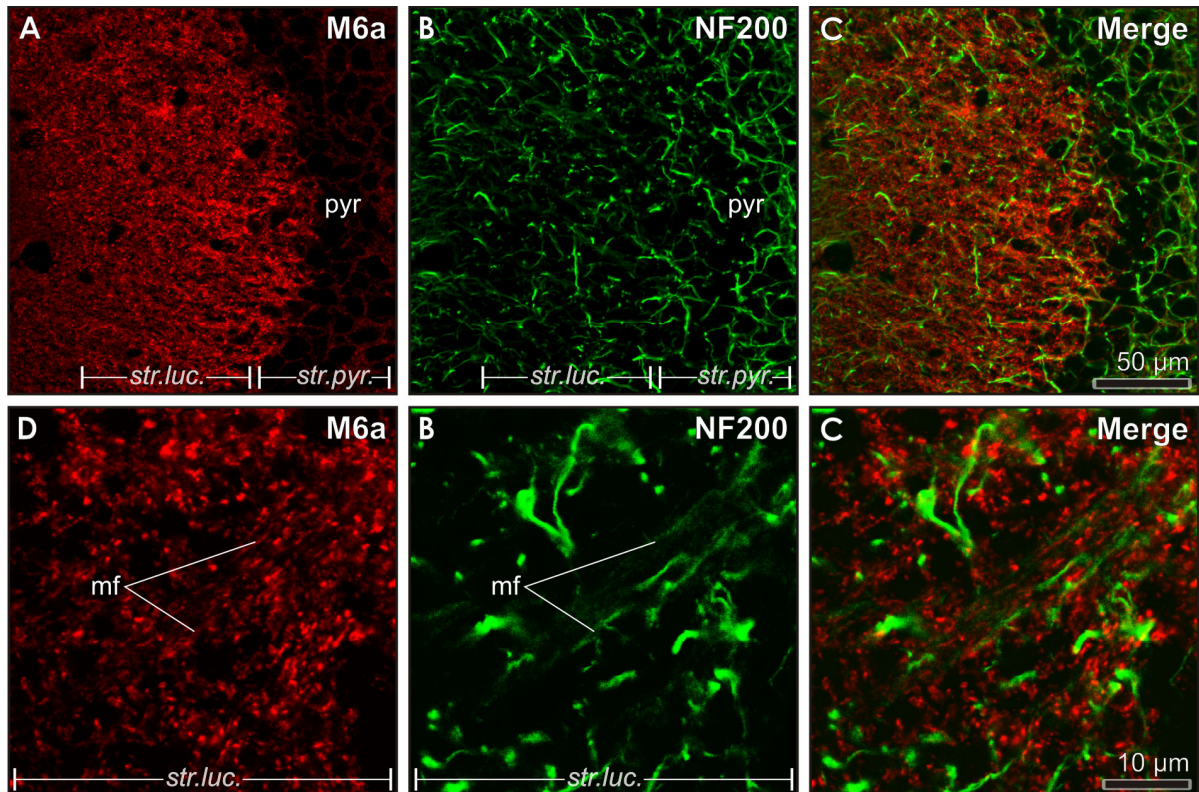


FIGURE 8. Immunolocalisation of M6a (Alexa 594, **red**) and neurofilament protein NF-200 (Alexa 488, **green**) in *stratum lucidum* of the hippocampus

FIGURE 6. Colocalisation of M6a with calbindin demonstrated with fluorescent antibodies (**A-C**). M6a colocalises with calbindin-immunoreactive mossy fibre projections targeting the proximal dendrites (**d**) of CA3 pyramidal neurons in *stratum lucidum* (**str.luc.**; **A-C, F**). Calbindin immunoreactivity (**B**) appears homogenously throughout mossy fibre projections, as might be expected for a cytoplasmic protein, whereas immunoreactivity for the membrane protein M6a (**A**) exhibits a punctate pattern of expression consistent with the interpretation that M6a is localised in the plasma membrane of mossy fibre axons (**mf**; **A, B, F**). At high magnification M6a immunoreactive puncta are visible at discrete sites of calbindin-immunoreactive mossy fibre projections (**F**, enlargement of the box shown in **C**). Colocalisation observed in the hilus is presumably attributable to M6a localised within the axons of mossy fibre collaterals innervating hilar targets (**D**). M6a does not appear to colocalise with calbindin-immunoreactive pyramidal cell bodies or dendrites in CA1 proper (**D**).

FIGURE 7. M6a and MAP-2 are not colocalised. M6a immunoreactivity in *stratum lucidum* (**str.luc.**) is clearly detected as parallel, fibre-like structures that pass between and surround MAP-2-immunoreactive dendrites (**d**) of CA3 pyramidal neurons (**A-C, F**; enlargement of the box shown in **C**). At this anatomical level of the dorsal hippocampus M6a-immunoreactive structures are oriented in plane with the optical slice, whereas the apical dendrites of CA3 pyramidal neurons are oriented more in the z-direction and thus regularly appear in cross section. Despite a close proximity to one another, M6a and MAP-2 do not colocalise at the level of the cell body or apical dendrites of pyramidal neurons in the CA3 subfield (**C, F**) or granule cells in the dentate gyrus (**E**). In the infralimbic prefrontal cortex M6a-immunoreactive elements come into direct apposition with MAP-2-immunoreactive pyramidal cell bodies and dendrites, but do not colocalise (**D**).

FIGURE 8. NF200-immunoreactive structures in the CA3 subfield of the hippocampus (**B, D**) could be assigned to one of two categories; i) thin, weakly immunoreactive fibres with a parallel orientation detected exclusively within the *stratum lucidum* (**D**); or ii) strongly immunoreactive fibres distributed in proximity to CA3 *stratum pyramidale* (**B; str.pyr.**), and to a lesser extent within *stratum lucidum* (**B; str.luc.**). M6a was detected in close alignment to NF-200-immunoreactive fibres of the first category, which represent presumptive mossy fibre axons (**F**). M6a did not associate with strongly stained NF-200-immunoreactive fibres of the secondary category, which based on location are likely to represent myelinated CA3 associational fibres projecting to targets within the *stratum radiatum*.

FIGURE 9. Colocalisation of M6a with synaptophysin in the hippocampus (**A-C, E, F**) and prefrontal cortex (**D**). Synaptophysin immunoreactivity in *stratum lucidum* (**str.luc.**) exhibits a distinctive 'ring-like' pattern of expression at this level of the dorsal hippocampus (**B**). Such a 'ring-like' pattern results from synaptophysin-positive nerve terminals surrounding immunonegative (dark) dendrites (**d**) which run perpendicularly to the optical slice. The mossy fibre terminals (**mft**) contain the synaptophysin immunoreactive organelles (presumptively vesicles; **F**). The M6a-immunopositive pattern is comprised of parallel, fibre-like structures (**mf**, mossy fibres) that come into close apposition with both dendrites and the synaptophysin-positive vesicles (**C, F**). Colocalisation of M6a and synaptophysin is observed as small puncta located at the periphery of compartments containing clustered synaptophysin-immunopositive vesicles (**mft**; mossy fibre terminals). More sites of colocalisation are found in the CA1 (**E**) subfield and infralimbic cortex (**D**), both of which exhibit small immunoreactive puncta which colocalise in proximity to pyramidal cell bodies and dendrites.

FIGURE 10. Colocalisation of M6a with VGLUT1 in the hippocampus (**A-C, E, F**) and prefrontal cortex (**D**). VGLUT1-immunoreactivity (**B**) in the *stratum lucidum* (**str.luc.**) is virtually identical to that observed with synaptophysin. VGLUT1-immunoreactive mossy fibre terminals (**mft**) ensheath proximal dendrites (**d**) emerging from CA3 *stratum pyramidale* (**str.pyr.**). The mossy fibre terminals contain VGLUT1-immunoreactive organelles (presumptively vesicles; **C, F**). Colocalisation with M6a is observed as small puncta located at the periphery of compartments containing clustered VGLUT1-immunopositive vesicles (**mft**, mossy fibre terminals). In the CA1 subfield of the hippocampus (**E**) and the infralimbic cortex (**D**) more sites of colocalisation are detected in apposition to pyramidal cell bodies and dendrites.

FIGURE 11. Colocalisation of M6a with VGAT in the hippocampus (**A-C, E, F; horizontal section**) and prefrontal cortex (**D**). VGAT immunoreactivity is abundant within *stratum pyramidale* (**str.pyr.**), of both CA3 (**B**) and CA1 (**E**) subfields and is expressed relatively sparsely in *stratum lucidum* (**str.luc.**). Within *stratum lucidum* VGAT-immunoreactive puncta are seen almost exclusively in direct apposition to apical dendrites from unlabeled CA3 pyramidal neurons. Please note that in contrast to the Figs. 6-10 which show coronal sections, CA3 pyramidal dendrites (**d**) are oriented in plane with the optical slice: M6a-immunoreactive fibres are oriented more in the z-direction (**A-C**). Partial colocalisation of M6a and VGAT (**yellow arrowheads; F**) in *stratum lucidum* is detected in proximity to apical dendrites of CA3 pyramidal neurons. colocalisation in the infralimbic cortex (**yellow arrowheads; D**) is detected almost exclusively at the level of the pyramidal cell body.

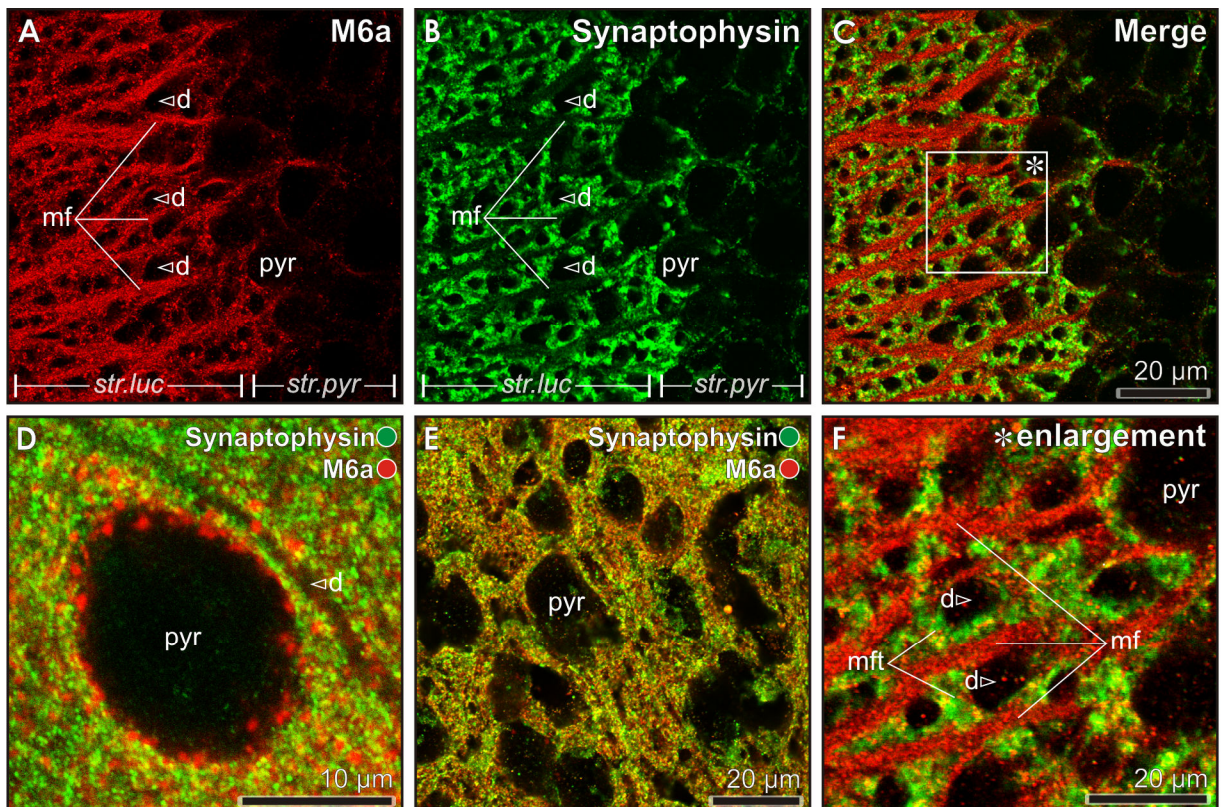


FIGURE 9. Immunolocalisation of M6a (Alexa 594, **red**) and synaptophysin (Alexa 488, **green**) in the hippocampus and prefrontal cortex.

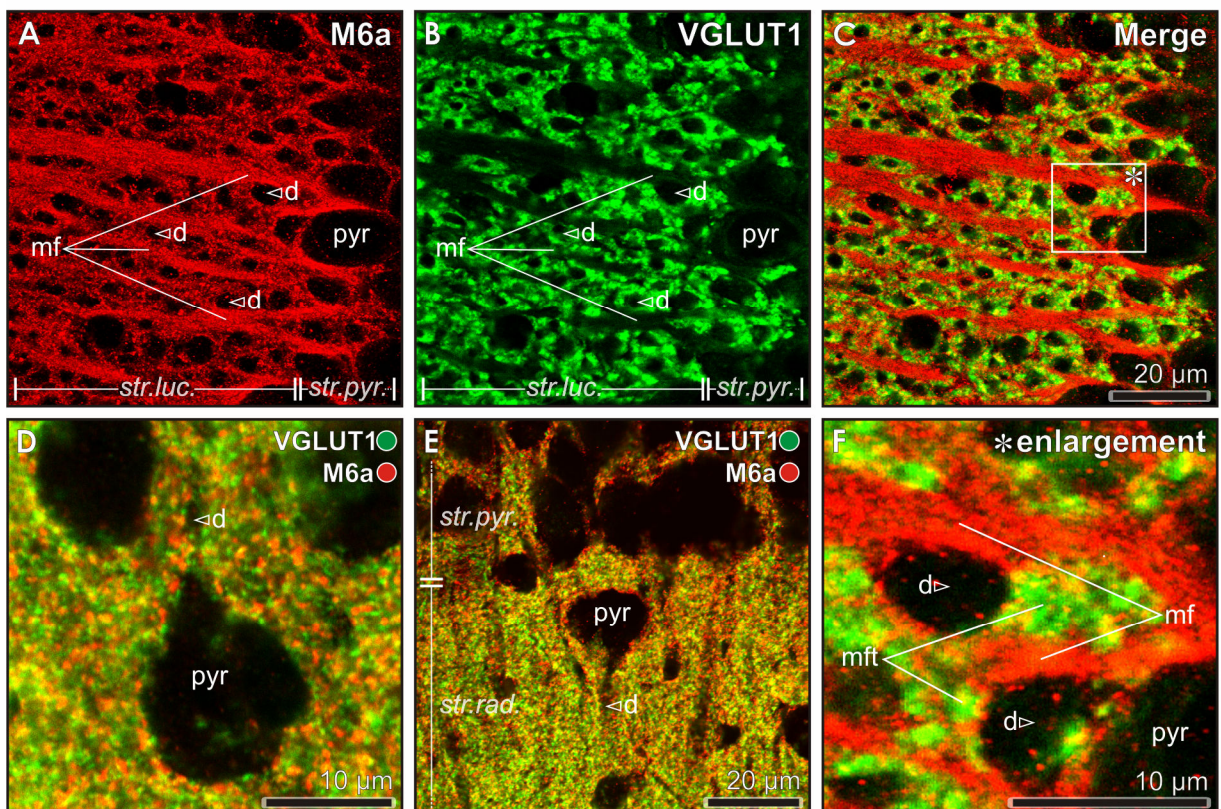


FIGURE 10. Immunolocalisation of M6a (Alexa 594, **red**) and vesicular glutamate transporter 1 (VGLUT1) (Alexa 488, **green**) in the hippocampus and prefrontal cortex.

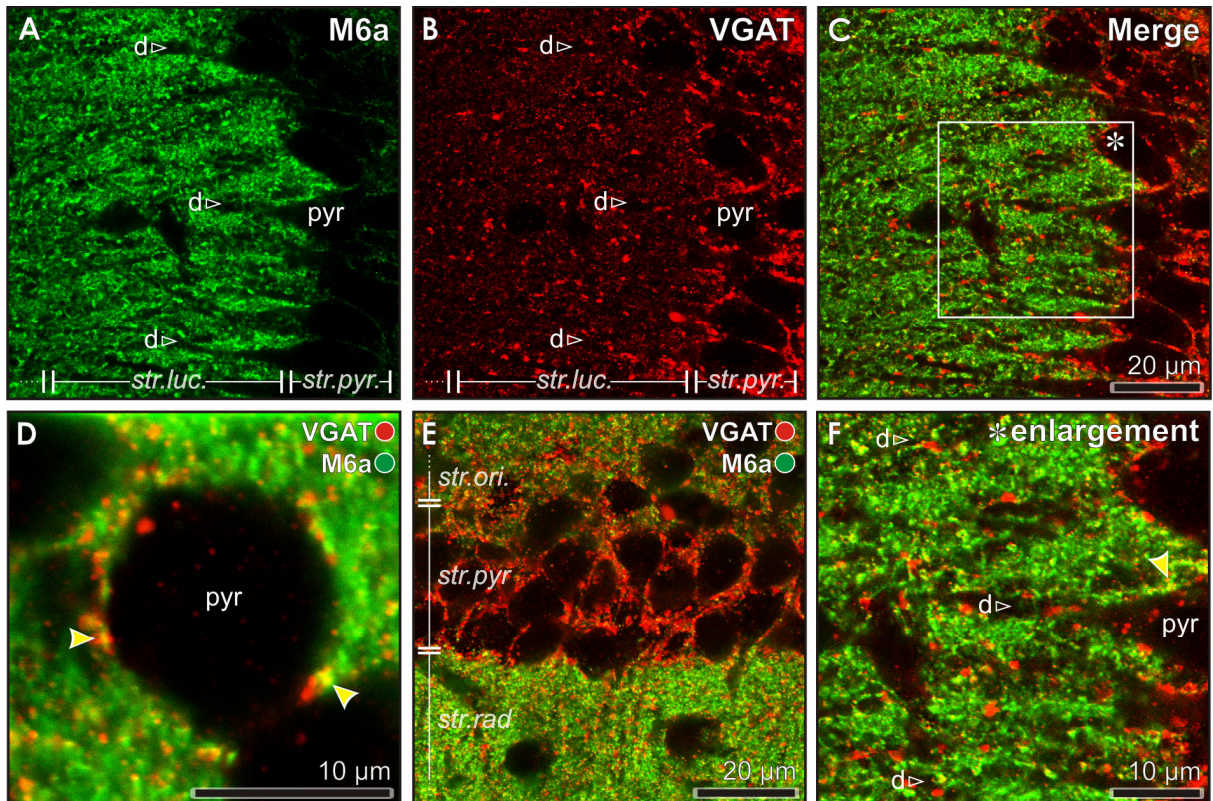


FIGURE 11. Immunolocalisation of M6a (Alexa 488, **green**) and vesicular GABA transporter (VGAT) (Alexa 568, **red**) in the hippocampus and prefrontal cortex.

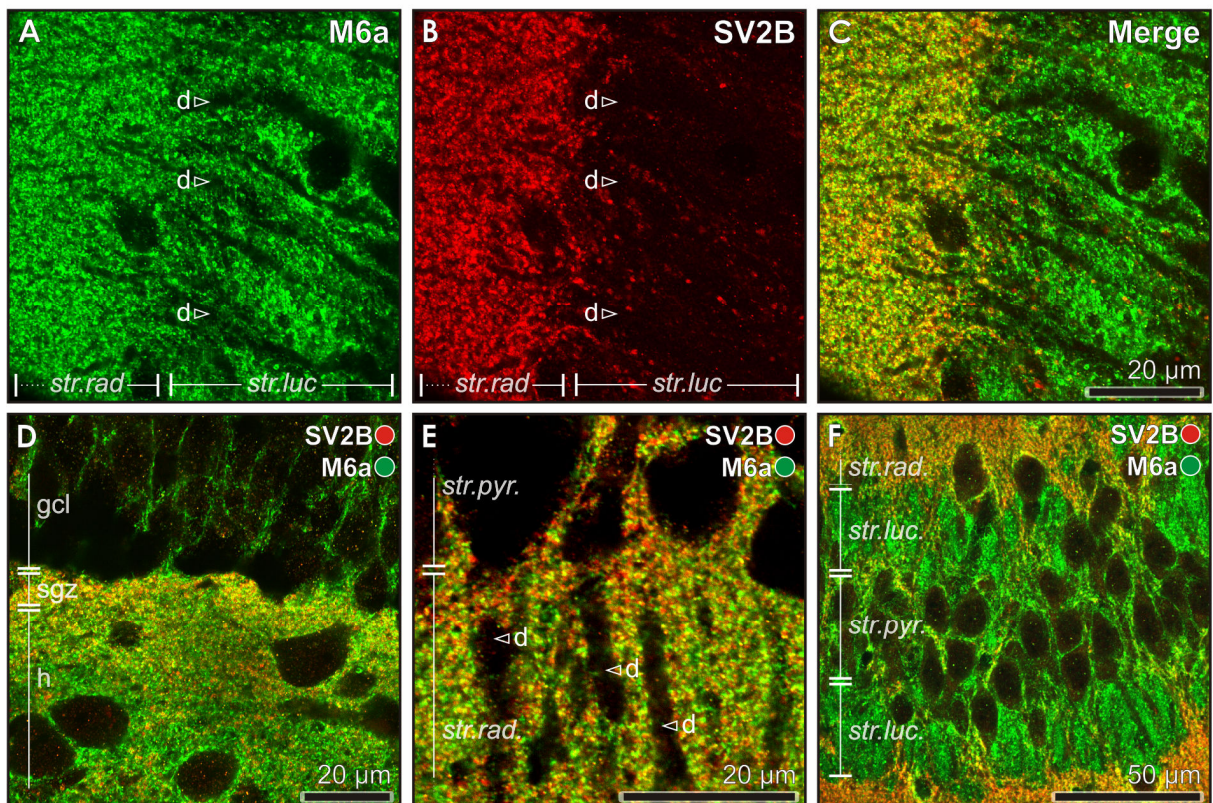


FIGURE 12. Immunolocalisation of M6a (Alexa 488, **green**) and synaptic vesicle protein type 2B (SV2B) (Alexa 568, **red**) in the hippocampus and prefrontal cortex.

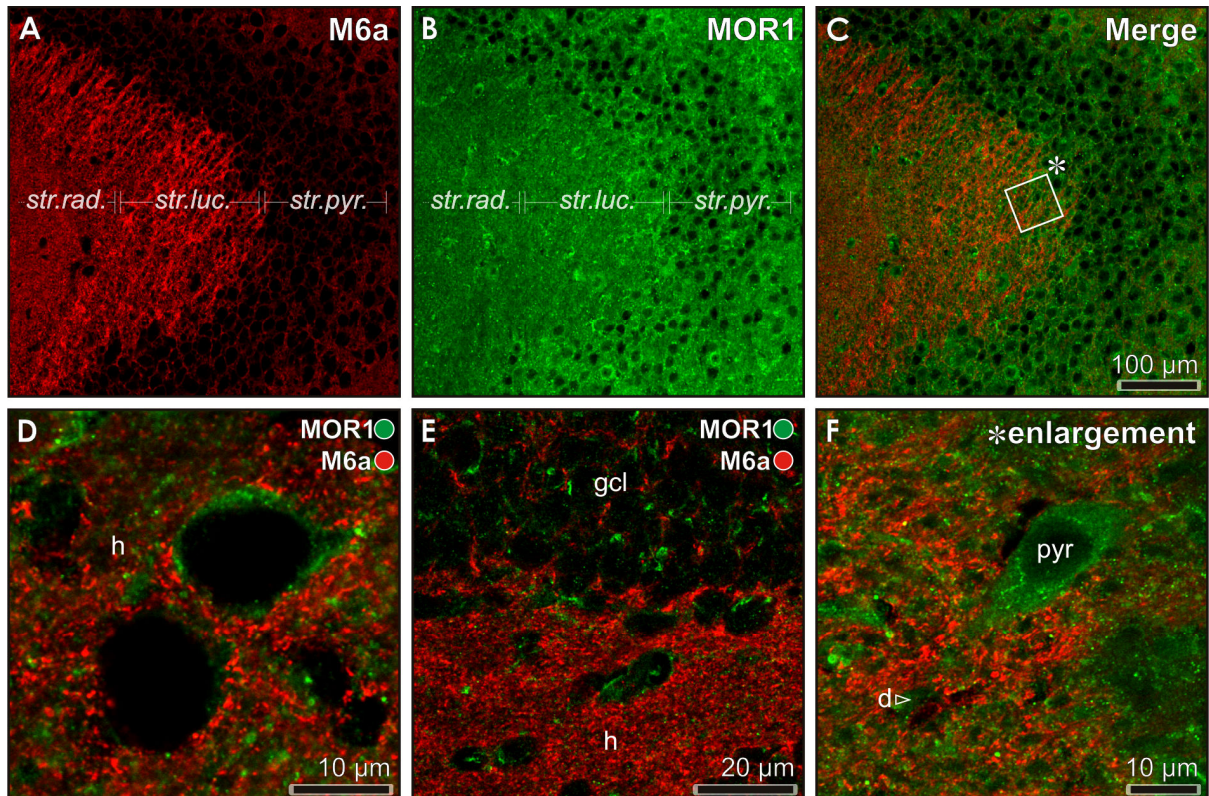


FIGURE 13. Immunolocalisation of M6a (Alexa 594, **red**) and isoform 1 of the μ -opioid receptor (MOR1) (Alexa 488, **green**) in the hippocampus.

FIGURE 12. Colocalisation of M6a with SV2B in the hippocampus (**A-F**). SV2B immunoreactivity is virtually absent from the *stratum lucidum* (**str.luc.**; **B**) since SV2B is not expressed by dentate granule cells and is consequently not detected within synaptic vesicles of mossy fibre terminals. SV2B thus serves as useful means of visualising the border between *stratum lucidum* and *stratum radiatum* (**str.rad.**; **C, F**). SV2B-positive synaptic terminals (non-mossy fibre) innervating the apical dendrites of CA3 pyramidal neurons (**d**; **A-B**) in the *stratum radiatum* colocalise with M6a (**C**). Colocalisation of M6a and SV2B is also observed at the proximal dendrites of CA1 pyramidal neurons (**d**; **E**) and at the subgranular zone (**sgz**) of the dentate gyrus (**D**).

FIGURE 13. Immunolocalisation M6a and MOR1 immunoreactivity in the hippocampus (**A-F**). MOR1 immunoreactivity was localised to the granule cell layer (**gcl**; **E**) of the dentate gyrus, certain neurons within the hilus (**h**; **D-E**), and *stratum pyramidale* (**str.pyr.**) of the CA3 subfield. M6a immunoreactivity is strongly expressed in *stratum lucidum* (**str.luc.**) and absent from *stratum pyramidale* (**A**): MOR1 immunoreactivity is minimally expressed within *stratum lucidum* and strongly expressed in *stratum pyramidale* (**B**). MOR1-positive neurons appeared to receive contacts from M6a-positive presynaptic fibres (**D,F**). No evidence indicating colocalisation of M6a and MOR1 was detected in any hippocampal region analysed.

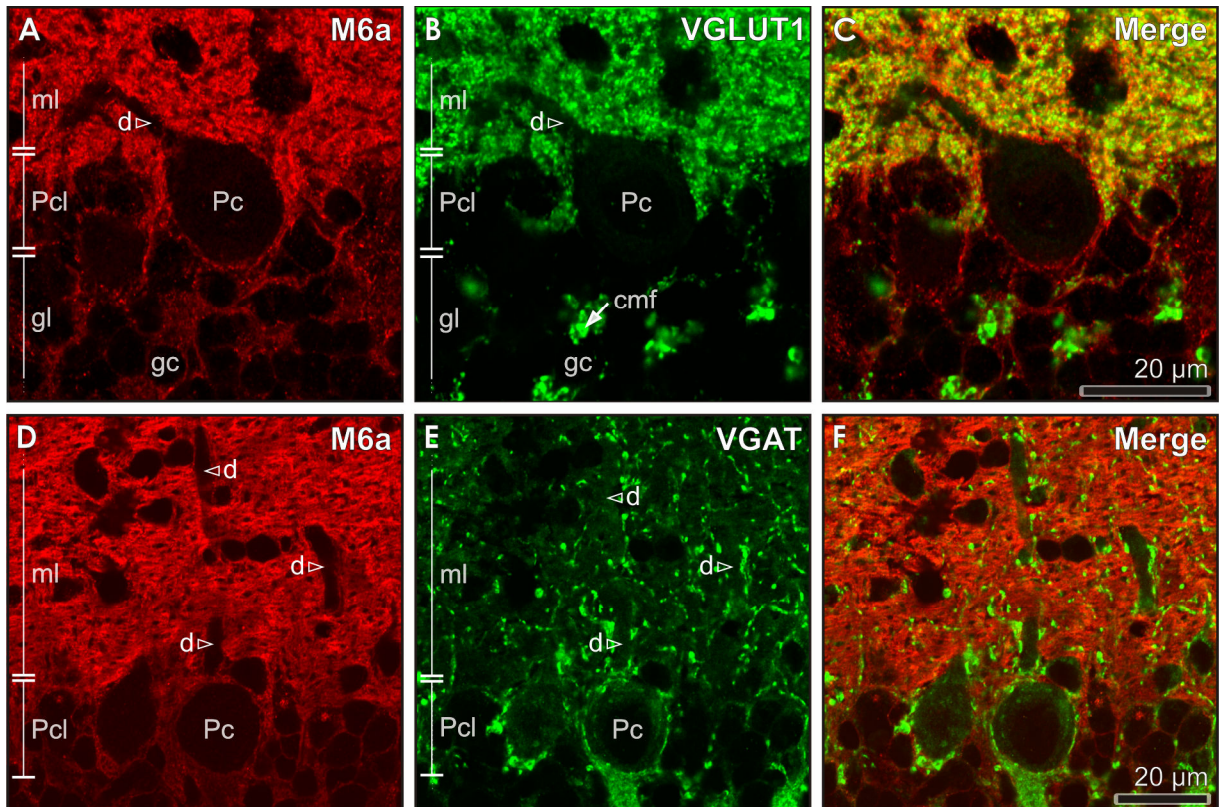


FIGURE 14. Immunolocalisation of M6a (Alexa 594, **red**) and VGLUT1 (Alexa 488, **green**; **A-C**) and VGAT (Alexa 488, **green**; **D-F**) in the cerebellum. M6a is distributed heavily within the cerebellar molecular layer (**ml**), the visualized pattern of immunoreactivity dependent on the relative orientation of the section: M6a-immunoreactive puncta within the molecular layer in panel **A** represent transected parallel fibres, whereas the extensive M6a-positive fibres visualized in panels **D** represent the same axons sectioned longitudinally. M6a colocalises with VGLUT1-positive puncta in proximity to Purkinje cell (**Pc**) dendrites (**d**) within the molecular layer, but not with large cerebellar mossy fibre (**cmf**) terminals in the granule layer (**gl**). M6a did not colocalise with VGAT in any cerebellar region examined.

cell dendrites. Similarly, in the infralimbic cortex punctuate M6a-immunoreactivity is located in direct apposition with MAP-2-immunoreactive pyramidal cell bodies and dendrites (**Fig.7; D**). M6a and MAP-2 immunoreactivity do not colocalise in any region examined despite exhibiting a close proximity to one another.

NF200 immunoreactivity detected by confocal LSM

NF200-immunoreactive fibres in the CA3 subfield (**Alexa 488, green; Fig.8; B**) could be assigned to one of two categories; i) weakly immunoreactive fibres with a parallel orientation detected exclusively within the *stratum lucidum*; or ii) strongly immunoreactive fibres with no apparent laminar preference. M6a immunoreactivity was detected in close alignment to weakly immunoreactive NF-200-immunoreactive fibres in the *stratum lucidum* (**Fig.8; F**), but colocalisation was not observed, perhaps reflecting the distance separating cytoskeletal NF200 and membrane-bound M6a. In contrast, M6a was not associated with the axonal membranes of strongly stained NF-200-immunoreactive fibres, which based on location and morphological characteristics are likely to represent CA3 associational fibres and axons of parvalbumin-containing inhibitory interneurons (Matsuda *et al.*, 2004). These fibres were of a larger calibre and were distributed in proximity to CA3 *stratum pyramidale* (***str.pyr.***), and to a lesser extent within *stratum lucidum* (***str.luc.***).

Synaptophysin immunoreactivity detected by confocal LSM

Synaptophysin immunoreactivity (**Alexa 488, green; Fig.9; B**) in the *stratum lucidum* (***str.luc.***) exhibits a distinctive 'ring-like' pattern of expression when viewed in coronal sections through this anatomical level of the dorsal hippocampus (Bregma -2.06 mm). The 'ring-like' appearance represents synaptophysin-immunopositive synaptic vesicles clustered within mossy fibre terminals in synaptic contact with the apical dendrites of CA3 pyramidal neurons. Unlabelled dendrites (**d**) transect the optical slice and consequently appear as a dark circle, or ellipse, surrounded by synaptophysin immunoreactivity. Along their course, M6a-immunoreactive fibres (**Alexa 594, red; Fig.9; A**) come into close apposition with multiple dendrites (dark round to ovoid structures). Despite their different patterns of immunoreactivity, partial

colocalisation of M6a and synaptophysin is observed, although typically as small puncta situated at the periphery of presumptive mossy fibre terminal membranes. In contrast, colocalisation within synaptophysin-immunoreactive clusters was only rarely observed. In both the CA1 subfield of the hippocampus (**Fig.9; E**) and the infralimbic cortex (**Fig.9; D**) M6a and synaptophysin are seen to colocalise as small immunoreactive puncta in apposition to cell bodies and proximal dendrites of pyramidal neurons.

VGLUT1 immunoreactivity detected by confocal LSM

VGLUT1 immunoreactivity (**Alexa 488, green; Fig.10; B**) in the *stratum lucidum* is highly comparable to that observed with synaptophysin. VGLUT1-immunoreactive mossy fibre terminals ensheath unlabelled dendrites (**d**) emerging from CA3 *stratum pyramidale* (**str.pyr.**) and colocalisation with M6a (**Alexa 594, red; Fig.10; A**) is observed as small puncta located predominantly in close proximity to the membranes of presumptive mossy fibre terminals. In both the CA1 subfield of the hippocampus (**Fig.10; E**) and the infralimbic cortex (**Fig.10; D**) M6a and VGLUT1 are seen to colocalise as immunoreactive puncta in apposition to cell bodies and proximal dendrites of pyramidal neurons.

In the cerebellum VGLUT1 immunoreactivity (**Fig.14; B**) is most heavily distributed in the molecular layer (**ml**), demonstrating the abundance of synaptic contacts made by parallel fibres onto the dendrites of Purkinje cells (**Pc**). In addition, large VGLUT1-immunoreactive cerebellar mossy fibre (**cmf**) terminals are seen making synaptic contact with granule cells (**gc**) within the cerebellar granule layer (**gl**). M6a colocalises with VGLUT1 exclusively within the molecular layer.

VGAT immunoreactivity as detected by confocal LSM

In the hippocampal formation VGAT-immunoreactive puncta (**Alexa 568, red; Fig.11; B**) are predominantly localised in direct apposition to pyramidal cell bodies within *stratum pyramidale* (**str.pyr.**), but are sparsely distributed in *stratum lucidum* (**str.luc.**). M6a does not colocalise with VGAT within the *stratum pyramidale*. Partial colocalisation of M6a and VGAT is occasionally observed within the *stratum lucidum* (**Fig.11; C, D**), CA1 stratum radiatum (**Fig.11; E**), and infralimbic cortex (**Fig.11; D**) in apposition to the cell bodies and proximal dendrites of pyramidal neurons.

In a region composed primarily of GABAergic neuronal subtypes, VGAT is predictably distributed throughout all cerebellar laminae (**Fig.14; E**): within the molecular layer (**ml**) VGAT-positive puncta (presumptive stellate cell terminals) are detected in apposition to the proximal dendritic arbors of Purkinje neurons; within the Purkinje cell layer (**Pcl**) VGAT is detected faintly within the cytoplasm of Purkinje cell somata and as puncta on the cell surface (presumptive basket cell terminals); in the granule layer (**gl**) VGAT-immunoreactive Purkinje axons intersect granule cells, which are surrounded by occasional VGAT puncta (presumptive Golgi cell terminals). M6a and VGAT are differentially distributed and do not colocalise in any cerebellar region investigated.

SV2B immunoreactivity detected by confocal LSM

The pattern of SV2B immunoreactivity (**Alexa 568, red ; Fig.12; B**) in the *stratum lucidum* of mice correlates closely with that observed in DAB stained rat sections. The abundance of SV2B-immunoreactive puncta in *stratum radiatum* ends abruptly at the border to *stratum lucidum*, wherein SV2B-immunoreactivity is virtually undetectable. Colocalisation of M6a (**Fig.12; A**) and SV2B is observed in apposition to distal apical dendrites of CA3 pyramidal neurons throughout the *stratum radiatum*

(**Fig.12; C**). Colocalisation was also observed in the dentate subgranular zone (**Fig.12; D**): M6a immunoreactivity is distributed both in the subgranular zone and in apposition to cell bodies of hilar neurons, whereas SV2B immunoreactivity is restricted to terminals innervating the subgranular zone. In the CA1 subfield of the hippocampus, colocalisation of M6a and SV2B is observed primarily in apposition to proximal apical dendrites extending into *stratum radiatum* (**Fig.12; E**).

MOR1 immunoreactivity detected by confocal LSM

MOR1 immunoreactivity (**Alexa 488, green**) as detected by confocal microscopy in the mouse hippocampal formation was localised to the granule cell layer (**Fig.13; E**) of the dentate gyrus, a subpopulation of neurons within the hilus (**Fig.13; E**), and the *stratum pyramidale* (**str.pyr.**) of the CA3 subfield (**Fig.13; B, C, F**). M6a and MOR1 exhibit contrasting patterns of immunoreactivity in the CA3 subfield of the hippocampus: M6a immunoreactivity is strongly expressed in *stratum lucidum* (**str.luc.**) and absent from the *stratum pyramidale* (**Fig 13; A**), whereas MOR1 immunoreactivity is minimally expressed within *stratum lucidum* and strongly expressed in *stratum pyramidale* (**Fig.13; B**). Neurons expressing MOR1 often appeared to receive contacts from M6a-immunopositive presynaptic fibres representing mossy fibre collaterals in the hilus and mossy fibre projections in the *stratum lucidum*. No colocalisation of M6a and MOR1 was detected in any hippocampal region analysed.

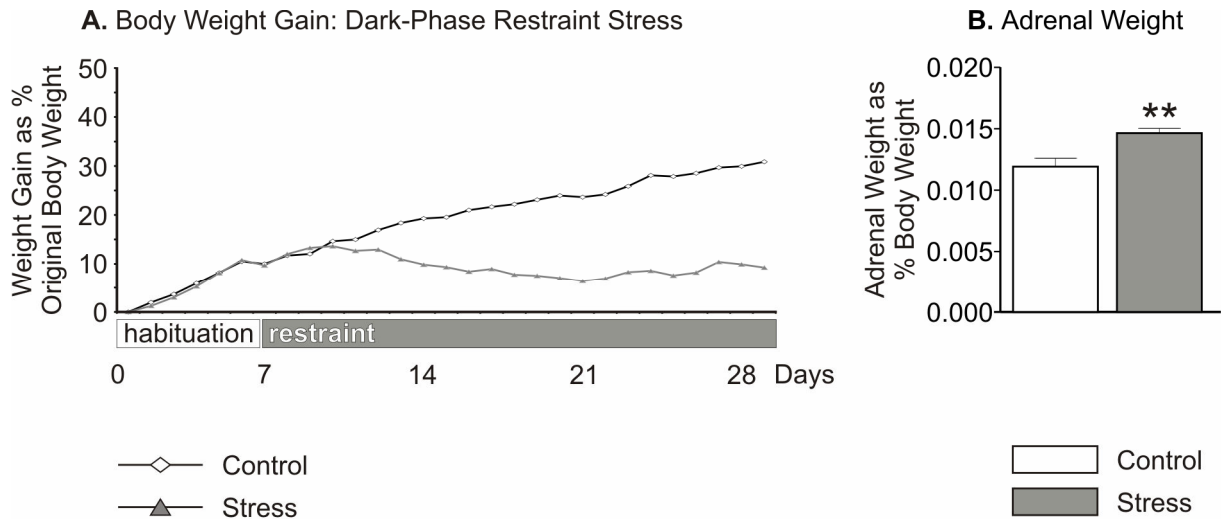


FIGURE 15. Effects of chronic restraint stress on body weight gain and adrenal weight. Animals exposed to chronic stress during the dark phase exhibited reduced body weight gain coinciding with the onset of restraint (**A**) and significantly increased adrenal weight (**B**) compared to controls. Significant differences between Control and Stress groups are indicated by asterisks ($n=9/\text{group}$; two tailed Student's t -test; **, $p<0.01$; *, $p<0.05$). Data are expressed as mean \pm SEM.

Chronic restraint stress

Chronic restraint during the dark phase reliably induced changes in both stress parameters analysed in this study; i) body weight gain (**Fig.15; A**) and ii) relative adrenal weight (**Fig.15; B**). Stressed animals exhibited a significantly reduced body weight gain compared to controls that was first observed after 4 days ($p<0.05$) of restraint stress. The mean body weight gain attained on the day of sacrifice was 31.4% and 9.1% (percentage of initial body weight) for Control and Stress animals, respectively. Stressed animals showed evidence of adrenal hypertrophy as indicated by significantly increased adrenal weight ($p<0.01$; **Fig.15; B**) expressed as a percentage of final body weight.

Real-time RT-PCR

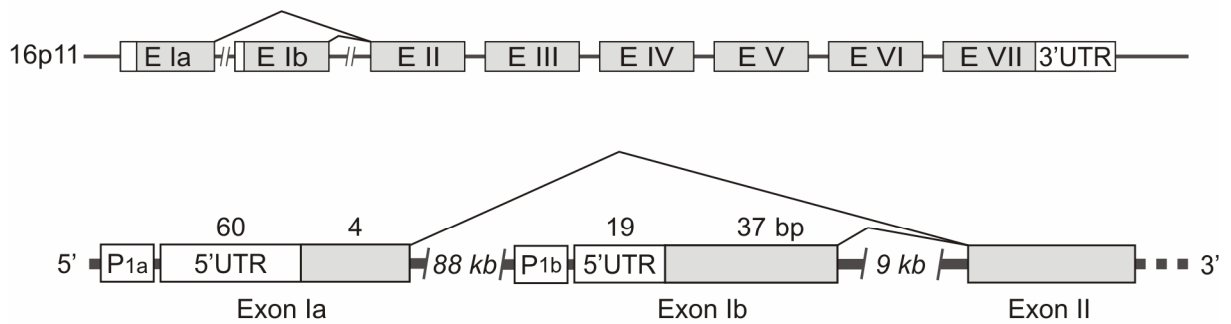
Constitutive expression of M6a isoforms in the brain and kidneys

A comparative real-time RT-PCR analysis of constitutive M6a expression was performed in the brain and kidneys using primers specific for; i) M6a isoform Ia, ii) M6a isoform Ib, and iii) the 3'-UTR region of the M6a transcript common to both isoforms. The results indicate that N-terminus variants of M6a are differentially expressed in the brain and polarised epithelial tissue in the kidneys. M6a isoform Ia was found to be ubiquitously expressed at a low level throughout the brain and kidneys: M6a isoform Ib was identified as the predominant isoform expressed in the brain, but was detected at very low levels in the kidneys (**Fig.16; B**). Moreover, M6a isoform Ib was differentially expressed within the brain regions examined. M6a isoform Ib was most abundantly expressed within the hippocampal formation (17% cyclophilin) with comparable levels of expression being detected in the prefrontal cortex and cerebellum (9% and 10% of cyclophilin expression, respectively).

Effects of chronic stress on M6a expression in the brain

The effect of 21 days chronic restraint stress on M6a expression in specific brain regions was quantified with real-time PCR analysis (**Fig.17**). M6a 3'-UTR primers revealed a significant down-regulation of M6a (65%, $p < 0.01$) in the hippocampus of stressed animals. Subsequent analyses with isoform-specific primers demonstrated that M6a isoform Ib (73%, $p < 0.05$), but not isoform Ia, is significantly reduced by stress in the hippocampus (**A**). RT-PCR detected no significant effect of stress on M6a expression in the prefrontal cortex, however, both isoforms Ia and Ib show a tendency towards upregulation by stress, but fail to reach significance (**B**). No significant effect of stress on M6a expression was observed in the cerebellum (**C**).

A. M6a gene: N-terminus variants (*Rattus Norvegicus*)



B. Constitutive expression of M6a isoforms in brain and kidney

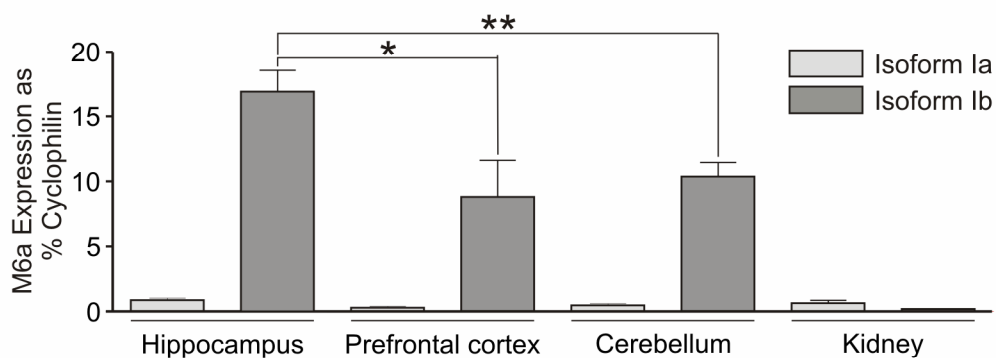


FIGURE 16. Constitutive expression of M6a isoforms Ia and Ib in the brain and kidneys as determined by quantitative RT-PCR. Two N-terminus variants of M6a are produced by usage of alternate transcription start sites corresponding to exons Ia and Ib (A; translated regions appear in grey). Exon Ia encodes a short N-terminal domain, whereas M6a isoform Ib encodes a longer N-terminal domain containing a putative PKC phosphorylation site (see Fig. 1). Three types of primers were developed for real-time RT-PCR analysis; i) primers recognizing the 3'-UTR region of M6a (A; common to all isoforms of M6a); ii) primers specific for M6a isoform Ia; and iii) primers specific for M6a isoform Ib. Constitutive expression of M6a isoforms Ia and Ib in the brain and kidneys as determined by quantitative real time RT-PCR (B). M6a isoform Ia appears ubiquitously expressed at low levels in the brain and kidney epithelia. By comparison, M6a isoform Ib is abundantly expressed in the brain (~20-fold higher expression than M6a isoform Ia), but very weakly expressed in the kidneys. (n=9; two tailed Student's *t*-test; **, $p < 0.01$; *, $p < 0.05$). Data are expressed as mean \pm SEM.

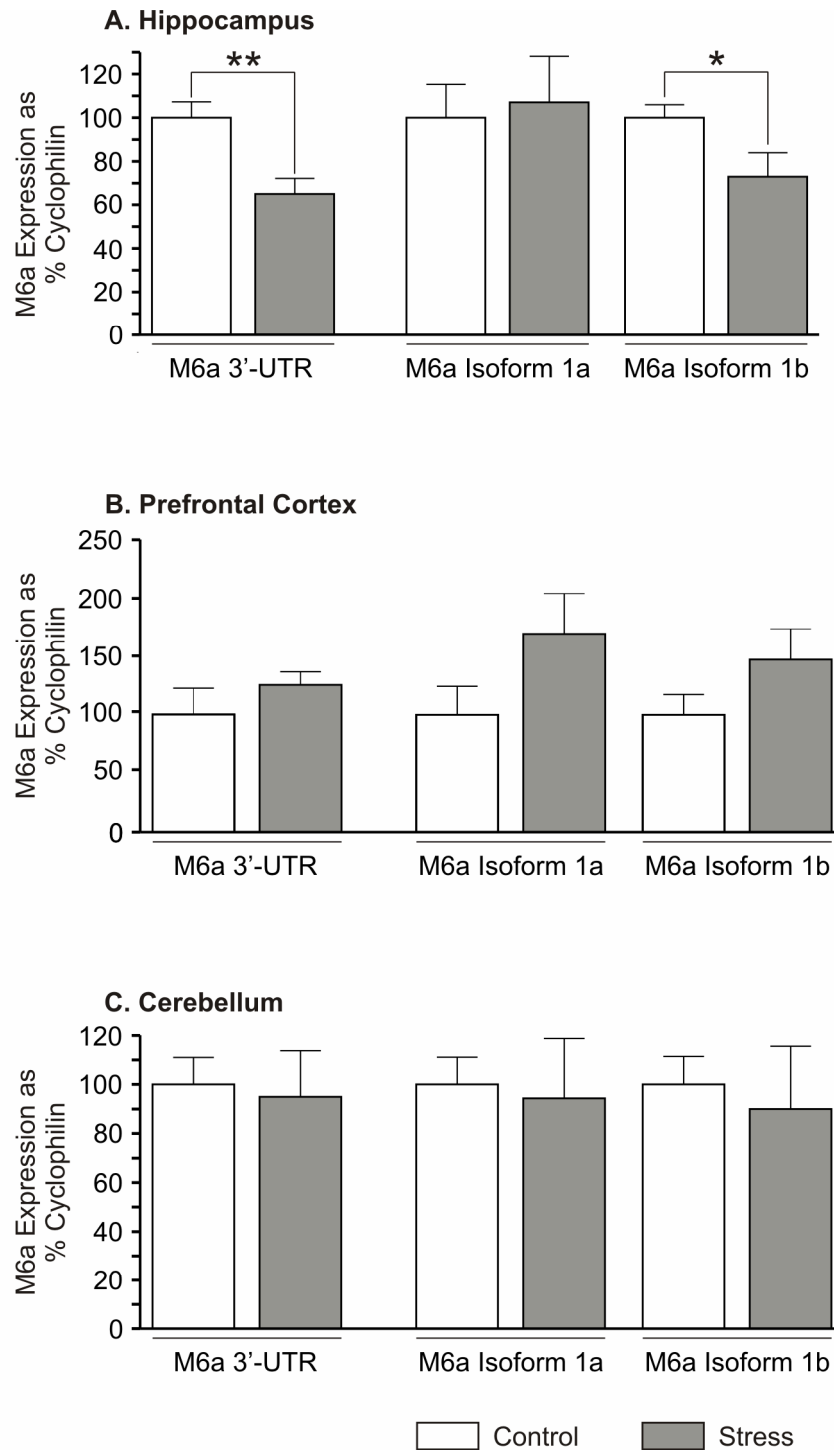


FIGURE 17. Quantitative real-time PCR analysis of M6a expression in the hippocampus (A), prefrontal cortex (B), and cerebellum (C) of chronically stressed rats. Initial analyses performed with M6a 3'-UTR (non-isoform-specific) primers revealed a significant stress-induced down-regulation of M6a in the hippocampus. Subsequent analyses with isoform-specific primers show that M6a isoform 1b, but not isoform 1a, is regulated by stress in the hippocampus. In the prefrontal cortex, both isoforms show a tendency towards upregulation, but fail to reach significance. No effect of stress on M6a expression was observed in the cerebellum. Significant differences between Control and Stress groups are indicated by asterisks (n=9/group; two tailed Student's *t*-test; **, $p < 0.01$; *, $p < 0.05$). Data are expressed as mean \pm SEM.

Quantitative *in situ* hybridisation

Quantitative *in situ* hybridisation was performed to investigate the effects of chronic restraint stress on M6a expression within precise subpopulations of hippocampal neurons (dentate granule cells and CA3 pyramidal neurons) and subareas of the medial prefrontal cortex of rats (**Fig.18**). Hybridisation signals comprised of exposed silver grains appear as black puncta clustered in the vicinity of cell bodies. Cell nuclei counterstained with methyl green appear green/blue. M6a expression in dentate gyrus (**A**) and CA3 stratum pyramidale (**B**) was reduced to approximately 85% ($p < 0.05$) of controls. No effect of stress on M6a expression was detected in the anterior cingulate cortex (**C**), however, significant increases of approximately 112% ($p < 0.05$) of controls were detected in the prelimbic cortex (**D**) and infralimbic cortex (**E**). Light micrographs illustrating hybridisation signals located to dentate granule cell bodies (**F**) and infralimbic pyramidal neurons (**G**).

Quantitative immunocytochemistry

Quantitative immunocytochemistry was performed to investigate the effects of chronic stress on the expression of M6a protein within the mossy fibres of animals exposed to stress and antidepressant treatment with the SSRI fluoxetine (**Fig.20**). The groups analysed included; *Control*, *Stress*, *Stress + Fluoxetine*, and *Control + Fluoxetine*. Densitometric measurements (expressed as relative optical density, ROD) of M6a immunoreactivity within *stratum lucidum* were not significantly different in any group analysed. Chronically stressed animals exhibited reduced ROD values in the *stratum lucidum*, but this effect failed to reach significance. This may be in part attributable to the relatively small sample size used in this experiment or the insufficient sensitivity of the DAB detection system to changes in antigen abundance.

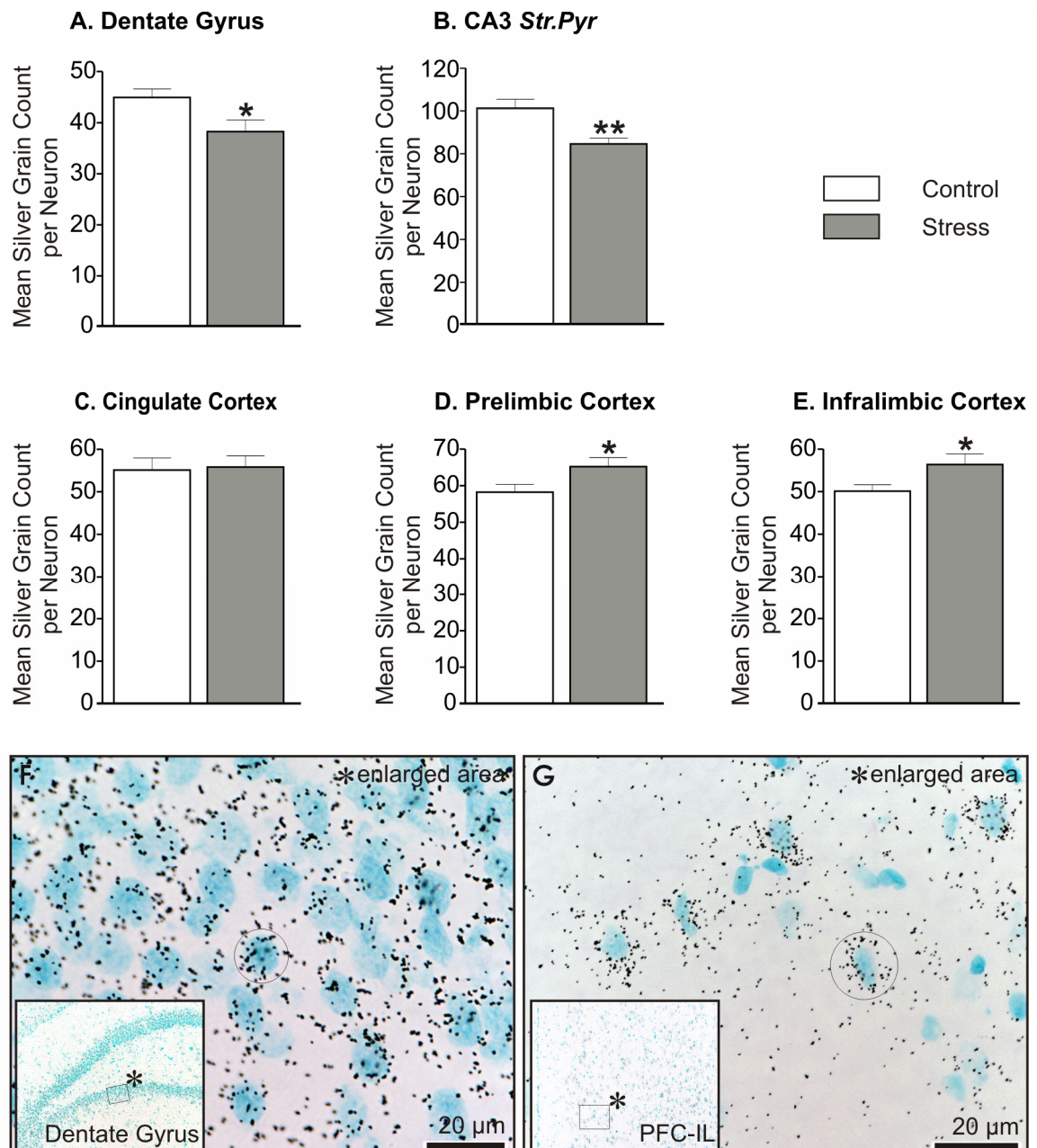


FIGURE 18. Quantitative *in situ* hybridization analysis of M6a expression in specific subregions of the hippocampus and prefrontal cortex were investigated in chronically stressed rats. M6a expression in granule cell layer of the dentate gyrus (**A**) and the CA3 *stratum pyramidale* (**B**) was reduced to 85.2% and 86.6 % of controls, respectively. Increases to 112.5% ($p < 0.01$) and 112.0% ($p < 0.01$) of controls were detected in the prelimbic cortex (**D**) and infralimbic cortex (**E**), respectively. No effect of stress on M6a expression was detected in the anterior cingulate cortex (**C**). Light micrographs illustrating hybridization signals located to granule cells in the dentate gyrus (**F**) and infralimbic pyramidal neurons in the prefrontal cortex (**G**). Hybridization signals comprised of exposed silver grains appear as black puncta clustered in the vicinity of cell bodies. Cell bodies counterstained with methyl green are visualised as blue/green ovoids. Black circles indicate the respective counting masks used to estimate mean neuronal silver grain numbers. Significant differences between Control and Stress groups are indicated by asterisks ($n = 9/\text{group}$; two tailed Student's *t*-test; **, $p < 0.01$; *, $p < 0.05$). Data are expressed as mean \pm SEM.

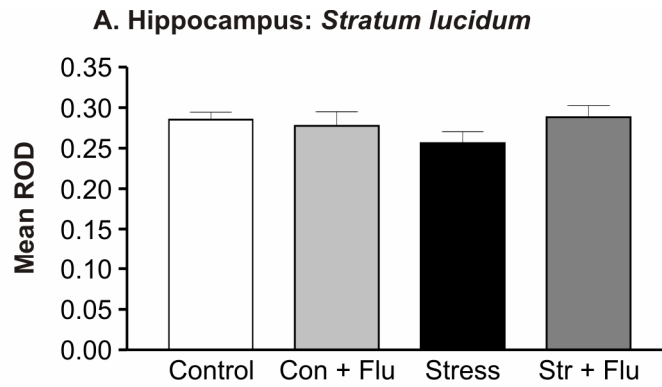


FIGURE 20. Effects of chronic stress and antidepressant treatment on M6a protein expression determined by quantitative immunocytochemistry (**A**). Densitometric measurement of M6a immunoreactivity within *stratum lucidum* failed to expose any significant effect of chronic stress on M6a protein expression in fluoxetine treated animals (Control + Flu, Stress + Flu). No effect of fluoxetine was observed in control animals (Con, Con + Flu). M6a protein expression was found to be reduced in stressed animals, but this reduction failed to reach significance. (n=6/group; two way ANOVA followed by Bonferroni *post hoc* test). Data are expressed as mean \pm SEM.

Discussion

Antibody specificity

Monoclonal anti-M6a from MBL (Nagoya, Japan) is currently the only commercially available antibody directed against the M6a antigen. The present study provides the first demonstration that this antibody is suitable for the immunolocalisation of M6a in paraformaldehyde-fixed brain sections. Moreover, the pattern of immunoreactivity obtained is antigen-specific: transgenic mice lacking M6a exhibited no immunoreactivity to the antibody. The monoclonal anti-M6a has proven effective in flow cytometry applications (unpublished data supplied by MBL, Nagoya, Japan) and sections stained in the absence of detergent (Triton X-100) demonstrated an identical pattern of immunoreactivity with respect to location and intensity providing a strong indication that within the membrane glycoprotein M6a, the epitope recognised by the monoclonal antibody is located in the extracellular part of the molecule. Antibody-epitope interactions were, however, severely diminished in glutaraldehyde-fixed sections (data not shown) indicating: i) glutaraldehyde-fixation may impair anti-M6a antibody penetration into tissue sections, and/or ii) the extensive protein cross-linking may alter the conformational integrity of the epitope rendering the antibody unsuitable for ultrastructural analyses. With respect to the latter possibility, the second extracellular loop is expected to be particularly susceptible to conformational modification owing to the presence of two putative disulfide bridges.

M6a is targeted to the axonal membrane of glutamatergic neurons

In situ hybridisation studies performed in the present study confirm that M6a is expressed exclusively by a subset of glutamatergic neurons in the adult rat CNS. The comparative confocal analyses performed aimed to extend existing knowledge on the distribution of M6a within the: i) hippocampus; ii) prefrontal cortex; and iii) cerebellum.

Dentate gyrus: mossy fibre pathway

The specific pattern of immunoreactivity detected in the hippocampal formation indicates that M6a expressed within the granule cells of the dentate gyrus is targeted to distal terminal regions of MF axons. The cytoplasmic calcium-binding protein calbindin D-28k is distributed within distinct neuronal populations in the hippocampal formation (Sequier *et al.*, 1990; Seress *et al.*, 1993) and provides a means of selectively visualizing hippocampal MFs converging on unlabelled postsynaptic targets within the hilus and *stratum lucidum*. Within these regions M6a exhibited extensive colocalisation with calbindin-immunoreactive MF axons in both dorsal and ventral divisions of the hippocampal formation. Focal M6a-immunoreactive puncta were visualised at distinct sites within the terminal regions of MF terminals, but were not observed within the cell body or dendrites of granule cells similarly visualised by calbindin or MAP-2 immunoreactivity.

The granule cells of the dentate gyrus have been described by some authors as 'the most unusual' neuronal population in the brain (Frotscher *et al.*, 2006), a view supported by the extraordinary anatomical, neurochemical, and electrophysiological properties characterising the dentate MF pathway (reviewed by Henze *et al.*, 2000). Ultrastructural analyses reveal three distinct types of MF terminal based on morphology and target specificity: i) giant MF boutons, ii) filopodial extensions, and iii) small *en passant* varicosities (reviewed by Acsady *et al.*, 1998; see **Fig.2**). First described more than a century ago (Golgi, 1886), giant MF boutons (diameter 4-10 μm) establish multiple asymmetrical synapses with hilar mossy cells (the only type of excitatory neuron in the hilus) and CA3 pyramidal neurons via elaborate spine-like structures, or 'thorny excrescences' (Gonzales *et al.*, 2001). Filopodial extensions protrude from giant MF boutons and are characterised by a thin stalk-like projection terminating in a bulbous varicosity (diameter 0.5-2 μm), whereas small *en passant*

varicosities are visible as swellings (diameter 0.5-1.5 μm) in the axon shaft itself. Whereas giant MF boutons mediate synaptic transmission between the dentate gyrus and the CA3 pyramidal neurons, filopodial extensions and small varicosities make synaptic contact almost exclusively with the dendrites of aspiny GABAergic interneurons within the hilus and *stratum lucidum* (Frotscher *et al.*, 1994; Acsady *et al.*, 1998). Moreover, MF terminals bearing the morphological characteristics of filopodial extensions and small varicosities greatly outnumber giant boutons such that the ratio of granule cell inputs to interneurons and principal neurons in the hippocampus has been estimated at approximately 5:1 (Acsady *et al.*, 1998). The functional ramifications of this are reflected in electrophysiological studies demonstrating that stimulation of the perforant path typically induces inhibitory postsynaptic potentials in CA3 pyramidal neurons under normal conditions (Müller & Misgeld, 1990). M6a was visualised as discrete puncta within the *stratum lucidum* consistent with either its aggregation within discrete membrane domains or sequestration within distinct axolemmal compartments. The distribution and estimated dimensions of focal M6a-immunoreactive puncta (diameter \sim 0.2-0.5 μm) within the *stratum lucidum* appears consistent with enrichment in MF filopodial extensions or small *en passant* varicosities. Unfortunately, this could not be confirmed by ultrastructural analysis in the present study because the antibody did not bind to M6a in glutaraldehyde-fixed tissue sections.

Pyramidal neurons: hippocampus

Pyramidal neurons forming the hippocampal *stratum pyramidale* were also found to express M6a mRNA, with no apparent difference in expression levels observed between CA subfields. Axonal projections from CA3 pyramidal neurons within the hippocampal formation include: Schaffer collaterals terminating on the dendrites of

CA1 pyramidal neurons within *stratum radiatum*, and ii) associational projections terminating on the apical dendrites of CA3 pyramidal neurons within *stratum radiatum*. Schaffer collaterals diverge extensively throughout the longitudinal axis of the hippocampal formation (Witter, 1993) and do not exhibit the lamellar organisation characterising the MF pathway. Accordingly, Schaffer collaterals are not visualised as a coherent fibre pathway in the present study and M6a targeted to the terminal regions of CA3 projections are primarily detected as synaptic puncta within the *stratum radiatum*.

Pyramidal neurons: prefrontal cortex

Within the medial prefrontal cortex M6a was found to be abundantly expressed in all cortical layers by large neurons bearing the morphological characteristics of pyramidal neurons. Moreover, pyramidal neurons within layers II/III of the medial prefrontal cortex exhibited comparable levels of expression in all medial prefrontal subareas examined (anterior cingulate, prelimbic and infralimbic cortex) as determined by quantitative *in situ* hybridisation. PFC pyramidal neurons receive synaptic inputs in an organized fashion with respect to their dendritic arborizations. Distal portions of the apical dendritic tree (layer I; molecular layer) receive inputs primarily from extracortical nuclei, such as the medial dorsal thalamic nuclei and hippocampal CA3 subfield (Swanson, 1977; Groenewegen *et al.*, 1997): proximal portions of apical and basilar dendrites receive inputs from local cortical circuits (Scheibel and Scheibel, 1977) that serve to amplify EPSPs generated in distal apical dendritic branches (Seamans *et al.*, 1997). M6a immunoreactivity was localised exclusively to small calibre axonal fibres, however, immunoreactive terminals detected in apposition to pyramidal neuron dendrites exhibited no preferential *localisation* to either proximal or distal segments of dendritic arborizations.

Cerebellar granule cells: parallel fibres

The combined *in situ* hybridisation and immunocytochemical approach used in the present study confirmed the findings of previous studies describing the differential pattern of M6a expression within the cerebellum (Yan *et al.*, 1996). Hybridisation signals were detected exclusively within the cerebellar granule layer, whereas M6a immunoreactivity was visualised predominantly within the molecular layer as thin fibres (~0.5 µm diameter) bearing the orientation and morphological characteristics of cerebellar parallel fibres (Wyatt *et al.*, 2005).

M6a and GABAergic neurons

In the present study M6a expression was found to be restricted to excitatory neurons in all regions examined. Early studies characterising the pattern of M6a expression in the cerebellum determined that Purkinje cells do not express M6a (Yan *et al.*, 1996). Since Purkinje cells represent just one of several GABAergic subtypes in the cerebellum, confocal immunolocalisation of VGAT was performed to visualise: stellate cell terminals contacting Purkinje cell dendrites; basket cell terminals contacting Purkinje cell bodies, and Golgi cell terminals contacting granule cells. M6a did not colocalise with VGAT in any cerebellar region examined indicating that M6a is not present in inhibitory neuronal populations in the cerebellum. Intrinsic inhibitory networks in the hippocampal formation comprise multiple subtypes of GABAergic interneurons located primarily within the hilus and *stratum radiatum*: interneurons represent only about 10% of the major hippocampal cell layers (Buzsaki, 1984). Neurons bearing the morphological characteristics of GABAergic interneurons (invaginated nucleus, dense Nissl staining) did not express M6a mRNA as determined by *in situ* hybridisation. Moreover, M6a did not colocalise with either calbindin-immunoreactive interneuron cell bodies or processes in *stratum radiatum*.

However, M6a immunoreactive puncta (presumptive terminals) were often observed surrounding the processes of calbindin-immunoreactive interneurons in *stratum lucidum*, indicating that M6a is likely to be expressed within axon terminals making synaptic contact with inhibitory interneurons in the hippocampal formation.

Colocalisation of M6a with synaptic vesicle markers

In the present study, confocal analysis with the monoclonal anti-M6a antibody revealed immunoreactivity to be partially colocalised with synaptic vesicle markers in glutamatergic axon terminals within the hippocampus, prefrontal cortex, and cerebellum. Previous immunoelectron microscopic studies performed with monoclonal anti-M6-7 antibody detected the antigen in membranes of cerebellar granule cell terminals and synaptic vesicles (Roussell *et al.*, 1998). In contrast to the antibody used in the present study, anti-M6-7 recognised an epitope within the C-terminus of both M6a and M6b. A more recent study investigating the protein composition of synaptic vesicle membranes identified M6a (and myelin PLP) within isolated synaptosomal fractions (Takamori *et al.*, 2006). It is, however, technically difficult to prepare subcellular fractions free of contamination and members of the proteolipid family, including M6a and PLP, are among the most abundantly expressed genes in the brain (Huminiacki *et al.*, 2003). In the present study, the discovered enrichment of M6a within terminals of the hippocampal MF pathway was serendipitous, in that it permitted immunolocalisation of M6a within an atypically large presynaptic structure, the giant MF bouton (diameter 4-10 μm). The dimensions of the presynaptic terminal are of considerable significance with respect to the resolving power of a standard confocal laser scanning microscope: due to diffraction, the maximum theoretical resolution achievable by confocal microscopy in the axial plane is approximately 200 nm (Born & Wolf, 1999). Therefore, antigens located within

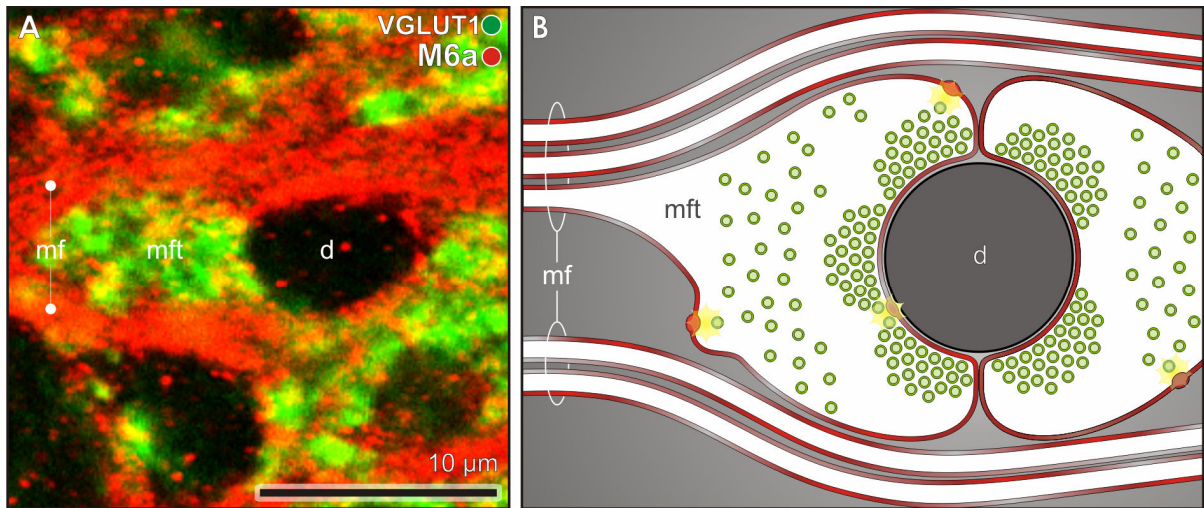


FIGURE 22. Colocalization of M6a (red) and VGLUT1 (green) in the *stratum lucidum* (A). The observed pattern of immunoreactivity is simplified schematically (B, details are not drawn to scale). M6a is localized to the plasma membrane of mossy fibre axons (mf) and mossy fibre terminals (mft), whereas VGLUT1 immunoreactivity is localised to the membranes of glutamatergic vesicles (sv) clustered within mossy fibre terminals. CA3 pyramidal dendrites (d) making contact with mossy fibre terminals are unlabeled and appear in cross section. Partial colocalization of M6a and VGLUT1 is observed on the plasma membrane of mossy fibre terminals, but is rarely in the midst of clustered VGLUT1-positive synaptic vesicles.

different subcellular structures, but situated in close proximity to one another, may be misinterpreted in LSM analyses as being colocalised. The vast dimensions of giant MF boutons provide a means of analysing the relative subcellular distribution of M6a within the presynaptic terminal while remaining within the resolving power of the LSM.

Within the hippocampal *stratum lucidum*, a region densely innervated by dentate MF projections, M6a exhibited a distinct pattern of colocalisation with the synaptic vesicle proteins synaptophysin and VGLUT1: sites of colocalisation were almost exclusively observed in the periphery of presumptive MF terminal membranes, but were rarely detected within central regions of the presynaptic compartment where VGLUT1-positive synaptic vesicles are clustered. These peripheral sites of colocalisation may occur as a result of close proximity between VGLUT1-positive vesicles and M6a within the terminal membrane. Such proximity may occur with more probability within the comparatively small presynaptic compartments exhibited by filopodial and small

varicose MF terminals. This would appear consistent with the punctuate pattern of M6a immunoreactivity demonstrated in the hippocampal *stratum lucidum* in the present study. Alternatively, this may reflect an association between M6a and membrane components mediating synaptic or endocytotic events in the presynaptic terminal, although such interactions are yet to be verified experimentally.

Chronic stress regulation of M6a expression

In the present study 21 days chronic restraint stress altered the transcriptional regulation of membrane glycoprotein M6a within the hippocampus and medial prefrontal cortex, brain regions that are known to undergo morphological changes/exhibit maladaptive plasticity in response to severe or prolonged stress.

M6a is downregulated by chronic stress in the hippocampus

In the present study, M6a mRNA was found to be downregulated by stress in the hippocampal formation of chronically restrained rats. This finding is consistent with previous data demonstrating reduced M6a expression in the hippocampus of psychosocially stressed tree shrews (Alfonso *et al.*, 2004b) and chronically restrained mice (Alfonso *et al.*, 2006), indicating that the effect of stress on hippocampal M6a expression is robustly conserved across species and is reproducible with different stress paradigms. From a methodological perspective, *in situ* hybridisation predictably demonstrated less sensitivity to stress-induced changes in hippocampal M6a expression compared to quantitative RT-PCR analyses, but enabled expression to be quantified within specific neuronal subtypes. Both granule cells of the dentate gyrus and pyramidal neurons within hippocampal region CA3 were found to respond to chronic restraint with highly comparable reductions in M6a expression. *In vitro* analyses of transgenic mice bearing targeted deletions of either M6a, M6b, or both,

indicate that these neuronally expressed proteolipids exhibit a degree of functional redundancy such that neurons coexpressing M6a and M6b appear able to compensate for selective reductions in either specific isoform (Burzynska, 2004). In contrast to M6a, proteolipid M6b is differentially expressed in the hippocampal formation: the expression of M6b is particularly weak in the dentate gyrus but enriched within the CA3 pyramidal neurons (Yan *et al.*, 1996). Hippocampal MF terminals, may therefore exhibit a particular sensitivity to altered M6a expression, although it must be considered that even very low expression of M6b may be sufficient to compensate for stress-induced reductions in M6a.

M6a is upregulated by chronic stress in the ventromedial prefrontal cortex

The prefrontal cortex comprises a heterogeneous collection of functionally distinct nuclei of which the ventromedial subareas (PL, IL) are particularly involved in the integration of visceral/autonomic and cognitive information ultimately contributing to the perception of stress. Quantitative RT-PCR permits the detection of changes in gene expression with an extremely high sensitivity, however, the anatomical specificity of data generated using this method relies on the ability to precisely excise the tissue/cells of interest. In an initial RT-PCR analysis, the entire prefrontal cortex was analysed and found to exhibit a tendency towards increased M6a expression in chronically restrained rats, but this tendency failed to reach significance. Since significant changes in gene expression within specific prefrontal subareas may be masked in a combined analysis of all subregions, quantitative *in situ* hybridisation was performed, revealing that M6a is indeed differentially regulated by stress within subareas of the prefrontal cortex. M6a expression was increased in pyramidal neurons (layers II/III) of prelimbic and infralimbic subareas, whereas no change of expression was observed in the anterior cingulate gyrus.

M6a is targeted to pyramidal axon terminals and associational connections in layers II/III of the medial prefrontal cortex modulate the electrophysiological response of pyramidal neurons to extracortical inputs terminating in distal portions of apical dendrites. Few studies have investigated the effects of chronic stress on presynaptic structures in the prefrontal cortex, however, dendritic remodelling observed in pyramidal neurons within layers II/III of the medial prefrontal cortex is thought to represent an adaptive response to altered synaptic input from extracortical sources such as the CA3 region of the hippocampus (Wellman, 2001). If stress-induced decreases in M6a expression detected within the hippocampal CA3 region have an adverse effect on synaptic transmission, it is conceivable that the increased M6a expression observed in prefrontal pyramidal neurons reflects an adaptive mechanism designed to strengthen associational contacts and in doing so, to sensitize pyramidal neurons to weakened inputs terminating on distal portions of dendritic arborizations.

Chronic stress selectively regulates expression of neuronal M6a isoform Ib

Quantitative RT-PCR analysis revealed that N-terminus variants of M6a are constitutively expressed at different levels within central and peripheral tissue: M6a isoform Ia is ubiquitously expressed at low levels in kidney epithelia and brain, whereas M6a isoform Ib is highly expressed within the brain, but expressed at very low levels in the kidneys. Consistent with the intense immunoreactivity exhibited by the hippocampal MF pathway, neuronal expression of M6a was found to be highest within the hippocampus. Since the monoclonal antibody recognises an epitope common to both N-terminus variants of M6a (M6a isoforms Ia & Ib) in the extracellular part of the molecule, the majority of immunoreactivity detected in the brain can be attributed to M6a isoform Ib. Immunoreactivity was exclusively localised to regions of axonal membranes. If M6a isoform Ia exhibits a different subcellular

location to M6a isoform 1b, this may not be detected by the applied immunocytochemical methods due to the low expression levels demonstrated by this isoform in the brain.

Chronic restraint was found to selectively downregulate neuronally expressed M6a isoform 1b in the hippocampus of chronically restrained rats as determined by quantitative real-time RT-PCR performed with isoform-specific primers. In contrast, M6a isoform 1a was unchanged by stress in the hippocampus. M6a was initially identified by subtractive hybridisation as a glucocorticoid-responsive gene in tree shrews chronically treated with cortisol (Alfonso *et al.*, 2004a). The isoform-specific effects of chronic stress identified in the present thesis indicate that stress-induced reductions in hippocampal M6a expression are likely to occur via glucocorticoid-mediated repression of transcriptional activity specifically within the promoter region of exon 1b in the M6a gene. This may occur either via DNA binding, or through interference with non-receptor transcription factors via protein-protein interactions (reviewed by Meijer, 2002). Previous studies have determined that the genes encoding proteolipids M6a and M6b exhibit a highly comparable organisation of the 5'-end with exons 1a and 1b specifying N-termini of short and full length, respectively (Werner *et al.*, 2001). The effects of stress on M6b expression remain to be investigated.

Time-course of stress-effects on M6a expression

Stress-induced changes in M6a expression may contribute to the development of maladaptive plasticity, or alternatively represent a downstream consequence of such changes. It is therefore important to determine the time-course of stress effects on M6a expression within brain regions exhibiting morphological changes in response to chronic stress exposure. In the hippocampus, structural changes in neuronal

architecture are typically observed after 14 -21 days of chronic restraint stress (Magarinos & McEwen, 1995b). Pyramidal neurons within the mPFC appear exquisitely sensitive to stress and dendritic remodelling has been observed after 7 days restraint stress (Wellman, 2001). The temporal pattern of M6a expression determined by real-time RT-PCR analysis in the hippocampus of chronically restrained mice demonstrates that M6a is progressively down-regulated with increasing exposure to stress, the effect reaching significance after 21 days of restraint (Alfonso *et al.*, 2006). Stress-induced changes in M6a expression observed in the present study similarly correspond to a time-point following the induction of dendritic modification in the hippocampus and medial prefrontal cortex. Significantly, the present study demonstrates that M6a is not a dendritic, but an axonal membrane component in glutamatergic neurons of the adult brain. As of yet, no data exists describing the time-course exhibited by stress-induced changes in presynaptic MF terminal morphology in the hippocampus. This may be of particular relevance since previous studies have postulated that stress-induced retraction of *dendrites* observed before in hippocampal region CA3 may represent adaptive changes to altered presynaptic input (Watanabe *et al.*, 1992b; Magarinos & McEwen, 1995a; McEwen *et al.*, 1997).

Functional implications of M6a in glutamatergic axon terminals

Cell adhesion

M6a has been identified as a potential mediator of cell-cell interactions potentially involved in axon fasciculation during development (Lund *et al.*, 1986; Lagenaur *et al.*, 1992). The dentate gyrus remains a primary neurogenic zone within the adulthood brain (Gould *et al.*, 2000; Fuchs *et al.*, 2004) and neuronal precursors born in the subgranular zone migrate locally into the granule cell layer where they subsequently

mature into functional granule cells (van Praag *et al.*, 2002). The MF pathway can therefore be viewed as a projection system undergoing perpetual development: even in adulthood, the MF pathway is to some extent composed of immature fibres in the process of elongation and target-seeking. Interestingly, cell adhesion molecules participating in axonal development appear differentially distributed in the MF pathway: NCAM is ubiquitously distributed throughout the MF pathway (Miller *et al.*, 1993), whereas polysialylated-NCAM was detected on axons and within small MF boutons preferentially innervating non-pyramidal neurons (Seki & Arai, 1999). With respect to the permissive and stabilising roles exhibited by sialylated and nonsialylated forms of NCAM on structural remodelling (reviewed by Bonfanti, 2006), respectively, the above findings suggest that small MF terminals may be equipped with a structural flexibility exceeding that of giant MF boutons. This may be of particular significance to the potential localisation of M6a within MF filopodial extensions and small *en passant* varicosities.

Ion channel function

Data from *in vitro* experiments suggest that M6a may function as a NGF-sensitive calcium channel under the regulation of PKC-mediated phosphorylation (Mukobata *et al.*, 2002). Intracellular calcium serves as a key regulatory component of neurotransmitter release, synaptic plasticity, and numerous second-messenger signalling pathways modulating the transcriptional efficiency of targeted genes (reviewed by West *et al.*, 2005). Consistent with their atypical anatomical and neurochemical properties, MF terminals exhibit a presynaptic form of synaptic plasticity rarely observed in other neural networks in the brain (Kobayashi *et al.*, 1999; Zalutsky & Nicoll, 1990, Nicoll *et al.*, 2005). Glutamate release at the MF terminal relies on calcium influx: candidate channels include P/Q- and N-type

voltage-gated calcium channels, however pharmacological analyses indicate that other calcium-permeable channels are likely to exist (Nicoll & Schmitz, 2005). Within the presynaptic MF terminal, calcium influx is necessary for the induction of mechanisms driving both potentiation and depression of synaptic efficacy, suggesting that calcium-dependent protein kinases with differential affinities for calcium may regulate MFT synaptic plasticity (Tong *et al.*, 1996; Kobayashi *et al.*, 1999). Mukobata and coworkers report that exogenous M6a expression (M6a isoform Ib, as identified by sequence analysis in the present study) augmented NGF-triggered calcium influx in PC12 cells, however, this effect was not observed in *Xenopus* oocytes in which receptor tyrosine kinase trkA and PKC are not constitutively expressed (Mukobata *et al.*, 2002). NGF was found to be downregulated by stress in the hippocampus of chronically restrained mice (Alfonso *et al.*, 2006). NGF signalling can serve as a potent modulator of axonal outgrowth/structural plasticity (Trivedi *et al.*, 2004) and pharmacological inhibition of tyrosine kinase receptor (trk) function impairs fasciculation and causes aberrant targeting of MF projections in the developing rat hippocampus (Tamura *et al.*, 2006). However, trkA expression is extremely weak in the dentate gyrus as determined by *in situ* hybridisation (Cellerino *et al.*, 1995) and trkA immunoreactivity was detected primarily in cholinergic nerve terminals originating in the medial septum, but not in mossy fibre terminals (Barker-Gibb *et al.*, 2003). Therefore, the differential distribution of M6a and trkA argues against the direct involvement of M6a in NGF-mediated signalling within the dentate MF pathway.

Opioid receptor interactions

In vitro studies have demonstrated that M6a interacts with the μ -opioid receptor (isoform 1; MOR1) to facilitate constitutive internalisation and promote receptor

recycling in transfected HEK 293 cells (Liang, 2004; Wu, 2006). Endogenous opioid peptides are elevated in response to stress (Chen *et al.*, 2004) and chronic morphine exposure has been shown to induce structural changes in pyramidal neurons within the prefrontal cortex (Robinson & Kolb, 1999) and hippocampus (Liao *et al.*, 2004). Hippocampal MF terminals contain and secrete various neuropeptides including enkephalin (Stengaard-Pederson, 1983), the endogenous ligand of MORs (Raynor *et al.*, 1994; Arvidsson *et al.*, 1995). Confocal analyses performed in the present thesis provided no evidence of colocalisation of M6a and MOR1 within MF terminals or any other hippocampal region investigated. Based on previous studies investigating the distribution of MOR1 in the hippocampus, the sparse immunoreactivity detected in the *stratum lucidum* can be attributed to the expression of MOR1 in somatodendritic and axonal compartments of GABAergic interneurons (Drake & Milner, 1999). M6a and MOR1 may be expressed within the same neuronal populations in select brain regions, as indicated by previous *in situ* hybridisation studies (Wu, 2006), however, the results of the present thesis confirm that in the hippocampal formation, M6a and MOR1 are targeted to different subcellular destinations. This differential distribution indicates that direct interactions between M6a and MOR1 in the hippocampus are improbable and unlikely to contribute to the development of stress-induced neuropathologies.

Potential interaction with cholesterol and lipid-enriched microdomains

Lipid-enriched microdomains, or lipid rafts, are hypothesised to serve as platforms for specific proteins and mediate important cellular processes, including intracellular membrane transport and cell signalling (Simons & Ikonen, 1997; Brown and London, 2000; Simons & Toomre, 2000). Proteolipid PLP interacts with cholesterol, a major component of lipid-enriched microdomains, during polarised transport from the Golgi

network to appropriate subcellular destinations in cultured oligodendrocytes (Simons *et al.*, 2000). Aberrant expression of PLP was found to perturb the cellular distribution of cholesterol between plasma membrane and late endosomal compartments and to induce missorting of raft components in cultured BHK cells (Simons *et al.*, 2002) and oligodendrocytes (Kramer-Albers *et al.*, 2006). Cholesterol promotes the formation and stability of lipid rafts in biological membranes (Cerneus *et al.*, 1993; Scheiffele *et al.*, 1997) and perturbations of cellular cholesterol have been associated with impaired protein trafficking, for example the excitatory amino acid transporter (Butchbach *et al.*, 2003), and impaired synaptic plasticity in hippocampal slices (Koudinov & Koudinova, 2005). M6a exhibits a polarised distribution in neurons and epithelial tissue, however, direct interactions between M6a and cholesterol/lipid rafts are yet to be demonstrated experimentally. Nevertheless, membrane-spanning protein domains have been identified as a potential determinant for raft association (Scheiffele *et al.*, 1997) and M6a and PLP share considerable homology within the exoplasmic half of the first TMD (amino acids 39-48). It therefore appears feasible that M6a may interact with lipid rafts in neurons and that stress-induced changes in M6a expression may modify the lipid composition or protein content of neuronal membranes with functional consequences for presynaptic structural integrity.

Stress-induced regulation of M6a may modulate MF activity

Stress-induced changes in M6a expression may contribute to the development of aberrant MF terminal morphology associated with exposure to chronic stress (Magarinos *et al.*, 1997; Sousa *et al.*, 2000). Inhibitory interneurons innervated by filopodial MF terminals and small *en passant* varicosities directly modulate excitatory transmission in the hippocampal formation via: i) inhibitory feedback to granule cells (Frotscher *et al.*, 1994; Seress & Ribak, 1983); and ii) feed-forward inhibition of CA3

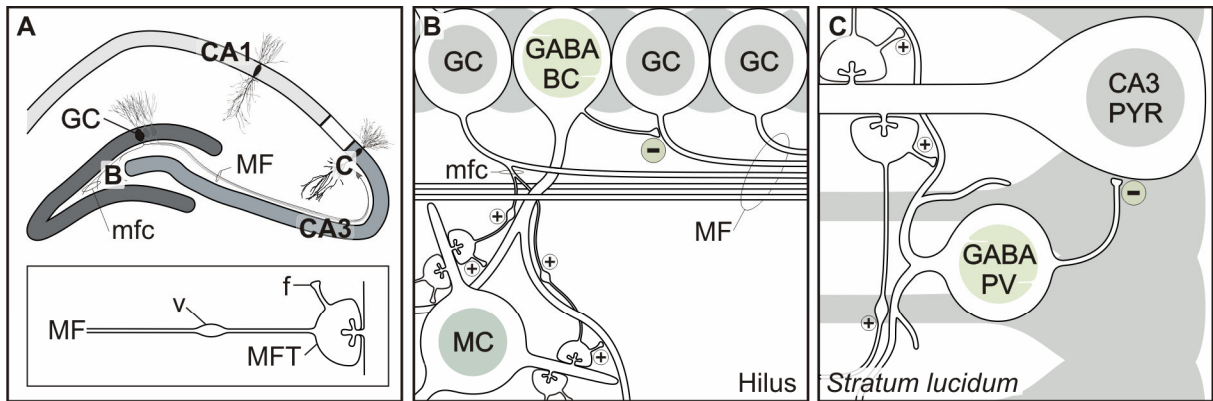


FIGURE 23. Schematic illustrating the divergent projections of the hippocampal mossy fibre (MF) pathway (modified according to Frotscher *et al.*, 1994 and Vida & Frotscher, 2000). Giant mossy fibre terminals (**MFT**) make synaptic contact with glutamatergic mossy cells (**MC**) in the hilus and CA3 pyramidal neurons in the *stratum lucidum* (**C**; **CA3 PYR**). Filipodial extensions (**f**) and small *en passant* varicosities (**v**) make synaptic almost exclusively with aspiny GABAergic interneurons. Shown here are potential pathways via which GABAergic neurons receiving MF input provide direct modulatory control over mossy fibre activity (**B**) and pyramidal neuron excitability (**C**). Basket cells in the hilus (**B**; **GABA BC**) provide direct inhibitory feedback to dentate granule cells (**GC**) initial axon segments: parvalbumin-immunoreactive interneurons in the *stratum lucidum* (**C**; **GABA PV**) provide direct feedforward inhibition to CA3 pyramidal neurons.

pyramidal neurons (Vida & Frotscher, 2000; see **Fig.23**). Maladaptive changes in MF terminal morphology induced by stress are likely to disrupt the inhibitory modulation of MF activity and may underlie the perturbations in hippocampal glutamatergic transmission associated with chronic stress (Lowey *et al.*, 1993). Interestingly, chronic stress was found to reduce the number of parvalbumin-immunoreactive interneurons in the hippocampal formation (Czeh *et al.*, 2005). Since neuronal loss has not yet been identified as a major consequence of stress exposure in the hippocampal formation (Volmann-Honsdorf *et al.*, 1997), reductions in parvalbumin immunoreactivity most probably reflect a reduction in parvalbumin expression. Such a reduction in calcium buffering capabilities is expected to enhance neuronal excitability and may serve as an adaptive measure designed to counteract stress-induced disturbances to MF terminal inputs. However, the effects of stress on the morphology of filopodial and small varicose MF terminals remain to be investigated.

Conclusion

The present findings identify the axonal membrane glycoprotein M6a as a stress target within the hippocampal formation and the medial prefrontal cortex. M6a is localised to distinct sites within the axonal membrane and terminal regions of excitatory neurons in the adult brain. The effects of stress on M6a expression are attributable to altered transcriptional activity of M6a isoform Ib, which was identified as the predominant isoform of M6a expressed in the brain. The present study indicates that M6a is unlikely to be directly involved in the stress-induced remodelling of dendritic arborizations. However, stress-induced reductions in M6a may compromise the structural integrity of glutamatergic nerve terminals and contribute to the development of maladaptive plasticity in stress-responsive brain regions.

List of References

- Acheson,A, Sunshine,JL, Rutishauser,U (1991): NCAM polysialic acid can regulate both cell-cell and cell-substrate interactions. *J.Cell Biol.* 114: 143-153.
- Acsady,L, Kamondi,A, Sik,A, Freund,T, Buzsaki,G (1998): GABAergic cells are the major postsynaptic targets of mossy fibers in the rat hippocampus. *J.Neurosci.* 18: 3386-3403.
- Alfonso,J, Aguero,F, Sanchez,DO, Flugge,G, Fuchs,E, Frasch,AC et al (2004a): Gene expression analysis in the hippocampal formation of tree shrews chronically treated with cortisol. *J.Neurosci.Res.* 78: 702-710.
- Alfonso,J, Pollevick,GD, Van Der Hart,MG, Flugge,G, Fuchs,E, Frasch,AC (2004b): Identification of genes regulated by chronic psychosocial stress and antidepressant treatment in the hippocampus. *Eur.J.Neurosci.* 19: 659-666.
- Alfonso,J, Fernandez,ME, Cooper,B, Flugge,G, Frasch,AC (2005a): The stress-regulated protein M6a is a key modulator for neurite outgrowth and filopodium/spine formation. *Proc.Natl.Acad.Sci.U.S.A* 102: 17196-17201.
- Alfonso,J, Frasch,AC, Flugge,G (2005b): Chronic stress, depression and antidepressants: effects on gene transcription in the hippocampus. *Rev.Neurosci.* 16: 43-56.
- Alfonso,J, Frick,LR, Silberman,DM, Palumbo,ML, Genaro,AM, Frasch,AC (2006): Regulation of hippocampal gene expression is conserved in two species subjected to different stressors and antidepressant treatments. *Biol.Psychiatry* 59: 244-251.
- Amaral,DG, Witter,MP (1989): The three-dimensional organization of the hippocampal formation: a review of anatomical data. *Neuroscience* 31: 571-591.
- Arvidsson,U, Riedl,M, Chakrabarti,S, Lee,JH, Nakano,AH, Dado,RJ et al (1995): Distribution and targeting of a mu-opioid receptor (MOR1) in brain and spinal cord. *J.Neurosci.* 15: 3328-3341.
- Auphan,N, DiDonato,JA, Rosette,C, Helmsberg,A, Karin,M (1995): Immunosuppression by glucocorticoids: inhibition of NF-kappa B activity through induction of I kappa B synthesis. *Science* 270: 286-290.
- Barker-Gibb,AL, Dougherty,KD, Einheber,S, Drake,CT, Milner,TA (2001): Hippocampal tyrosine kinase A receptors are restricted primarily to presynaptic vesicle clusters. *J.Comp Neurol.* 430: 182-199.
- Baumrind,NL, Parkinson,D, Wayne,DB, Heuser,JE, Pearlman,AL (1992): EMA: a developmentally regulated cell-surface glycoprotein of CNS neurons that is concentrated at the leading edge of growth cones. *Dev.Dyn.* 194: 311-325.
- Bonfanti,L (2006): PSA-NCAM in mammalian structural plasticity and neurogenesis. *Prog.Neurobiol.* 80: 129-164.

- Born,M and Wolf,E. (1999):Principles of Optics.Cambridge Univ. Press, Cambridge
- Botteron,KN, Raichle,ME, Drevets,WC, Heath,AC, Todd,RD (2002): Volumetric reduction in left subgenual prefrontal cortex in early onset depression. *Biol.Psychiatry* 51: 342-344.
- Brown,DA, London,E (2000): Structure and function of sphingolipid- and cholesterol-rich membrane rafts. *J.Biol.Chem.* 275: 17221-17224.
- Brown,SM, Henning,S, Wellman,CL (2005): Mild, short-term stress alters dendritic morphology in rat medial prefrontal cortex. *Cereb.Cortex* 15: 1714-1722.
- Burzynska AZ. Aunctions of proteolipids M6A and M6B in neuronal outgrowth and connectivity: an *in vivo* study. (2005): (Dissertation) Max-Planck-Institute of Experimental Medicine.
- Butchbach,ME, Tian,G, Guo,H, Lin,CL (2004): Association of excitatory amino acid transporters, especially EAAT2, with cholesterol-rich lipid raft microdomains: importance for excitatory amino acid transporter localization and function. *J.Biol.Chem.* 279: 34388-34396.
- Buzsaki,G (1984): Feed-forward inhibition in the hippocampal formation. *Prog.Neurobiol.* 22: 131-153.
- Cellerino,A (1996): Expression of messenger RNA coding for the nerve growth factor receptor trkA in the hippocampus of the adult rat. *Neuroscience* 70: 613-616.
- Cerneus,DP, Ueffing,E, Posthuma,G, Strous,GJ, van der,EA (1993): Detergent insolubility of alkaline phosphatase during biosynthetic transport and endocytosis. Role of cholesterol. *J.Biol.Chem.* 268: 3150-3155.
- Chen,JX, Li,W, Zhao,X, Yang,JX, Xu,HY, Wang,ZF et al (2004): Changes of mRNA expression of enkephalin and prodynorphin in hippocampus of rats with chronic immobilization stress. *World J.Gastroenterol.* 10: 2547-2549.
- Chrivia,JC, Kwok,RP, Lamb,N, Hagiwara,M, Montminy,MR, Goodman,RH (1993): Phosphorylated CREB binds specifically to the nuclear protein CBP. *Nature* 365: 855-859.
- Conrad,CD, Galea,LA, Kuroda,Y, McEwen,BS (1996): Chronic stress impairs rat spatial memory on the Y maze, and this effect is blocked by tianeptine pretreatment. *Behav.Neurosci.* 110: 1321-1334.
- Conrad,CD, LeDoux,JE, Magarinos,AM, McEwen,BS (1999): Repeated restraint stress facilitates fear conditioning independently of causing hippocampal CA3 dendritic atrophy. *Behav.Neurosci.* 113: 902-913.
- Cook,SC, Wellman,CL (2004): Chronic stress alters dendritic morphology in rat medial prefrontal cortex. *J.Neurobiol.* 60: 236-248.

- Czeh,B, Simon,M, Van Der Hart,MG, Schmelting,B, Hesselink,MB, Fuchs,E (2005): Chronic stress decreases the number of parvalbumin-immunoreactive interneurons in the hippocampus: prevention by treatment with a substance P receptor (NK1) antagonist. *Neuropsychopharmacology* 30: 67-79.
- Dalley,JW, Cardinal,RN, Robbins,TW (2004): Prefrontal executive and cognitive functions in rodents: neural and neurochemical substrates. *Neurosci.Biobehav.Rev.* 28: 771-784.
- Diorio,D, Viau,V, Meaney,MJ (1993): The role of the medial prefrontal cortex (cingulate gyrus) in the regulation of hypothalamic-pituitary-adrenal responses to stress. *J.Neurosci.* 13: 3839-3847.
- Doherty,P, Cohen,J, Walsh,FS (1990): Neurite outgrowth in response to transfected N-CAM changes during development and is modulated by polysialic acid. *Neuron* 5: 209-219.
- Drake,CT, Milner,TA (1999): Mu opioid receptors are in somatodendritic and axonal compartments of GABAergic neurons in rat hippocampal formation. *Brain Res.* 849: 203-215.
- Drevets,WC, Price,JL, Simpson,JR, Jr., Todd,RD, Reich,T, Vannier,M et al (1997): Subgenual prefrontal cortex abnormalities in mood disorders. *Nature* 386: 824-827.
- Evans,RM, Hollenberg,SM (1988): Cooperative and positional independent trans-activation domains of the human glucocorticoid receptor. *Cold Spring Harb.Symp.Quant.Biol.* 53 Pt 2: 813-818.
- Flugge,G, van Kampen,M, Mijster,MJ (2004): Perturbations in brain monoamine systems during stress. *Cell Tissue Res.* 315: 1-14.
- Folch,J, Lees,M (1951): Proteolipides, a new type of tissue lipoproteins; their isolation from brain. *J.Biol.Chem.* 191: 807-817.
- Frotscher,M, Soriano,E, Misgeld,U (1994): Divergence of hippocampal mossy fibers. *Synapse* 16: 148-160.
- Frotscher,M, Jonas,P, Sloviter,RS (2006): Synapses formed by normal and abnormal hippocampal mossy fibers. *Cell Tissue Res.* 326: 361-367.
- Fryszak,RJ, Neafsey,EJ (1991): The effect of medial frontal cortex lesions on respiration, "freezing," and ultrasonic vocalizations during conditioned emotional responses in rats. *Cereb.Cortex* 1: 418-425.
- Fuchs,E, Flugge,G, Ohl,F, Lucassen,P, Vollmann-Honsdorf,GK, Michaelis,T (2001): Psychosocial stress, glucocorticoids, and structural alterations in the tree shrew hippocampus. *Physiol Behav.* 73: 285-291.
- Fuchs,E, Czeh,B, Kole,MH, Michaelis,T, Lucassen,PJ (2004): Alterations of neuroplasticity in depression: the hippocampus and beyond. *Eur.Neuropsychopharmacol.* 14 Suppl 5: S481-S490.

- Gabbott,PL, Dickie,BG, Vaid,RR, Headlam,AJ, Bacon,SJ (1997): Local-circuit neurones in the medial prefrontal cortex (areas 25, 32 and 24b) in the rat: morphology and quantitative distribution. *J.Comp Neurol.* 377: 465-499.
- Golgi C. (1886): *Studii sulla fina anatomica degli organi centrali del sistema nervoso.* Milan
- Gomez,F, Houshyar,H, Dallman,MF (2002): Marked regulatory shifts in gonadal, adrenal, and metabolic system responses to repeated restraint stress occur within a 3-week period in pubertal male rats. *Endocrinology* 143: 2852-2862.
- Gonzales,RB, DeLeon Galvan,CJ, Rangel,YM, Claiborne,BJ (2001): Distribution of thorny excrescences on CA3 pyramidal neurons in the rat hippocampus. *J.Comp Neurol.* 430: 357-368.
- Gould,E, Tanapat,P, Rydel,T, Hastings,N (2000): Regulation of hippocampal neurogenesis in adulthood. *Biol.Psychiatry* 48: 715-720.
- Gow,A (1997): Redefining the lipophilin family of proteolipid proteins. *J.Neurosci.Res.* 50: 659-664.
- Gow,A, Gragerov,A, Gard,A, Colman,DR, Lazzarini,RA (1997): Conservation of topology, but not conformation, of the proteolipid proteins of the myelin sheath. *J.Neurosci.* 17: 181-189.
- Grewal,SS, York,RD, Stork,PJ (1999): Extracellular-signal-regulated kinase signalling in neurons. *Curr.Opin.Neurobiol.* 9: 544-553.
- Groenewegen,HJ, Wright,CI, Uylings,HB (1997): The anatomical relationships of the prefrontal cortex with limbic structures and the basal ganglia. *J.Psychopharmacol.* 11: 99-106.
- Helm,KA, Han,JS, Gallagher,M (2002): Effects of cholinergic lesions produced by infusions of 192 IgG-saporin on glucocorticoid receptor mRNA expression in hippocampus and medial prefrontal cortex of the rat. *Neuroscience* 115: 765-774.
- Henze,DA, Urban,NN, Barrionuevo,G (2000): The multifarious hippocampal mossy fiber pathway: a review. *Neuroscience* 98: 407-427.
- Holsboer,F, Gerken,A, Steiger,A, Benkert,O, Muller,OA, Stalla,GK (1984): Corticotropin-releasing-factor induced pituitary-adrenal response in depression. *Lancet* 1: 55.
- Huminiacki,L, Lloyd,AT, Wolfe,KH (2003): Congruence of tissue expression profiles from Gene Expression Atlas, SAGEmap and TissueInfo databases. *BMC.Genomics* 4: 31.
- Joels,M, Karst,H, Alfarez,D, Heine,VM, Qin,Y, van Riel,E et al (2004): Effects of chronic stress on structure and cell function in rat hippocampus and hypothalamus. *Stress.* 7: 221-231.
- Kim,JJ, Diamond,DM (2002): The stressed hippocampus, synaptic plasticity and lost memories. *Nat.Rev.Neurosci.* 3: 453-462.

- Kiss,JZ, Muller,D (2001): Contribution of the neural cell adhesion molecule to neuronal and synaptic plasticity. *Rev.Neurosci.* 12: 297-310.
- Kobayashi,K, Manabe,T, Takahashi,T (1999): Calcium-dependent mechanisms involved in presynaptic long-term depression at the hippocampal mossy fibre-CA3 synapse. *Eur.J.Neurosci.* 11: 1633-1638.
- Koudinov,AR, Koudinova,NV (2005): Cholesterol homeostasis failure as a unifying cause of synaptic degeneration. *J.Neurol.Sci.* 229-230: 233-240.
- Kramer-Albers,EM, Gehrig-Burger,K, Thiele,C, Trotter,J, Nave,KA (2006): Perturbed interactions of mutant proteolipid protein/DM20 with cholesterol and lipid rafts in oligodendroglia: implications for dysmyelination in spastic paraplegia. *J.Neurosci.* 26: 11743-11752.
- Kriz,J, Zhu,Q, Julien,JP, Padjen,AL (2000): Electrophysiological properties of axons in mice lacking neurofilament subunit genes: disparity between conduction velocity and axon diameter in absence of NF-H. *Brain Res.* 885: 32-44.
- Krugers,HJ, Douma,BR, Andringa,G, Bohus,B, Korf,J, Luiten,PG (1997): Exposure to chronic psychosocial stress and corticosterone in the rat: effects on spatial discrimination learning and hippocampal protein kinase Cgamma immunoreactivity. *Hippocampus* 7: 427-436.
- Kuipers,SD, Trentani,A, den Boer,JA, ter Horst,GJ (2003): Molecular correlates of impaired prefrontal plasticity in response to chronic stress. *J.Neurochem.* 85: 1312-1323.
- Lagenaur,C, Kunemund,V, Fischer,G, Fushiki,S, Schachner,M (1992): Monoclonal M6 antibody interferes with neurite extension of cultured neurons. *J.Neurobiol.* 23: 71-88.
- Lees M., Brostoff S.L. (1984): Proteins of myelin in "Myelin" 2nd edition (P. Morell) Plenum Press, New York, pp. 197-224.
- Liang Y. (2004): Identifizierung und Charakterisierung von μ -Opioidrezeptor-interagierenden Proteinen. (Dissertation) Fakultät für Naturwissenschaften der Otto-von-Guericke-Universität Magdeburg.
- Liao,D, Lin,H, Law,PY, Loh,HH (2005): Mu-opioid receptors modulate the stability of dendritic spines. *Proc.Natl.Acad.Sci.U.S.A* 102: 1725-1730.
- Lowy,MT, Gault,L, Yamamoto,BK (1993): Adrenalectomy attenuates stress-induced elevations in extracellular glutamate concentrations in the hippocampus. *J.Neurochem.* 61: 1957-1960.
- Lozovaya,N, Miller,AD (2003): Chemical neuroimmunology: health in a nutshell bidirectional communication between immune and stress (limbic-hypothalamic-pituitary-adrenal) systems. *Chembiochem.* 4: 466-484.
- Luine,V, Villegas,M, Martinez,C, McEwen,BS (1994): Stress-dependent impairments of spatial memory. Role of 5-HT. *Ann.N.Y.Acad.Sci.* 746: 403-404.

- Lund,RD, Perry,VH, Lagenaur,CF (1986): Cell surface changes in the developing optic nerve of mice. *J.Comp Neurol.* 247: 439-446.
- Magarinos,AM, McEwen,BS (1995a): Stress-induced atrophy of apical dendrites of hippocampal CA3c neurons: involvement of glucocorticoid secretion and excitatory amino acid receptors. *Neuroscience* 69: 89-98.
- Magarinos,AM, McEwen,BS (1995b): Stress-induced atrophy of apical dendrites of hippocampal CA3c neurons: comparison of stressors. *Neuroscience* 69: 83-88.
- Magarinos,AM, McEwen,BS, Flugge,G, Fuchs,E (1996): Chronic psychosocial stress causes apical dendritic atrophy of hippocampal CA3 pyramidal neurons in subordinate tree shrews. *J.Neurosci.* 16: 3534-3540.
- Magarinos,AM, Verdugo,JM, McEwen,BS (1997): Chronic stress alters synaptic terminal structure in hippocampus. *Proc.Natl.Acad.Sci.U.S.A* 94: 14002-14008.
- Matsuda,S, Kobayashi,Y, Ishizuka,N (2004): A quantitative analysis of the laminar distribution of synaptic boutons in field CA3 of the rat hippocampus. *Neurosci.Res.* 49: 241-252.
- McEwen,BS, Cameron,H, Chao,HM, Gould,E, Magarinos,AM, Watanabe,Y et al (1993): Adrenal steroids and plasticity of hippocampal neurons: toward an understanding of underlying cellular and molecular mechanisms. *Cell Mol.Neurobiol.* 13: 457-482.
- McEwen,BS, Conrad,CD, Kuroda,Y, Frankfurt,M, Magarinos,AM, McKittrick,C (1997): Prevention of stress-induced morphological and cognitive consequences. *Eur.Neuropsychopharmacol.* 7 Suppl 3: S323-S328.
- McEwen,BS, Magarinos,AM (1997): Stress effects on morphology and function of the hippocampus. *Ann.N.Y.Acad.Sci.* 821: 271-284.
- McEwen,BS, Magarinos,AM (2001): Stress and hippocampal plasticity: implications for the pathophysiology of affective disorders. *Hum.Psychopharmacol.* 16: S7-S19.
- McKittrick,CR, Magarinos,AM, Blanchard,DC, Blanchard,RJ, McEwen,BS, Sakai,RR (2000): Chronic social stress reduces dendritic arbors in CA3 of hippocampus and decreases binding to serotonin transporter sites. *Synapse* 36: 85-94.
- Meier,S, Brauer,AU, Heimrich,B, Nitsch,R, Savaskan,NE (2004): Myelination in the hippocampus during development and following lesion. *Cell Mol.Life Sci.* 61: 1082-1094.
- Meijer,OC (2002): Coregulator proteins and corticosteroid action in the brain. *J.Neuroendocrinol.* 14: 499-505.
- Meyer,U, van Kampen,M, Isovich,E, Flugge,G, Fuchs,E (2001): Chronic psychosocial stress regulates the expression of both GR and MR mRNA in the hippocampal formation of tree shrews. *Hippocampus* 11: 329-336.

- Miller,PD, Chung,WW, Lagenaur,CF, DeKosky,ST (1993): Regional distribution of neural cell adhesion molecule (N-CAM) and L1 in human and rodent hippocampus. *J.Comp Neurol.* 327: 341-349.
- Mukobata,S, Hibino,T, Sugiyama,A, Urano,Y, Inatomi,A, Kanai,Y et al (2002): M6a acts as a nerve growth factor-gated Ca(2+) channel in neuronal differentiation. *Biochem.Biophys.Res.Comm.* 297: 722-728.
- Muller,W, Misgeld,U (1990): Inhibitory role of dentate hilus neurons in guinea pig hippocampal slice. *J.Neurophysiol.* 64: 46-56.
- Nave,KA, Lai,C, Bloom,FE, Milner,RJ (1987): Splice site selection in the proteolipid protein (PLP) gene transcript and primary structure of the DM-20 protein of central nervous system myelin. *Proc.Natl.Acad.Sci.U.S.A* 84: 5665-5669.
- Nicoll,RA, Schmitz,D (2005): Synaptic plasticity at hippocampal mossy fibre synapses. *Nat.Rev.Neurosci.* 6: 863-876.
- Obayashi H, Katagiri-Abe T, Ichimura T, Tanaka H, Gejyo F, Arakawa M et al (2002): Expression and intracellular traffic of the newly synthesized FLAG-tagged M6a glycoprotein. *Acta Medica et Biologica* 50: 71-82.
- Ostrander,MM, Richtand,NM, Herman,JP (2003): Stress and amphetamine induce Fos expression in medial prefrontal cortex neurons containing glucocorticoid receptors. *Brain Res.* 990: 209-214.
- Paxinos G and Watson C. (1986): The rat brain in stereotaxic coordinates. Second Edition. Academic Press., New York.
- Peirson,SN, Butler,JN, Foster,RG (2003): Experimental validation of novel and conventional approaches to quantitative real-time PCR data analysis. *Nucleic Acids Res.* 31: e73.
- Perez-Cruz, C, Müller-Keuker, J, Heilbronner, U, Fuchs, E, Flüggé,G (2006): Morphology of pyramidal neurons in the rat prefrontal cortex: Lateralized dendritic remodelling by chronic stress. *Neural Plasticity*, in press
- Popot,JL, Pham,DD, Dautigny,A (1991): Major myelin proteolipid: the 4-alpha-helix topology. *J.Membr.Biol.* 123: 278.
- Radley,JJ, Sisti,HM, Hao,J, Rocher,AB, McCall,T, Hof,PR et al (2004): Chronic behavioral stress induces apical dendritic reorganization in pyramidal neurons of the medial prefrontal cortex. *Neuroscience* 125: 1-6.
- Raynor,K, Kong,H, Law,S, Heerding,J, Tallent,M, Livingston,F et al (1996): Molecular biology of opioid receptors. *NIDA Res.Monogr* 161: 83-103.
- Reul,JM, de Kloet,ER (1985): Two receptor systems for corticosterone in rat brain: microdistribution and differential occupation. *Endocrinology* 117: 2505-2511.
- Ririe,KM, Rasmussen,RP, Wittwer,CT (1997): Product differentiation by analysis of DNA melting curves during the polymerase chain reaction. *Anal.Biochem.* 245: 154-160.

- Robinson,TE, Kolb,B (1999): Morphine alters the structure of neurons in the nucleus accumbens and neocortex of rats. *Synapse* 33: 160-162.
- Roussel,G, Trifilieff,E, Lagenaur,C, Nussbaum,JL (1998): Immunoelectron microscopic localization of the M6a antigen in rat brain. *J.Neurocytol.* 27: 695-703.
- Rygula,R, Abumaria,N, Domenici,E, Hiemke,C, Fuchs,E (2006): Effects of fluoxetine on behavioral deficits evoked by chronic social stress in rats. *Behav.Brain Res.* 174: 188-192.
- Sandi,C, Davies,HA, Cordero,MI, Rodriguez,JJ, Popov,VI, Stewart,MG (2003): Rapid reversal of stress induced loss of synapses in CA3 of rat hippocampus following water maze training. *Eur.J.Neurosci.* 17: 2447-2456.
- Sapolsky,RM, McEwen,BS, Rainbow,TC (1983): Quantitative autoradiography of [3H]corticosterone receptors in rat brain. *Brain Res.* 271: 331-334.
- Sapolsky,RM, Krey,LC, McEwen,BS (1984): Stress down-regulates corticosterone receptors in a site-specific manner in the brain. *Endocrinology* 114: 287-292.
- Scheibel,ME, Scheibel,AB (1977): The anatomy of constancy. *Ann.N.Y.Acad.Sci.* 290: 421-435.
- Scheiffele,P, Roth,MG, Simons,K (1997): Interaction of influenza virus haemagglutinin with sphingolipid-cholesterol membrane domains via its transmembrane domain. *EMBO J.* 16: 5501-5508.
- Schweitzer,J, Becker,T, Schachner,M, Nave,KA, Werner,H (2006): Evolution of myelin proteolipid proteins: gene duplication in teleosts and expression pattern divergence. *Mol.Cell Neurosci.* 31: 161-177.
- Seamans,JK, Gorelova,NA, Yang,CR (1997): Contributions of voltage-gated Ca²⁺ channels in the proximal versus distal dendrites to synaptic integration in prefrontal cortical neurons. *J.Neurosci.* 17: 5936-5948.
- Seib,LM, Wellman,CL (2003): Daily injections alter spine density in rat medial prefrontal cortex. *Neurosci.Lett.* 337: 29-32.
- Seki,T, Rutishauser,U (1998): Removal of polysialic acid-neural cell adhesion molecule induces aberrant mossy fiber innervation and ectopic synaptogenesis in the hippocampus. *J.Neurosci.* 18: 3757-3766.
- Seki,T, Arai,Y (1999): Different polysialic acid-neural cell adhesion molecule expression patterns in distinct types of mossy fiber boutons in the adult hippocampus. *J.Comp Neurol.* 410: 115-125.
- Selye,H (1998): A syndrome produced by diverse nocuous agents (1936). *J.Neuropsychiatry Clin.Neurosci.* 10: 230-231.
- Sequier,JM, Hunziker,W, Andressen,C, Celio,MR (1990): Calbindin D-28k Protein and mRNA Localization in the Rat Brain. *Eur.J.Neurosci.* 2: 1118-1126.

- Seress,L, Ribak,CE (1983): GABAergic cells in the dentate gyrus appear to be local circuit and projection neurons. *Exp.Brain Res.* 50: 173-182.
- Seress,L, Gulyas,AI, Ferrer,I, Tunon,T, Soriano,E, Freund,TF (1993): Distribution, morphological features, and synaptic connections of parvalbumin- and calbindin D28k-immunoreactive neurons in the human hippocampal formation. *J.Comp Neurol.* 337: 208-230.
- Sheetz,MP, Baumrind,NL, Wayne,DB, Pearlman,AL (1990): Concentration of membrane antigens by forward transport and trapping in neuronal growth cones. *Cell* 61: 231-241.
- Sheline,YI, Wang,PW, Gado,MH, Csernansky,JG, Vannier,MW (1996): Hippocampal atrophy in recurrent major depression. *Proc.Natl.Acad.Sci.U.S.A* 93: 3908-3913.
- Sheng,M, McFadden,G, Greenberg,ME (1990): Membrane depolarization and calcium induce c-fos transcription via phosphorylation of transcription factor CREB. *Neuron* 4: 571-582.
- Shors,TJ, Seib,TB, Levine,S, Thompson,RF (1989): Inescapable versus escapable shock modulates long-term potentiation in the rat hippocampus. *Science* 244: 224-226.
- Simons,K, Ikonen,E (1997): Functional rafts in cell membranes. *Nature* 387: 569-572.
- Simons,K, Toomre,D (2000): Lipid rafts and signal transduction. *Nat.Rev.Mol.Cell Biol.* 1: 31-39.
- Simons,M, Kramer,EM, Thiele,C, Stoffel,W, Trotter,J (2000): Assembly of myelin by association of proteolipid protein with cholesterol- and galactosylceramide-rich membrane domains. *J.Cell Biol.* 151: 143-154.
- Simons,M, Kramer,EM, Macchi,P, Rathke-Hartlieb,S, Trotter,J, Nave,KA et al (2002): Overexpression of the myelin proteolipid protein leads to accumulation of cholesterol and proteolipid protein in endosomes/lysosomes: implications for Pelizaeus-Merzbacher disease. *J.Cell Biol.* 157: 327-336.
- Sousa,N, Lukoyanov,NV, Madeira,MD, Almeida,OF, Paula-Barbosa,MM (2000): Reorganization of the morphology of hippocampal neurites and synapses after stress-induced damage correlates with behavioral improvement. *Neuroscience* 97: 253-266.
- Stengaard-Pedersen,K (1983): Comparative mapping of opioid receptors and enkephalin immunoreactive nerve terminals in the rat hippocampus. A radiohistochemical and immunocytochemical study. *Histochemistry* 79: 311-333.
- Stewart,MG, Davies,HA, Sandi,C, Kraev,IV, Rogachevsky,VV, Peddie,CJ et al (2005): Stress suppresses and learning induces plasticity in CA3 of rat hippocampus: a three-dimensional ultrastructural study of thorny excrescences and their postsynaptic densities. *Neuroscience* 131: 43-54.

- Sullivan, RM, Gratton, A (1999): Lateralized effects of medial prefrontal cortex lesions on neuroendocrine and autonomic stress responses in rats. *J. Neurosci.* 19: 2834-2840.
- Swanson, LW (1977): The anatomical organization of septo-hippocampal projections. *Ciba Found. Symp.* 25-48.
- Takamori, S, Holt, M, Stenius, K, Lemke, EA, Gronborg, M, Riedel, D et al (2006): Molecular anatomy of a trafficking organelle. *Cell* 127: 831-846.
- Tamura, M, Koyama, R, Ikegaya, Y, Matsuki, N, Yamada, MK (2006): K252a, an inhibitor of Trk, disturbs pathfinding of hippocampal mossy fibers. *Neuroreport* 17: 481-486.
- Tang, J, Landmesser, L, Rutishauser, U (1992): Polysialic acid influences specific pathfinding by avian motoneurons. *Neuron* 8: 1031-1044.
- Tong, G, Malenka, RC, Nicoll, RA (1996): Long-term potentiation in cultures of single hippocampal granule cells: a presynaptic form of plasticity. *Neuron* 16: 1147-1157.
- Trentani, A, Kuipers, SD, ter Horst, GJ, den Boer, JA (2002): Selective chronic stress-induced in vivo ERK1/2 hyperphosphorylation in medial prefrontocortical dendrites: implications for stress-related cortical pathology? *Eur. J. Neurosci.* 15: 1681-1691.
- Trivedi, N, Marsh, P, Goold, RG, Wood-Kaczmar, A, Gordon-Weeks, PR (2005): Glycogen synthase kinase-3beta phosphorylation of MAP1B at Ser1260 and Thr1265 is spatially restricted to growing axons. *J. Cell Sci.* 118: 993-1005.
- Uylings, HB, Groenewegen, HJ, Kolb, B (2003): Do rats have a prefrontal cortex? *Behav. Brain Res.* 146: 3-17.
- Van Eden, CG, Kros, JM, Uylings, HB (1990): The development of the rat prefrontal cortex. Its size and development of connections with thalamus, spinal cord and other cortical areas. *Prog. Brain Res.* 85: 169-183.
- van Praag, H, Schinder, AF, Christie, BR, Toni, N, Palmer, TD, Gage, FH (2002): Functional neurogenesis in the adult hippocampus. *Nature* 415: 1030-1034.
- Venero, C, Tilling, T, Hermans-Borgmeyer, I, Herrero, AI, Schachner, M, Sandi, C (2004): Water maze learning and forebrain mRNA expression of the neural cell adhesion molecule L1. *J. Neurosci. Res.* 75: 172-181.
- Vertes, RP (2004): Differential projections of the infralimbic and prelimbic cortex in the rat. *Synapse* 51: 32-58.
- Vida, I, Frotscher, M (2000): A hippocampal interneuron associated with the mossy fiber system. *Proc. Natl. Acad. Sci. U.S.A* 97: 1275-1280.
- Vollmann-Honsdorf, GK, Flugge, G, Fuchs, E (1997): Chronic psychosocial stress does not affect the number of pyramidal neurons in tree shrew hippocampus. *Neurosci. Lett.* 233: 121-124.

- Watanabe,Y, Gould,E, McEwen,BS (1992): Stress induces atrophy of apical dendrites of hippocampal CA3 pyramidal neurons. *Brain Res.* 588: 341-345.
- Watanabe,Y, Gould,E, Cameron,HA, Daniels,DC, McEwen,BS (1992): Phenytoin prevents stress- and corticosterone-induced atrophy of CA3 pyramidal neurons. *Hippocampus* 2: 431-435.
- Wellman,CL (2001): Dendritic reorganization in pyramidal neurons in medial prefrontal cortex after chronic corticosterone administration. *J.Neurobiol.* 49: 245-253.
- Werner,H, Dimou,L, Klugmann,M, Pfeiffer,S, Nave,KA (2001): Multiple splice isoforms of proteolipid M6B in neurons and oligodendrocytes. *Mol.Cell Neurosci.* 18: 593-605.
- West,AE, Chen,WG, Dalva,MB, Dolmetsch,RE, Kornhauser,JM, Shaywitz,AJ et al (2001): Calcium regulation of neuronal gene expression. *Proc.Natl.Acad.Sci.U.S.A* 98: 11024-11031.
- White J, Lagenaur C, Yan Y, Salama G (1993): A novel cation channel involved in neurite extension. *Biophys.J.* [Suppl.] 64: A98.
- Wood,GE, Young,LT, Reagan,LP, McEwen,BS (2003): Acute and chronic restraint stress alter the incidence of social conflict in male rats. *Horm.Behav.* 43: 205-213.
- Woolley,CS, Gould,E, McEwen,BS (1990): Exposure to excess glucocorticoids alters dendritic morphology of adult hippocampal pyramidal neurons. *Brain Res.* 531: 225-231.
- Wu D. (2006): Das Glykoprotein M6a beeinflusst Endozytose und Rezyklisierung, sowie die Desensibilisierung des μ -Opioidrezeptors. (Dissertation) Fakultät für Naturwissenschaften der Otto-von-Guericke-Universität Magdeburg.
- Wyatt,KD, Tanapat,P, Wang,SS (2005): Speed limits in the cerebellum: constraints from myelinated and unmyelinated parallel fibers. *Eur.J.Neurosci.* 21: 2285-2290.
- Yan,Y, Lagenaur,C, Narayanan,V (1993): Molecular cloning of M6: identification of a PLP/DM20 gene family. *Neuron* 11: 423-431.
- Yan,Y, Narayanan,V, Lagenaur,C (1996): Expression of members of the proteolipid protein gene family in the developing murine central nervous system. *J.Comp Neurol.* 370: 465-478.
- Yin,X, Watanabe,M, Rutishauser,U (1995): Effect of polysialic acid on the behavior of retinal ganglion cell axons during growth into the optic tract and tectum. *Development* 121: 3439-3446.
- Zalutsky,RA, Nicoll,RA (1990): Comparison of two forms of long-term potentiation in single hippocampal neurons. *Science* 248: 1619-1624.
- Zhang,H, Miller,RH, Rutishauser,U (1992): Polysialic acid is required for optimal growth of axons on a neuronal substrate. *J.Neurosci.* 12: 3107-3114.

List of Figures

Figure 1:	Basic protein structure of membrane glycoprotein M6a	10
Figure 2:	Synaptic organisation of the hippocampal mossy fibre pathway	17
Figure 3:	M6a expression in the rat brain as determined by radioactive <i>in situ</i> hybridisation	38
Figure 4:	M6a immunoreactivity in the mouse brain: specificity of the anti-M6a antibody	39
Figure 5:	Immunocytochemical detection of different antigens in the hippocampus of the rat	41-44
Figure 6:	Immunolocalisation of M6a and calbindin in the hippocampus and prefrontal cortex	49
Figure 7:	Immunolocalisation of M6a and microtubule-associated protein 2 (MAP-2) in the hippocampus and prefrontal cortex	49
Figure 8:	Immunolocalisation of M6a and neurofilament protein NF-200 in the <i>stratum lucidum</i> of the hippocampus	50
Figure 9:	Immunolocalisation of M6a and synaptophysin in the hippocampus and prefrontal cortex	52
Figure 10:	Immunolocalisation of M6a and vesicular glutamate transporter 1 (VGLUT1) in the hippocampus and prefrontal cortex	52
Figure 11:	Immunolocalisation of M6a and vesicular GABA transporter (VGAT) in the hippocampus and prefrontal cortex	53
Figure 12:	Immunolocalisation of M6a and synaptic vesicle protein type 2B (SV2B) in the hippocampus and prefrontal cortex	53
Figure 13:	Immunolocalisation of M6a and isoform 1 of the μ -opioid receptor (MOR1) in the hippocampus	54
Figure 14:	Immunolocalisation of M6a and VGLUT1 and VGAT in the cerebellum	55
Figure 15:	Effects of chronic restraint stress on body weight gain and adrenal weight	60

Figure 16:	Constitutive expression of M6a isoforms Ia and Ib in the brain and kidneys	62
Figure 17:	Quantitative real-time PCR analysis of M6a expression in the hippocampus, prefrontal cortex, and cerebellum of chronically stressed rats	63
Figure 18:	Quantitative <i>in situ</i> hybridisation analysis of M6a expression in the hippocampus and prefrontal cortex of chronically stressed rats	65
Figure 19:	Effects of chronic stress and antidepressant treatment on M6a protein expression determined by quantitative immunocytochemistry	66
Figure 20:	Colocalisation of M6a with synaptic vesicle markers in giant mossy fibre terminals	73
Figure 21:	Divergence of the hippocampal mossy fibre pathway: direct modulation of inhibitory interneuron activity	83

List of Tables

Table 1:	Antibody list	28
Table 2:	Antibodies and fluorophores used in confocal colocalisation experiments	29
Table 3:	Primer list for quantitative real-time RT-PCR	32

Publications

Alfonso,J, Fernandez,ME, **Cooper,B**, Flugge,G, Frasn,AC (2005)

The stress-regulated protein M6a is a key modulator for neurite outgrowth and filopodium/spine formation. *Proc.Natl.Acad.Sci.U.S.A* 102: 17196-17201.

Acknowledgements

First and foremost I would like to thank Prof. Gabriele Flügge for her supervision and constant support throughout my Ph.D. thesis. I am also grateful to Prof. Eberhard Fuchs for allowing me the opportunity to work in the Clinical Neurobiology Laboratory.

For the generous donation of the M6a knockout mouse and for providing invaluable insight into the world of proteolipids I am thankful to Prof. Klaus-Armin Nave and Dr. Hauke Werner from the Neurogenetics Laboratory (Max Planck Institute for Experimental Medicine, Göttingen).

I would like to acknowledge Prof. Eckart Rüther and Prof. Ursula Havemann-Reinecke (Clinic of Psychiatry and Psychotherapy, Göttingen) for their contributions as members of my thesis committee.

For his assistance in interpreting confocal data within the hippocampal formation I am grateful for the kind assistance of Prof. Laszlo Seress (University of Pecs, Hungary)

I would also like to thank the members of the Neuroscience Program Coordination office. I am especially grateful to Prof. Michael Hörner for providing much appreciated support throughout my Ph.D. thesis.

Finally, I would like to extend my appreciation to members, past and present, of the Clinical Neurobiology Laboratory. Special thanks go to Dr. Jeanine Müller-Keuker for teaching me the hidden arts of Corel, to Dr. Boldizsar Czeh for his insightful discussions regarding my work, and to Dr. Nashat Abumaria for sharing his experience regarding gene expression analysis – and his impressive musical abilities. For superb technical assistance I am extremely grateful to Anna Hoffmann, Stephanie Gleisberg and Susanne Bauch, without whom entropy would certainly have prevailed.

Curriculum Vitae

Personal Data

Name: Benjamin Cooper
Date and place of birth: 26.05.1977
Nationality: New Zealand / United Kingdom
Contact information: Kreuzberggring 22, 37075, Göttingen, Germany
Email: bcooper@gmx.de

Education

10/2003 - 03&2007 Ph.D. thesis in the Graduate Program Neuroscience, University of Göttingen, performed at the German Primate Center in the Laboratory of Clinical Neurobiology. Laboratory head: Prof. E. Fuchs. Supervisor: Prof. G. Flügge.

09/2002 - 09/2003 M.Sc. in the Graduate Program Neuroscience, University of Göttingen, Germany

03/1995 - 02/1999 BSc. Neuroscience (honours: 1st Class) University of Otago, Dundedin, New Zealand

Stipends and Awards

2003-2006 Georg-Christoph-Lichtenberg thesis grant from the Government of Lower Saxony, Germany

Employment

04/1999 – 03/2001 Research assistant: Neuroanatomy
Focus: Transmission electron microscopy
Department of Anatomy and Structural Biology,
University of Otago, Dunedin, New Zealand.